4-21-2022 2:00 PM

Flexible Modelling of Time-dependent Covariate Effects with Correlated Competing Risks: Application to Hereditary Breast and Ovarian Cancer Families

Seungwoo Lee, *The University of Western Ontario*

Supervisor: Choi, Yun-Hee, *The University of Western Ontario*

A thesis submitted in partial fulfillment of the requirements for the Master of Science degree in Biostatistics

Abstract

This thesis aims to develop a flexible approach for modelling time-dependent covariate effects on event risk using B-splines in the presence of correlated competing risks. The performance of the proposed model was evaluated via simulation in terms of the bias and precision of the estimation of the parameters and penetrance functions. In addition, we extended the concordance index to account for time-dependent effects and competing events simultaneously and demonstrated its inference procedures. We applied our proposed methods to data rising from the BRCA1 mutation families from the breast cancer family registry to evaluate the time-dependent effects of mammographic screening and prophylactic surgery on breast cancer risks, where ovarian cancer and death from other causes are competing events. Different time-dependent models were evaluated via time-dependent C-index and Brier scores.

Keywords: family data; correlated frailty model; competing risks, time-dependent covariate; time-dependent effect; breast and ovarian cancers; B-spline; prediction; concordance index; Brier score

Summary for Lay Audience

Hereditary breast and ovarian cancer syndrome families have significantly higher lifetime risks of developing breast and ovarian cancer than the general population. Preventive interventions such as mammographic screening (MS) and risk-reducing salpingo-oophorectomy (RRSO) can potentially reduce associated cancer risks. However, since the statuses and effects of these interventions vary over time and individuals may experience multiple cancers, the evaluation of these interventions is complicated.

To understand how the interventions affect the risk of developing breast cancer in the presence of other events, we used a statistical method called the correlated frailty competing risks model, which is applicable for family data with multiple events. To flexibly evaluate the effect of interventions, we incorporated a flexible approach, B-spline, instead of assuming the shape of the effect of RRSO on breast cancer. We further extended the concordance index, which is a common measure used to describe the predictive ability of a model to simultaneously account for the multiple events and changes in the interventions' statuses. We applied our proposed method to BRCA1 mutation carrier families recruited through the Breast Cancer Family Registry to evaluate the time-dependent effects of MS and RRSO on breast cancer risks in the presence of ovarian cancer and death from the other causes as competing events. Then, the predictive abilities of the models were compared by using the extended concordance index.

Acknowledgments

I would like to express my deepest gratitude to my supervisor, Dr. Yun-Hee Choi, for her countless hours of support throughout my studies. Without her invaluable guidance and encouragement, this thesis would not have been possible. I feel fortunate to have worked with her on my thesis. She has set an example of excellence as an advisor, instructor, and researcher. I am also grateful to my supervisory committee member, Dr. Guanyoung Zou, for his valuable feedback on the thesis.

I would like to thank the Canadian Statistical Sciences Institute (CANSSI) and the Department of Epidemiology and Biostatistics for their financial support throughout my study at Western.

I would like to note that the content of this manuscript does not necessarily reflect the views or policies of the National Cancer Institute or any of the collaborating centers in the Breast Cancer Family Registry (BCFR), nor does mention of trade names, commercial products, or organizations imply endorsement by the USA Government or the BCFR.

Finally, I would like to thank my parents for their support and encouragement throughout all my studies, as well as friends from the Department of Epidemiology and Biostatistics who helped me a lot in completing the thesis.

Table of Contents

List of Tables

List of Figures

List of Abbreviations

AIC	Akaike Information Criterion
ASE	Average Standard Error
AUC	Area Under the Receiver Operating Characteristic Curve
BC	Breast Cancer
BCFR	Breast Cancer Family Registries
BS	B-Spline
C-index	Concordance Index
CO	Cox and Oakes
ECP	Empirical Coverage Percentage
ESE	Empirical Standard Error
GCV	Generalized Cross-Validation
HBOC	Hereditary Breast and Ovarian Cancer
HR	Hazard Ratio
IBS	Integrated Brier Score
ICC	Intracluster Correlation Coefficient
IPCW	Inverse Probability of Censoring Weight
MS	Mammographic Screening
MSE	Mean Squared Error
OC	Ovarian Cancer
PBIAS	Percentage Bias
PE	Permanent Exposure
PH	Proportional Hazard
RRM	Risk-Reducing Mastectomy
RRSO	Risk-Reducing Salpingo-Oophorectomy
TDC	Time-Dependent Covariate
TDE	Time-Dependent Effect
TDUC	Time-Dependent Uno's C-index
TIC	Time Independent Covariate

Chapter 1 Introduction

1.1 Motivation

Hereditary breast and ovarian cancer syndrome (HBOC) is an inherited cancer susceptibility syndrome caused mostly by mutations in BRCA 1 or 2 genes. As a hereditary condition, family members from HBOC are at high risk of developing breast cancer (BC) or ovarian cancer (OC). Members in HBOC families have significantly higher lifetime risks of developing BC and OC than the general population, where HBOC represents about 5 to 10% of all BCs and 18% of all OCs (Larsen et al., 2014; Ring and Modesitt, 2018). When mutated, this gene increases the risk of cancer, specifically BC and OC. The lifetime risk of BC for female carriers of BRCA 1 mutation is estimated to range from 46% to 87% (Petrucelli et al., 2022; Satagopan et al., 2001; Chen et al., 2006).

Preventive interventions such as mammographic screening (MS), risk-reducing mastectomy (RRM) and risk-reducing salpingo-oophorectomy (RRSO) can potentially limit the risk of associated cancer (Petrucelli et al., 2022). To understand the effect of interventions, precise estimates of the remaining cancer risk following interventions are tremendously important to help practitioners effectively treat families with HBOC. In particular, the occurrence of interventions may vary in time for different individuals, and their effects could also vary over time.

Motivated by studies to HBOC families, our interest lies in developing statistical methods for the estimation of time-dependent effects of preventive interventions on the BC risk in the presence of competing events such as OC or death. Specifically, we aim to develop a flexible model that can evaluate the time-dependent intervention effect on the risk of BC. We focus on addressing three statistical challenges arising from modelling HBOC family data: competing risk, time-dependent covariate (TDC), and time-dependent effect (TDE).

1.2 Correlated competing risks

Standard survival data often assumes one to experience only one type of event over a follow-up period. However, such an assumption may not be appropriate as subjects may experience more than one type of event. For instance, members of HBOC families often experience multiple cancers such as BC, OC or death from other causes. When the first event among BC, OC, and death is the event of interest, we need to consider competition among them. For example, if an individual experiences OC as the first event, the other events cannot be the first event. More obliviously, if individuals died before developing BC or OC, they cannot experience BC or OC. Hence, in this sense, the occurrence of a competing event precludes the occurrence of the other events as the first event, vice versa.

Conventional survival analysis methods, such as the Kaplan-Meier estimates or Cox proportional hazard model, treat the occurrence of the competing events as censored, assuming censoring is non-informative. The non-informative censoring assumption implies that the censoring mechanism is independent of the survival time. In other words, those who remain in the follow-up and those who are censored have the same future risk of experiencing an event of interest. However, treating the occurrence of competing risk as a censoring event would lead to overestimating the risk of the event of interest because it violates the assumption of non-informative censoring as the competing events would alter the risk of the event of interest. For example, Berry et al. (2010) showed that ignoring competing risks overestimated the risk of second hip fracture associated with age at the time of the first hip fracture in the Framingham Osteoporosis Study. The hazard ratio of the age at the time of the first hip fracture using the standard Cox model and competing risk regression were 1.3 and 0.9, respectively, indicating that advancing age of first hip fracture increases the risk of second hip fracture under the Cox model. In contrast, the competing risk regression suggested that advancing age lowers the risk of second hip fracture.

When data arise from clustered/family-based studies under competing risk settings, individuals with competing events may be correlated within a cluster because of unobserved cluster effects across individuals. Zhou et al. (2012) referred to such data as

clustered competing risks. For clustered data, it is common to share the same random effect within a cluster to account for the potential dependence across the individuals within clusters and assign the random cluster effects to each cause of failure in the presence of competing risks. However, in a more complex situation, the competing events are likely to be related, leading to the potential dependence across causes in individuals within a cluster. Ignoring the dependence of the competing events by using independent cluster effects across competing events within each cluster can result in biased parameter estimates. For instance, Rutten-Budde et al. (2019) demonstrated that when the frailties are correlated, the independent frailty model generally results in over- or under-estimating the frailty variance and large root mean square error for a small or large number of clusters. Thus, the independent assumption of frailties for competing risks is not appropriate for the clustered competing risk data in the presence of correlation between the events.

1.3 Time-dependent covariates

Covariates can be classified as time-independent and time-dependent. Time-independent covariates (TICs) are often measured at the beginning of the study (baseline) or a single time-point and remain fixed throughout the entire duration of follow-up. Examples include sex, mutation status, or treatment status assigned at the beginning of the study that does not change over time. In contrast, some covariates may be repeatedly measured during the follow-up period and whose values are subject to change over time, referred to as TDCs. For instance, in the study of the BC risk among HBOC families, the RRSO status can be seen as a binary TDC, which takes the value of 0 prior to surgery and 1 afterwards. Other examples of TDC include blood pressure, CD4 count, or weights collected at periodic intervals, whose value would change over time.

It is a common mistake that treats TDC as TIC, which would lead to biased results. Consider a binary TDC indicating intervention such as RRSO, which would occur at some time during follow-up. If RRSO is considered as a TIC, classifying those who ever underwent RRSO as being treated regardless of surgery time, where the time even

before RRSO would be considered as exposure to RRSO, the recorded exposure time for treated individuals is much longer than their true exposure time. Then, it would result in exaggerating the benefit of the intervention or conversely underestimating the risk (Suissa, 2008). Thus, it is essential to incorporate TDCs within models correctly in analyses. For instance, Beyersmann et al. (2008) studied the effects of nosocomial pneumonia on length of stay in intensive care units, where the occurrence of nosocomial infection is the time-dependent covariate with a value of 0 before infection and 1 after the infection appears. They demonstrated that the effect of nosocomial pneumonia was -1.02 with a hazard ratio of 0.36 when the infection status was erroneously treated as a TIC. In contrast, treating nosocomial pneumonia as a TDC correctly yielded an effect estimate of -0.28 with a hazard ratio of 0.75. The estimated effect of nosocomial pneumonia indicates a lower length of stay in intensive care units. The results show that the benefit of nosocomial pneumonia is overestimated if the time-dependent nature of exposure is ignored.

1.4 Time dependent effect

The Cox proportional hazard model requires the proportionality assumption that the hazard for those with the risk factor is proportional to the hazard of those without the risk factor. In other words, the relative hazard of an event or the effect of a given covariate in the model is assumed to be constant over time. This assumption is referred to as the proportional hazard (PH) assumption and is vital to the correct use of the Cox PH model. However, the ratio of hazards may not be constant over time when the effect of the covariate in the hazard function varies over time (Therneau and Grambsch, 2000). For example, under the PH assumption, the effect of RRSO on the risk of BC is the same for those who have recently undergone RRSO and those who underwent RRSO far in the past. However, this assumption would be violated if the effect of RRSO on BC changed over the follow-up period. Warwick et al. (2004) studied the time-dependent effect of some prognostic factors in women on breast carcinomas, such as tumour size, lymph node status and histologic grade. They showed that the effects of the prognostic factors differed and diminished over time, yielding a vital role of TDE, especially for long-term

survival, where the effects of the prognostic factors on the event of interest are more significant for those who survived longer than those who did not.

It is essential to understand that TDEs may manifest differently, with different patterns over time. Thus, depending on the nature of variables, different shapes of TDE trajectories can be considered. Keown-Stoneman et al. (2018) examined the effect of colon cancer recurrence on death using both a permanent exposure (constant effect) model and an exponential decay effect model. Although both models demonstrated that cancer recurrence increases the hazard of death, the AIC and likelihood ratio test suggested that the exponential decay model is a better fitting model. Thus, understanding the nature of time-dependent changes in treatment status is crucial to modelling risk effectively because early and late intervention may have different impacts on the risk of developing BC.

1.5 Objectives

To address the abovementioned statistical challenges, this thesis extends the cause-specific correlated frailty competing risk model proposed by Choi et al. (2021) for more flexible modelling of time-dependent effects. It also demonstrates time-dependent performance measures to evaluate the predictive ability of the proposed model that accounts for clustered, competing events and time-dependent covariates.

This thesis has two primary objectives: (1) to flexibly model time-dependent covariates within clustered competing risk models; and (2) to evaluate the performance of the proposed model for time-dependent covariates. To address objective (1), a flexible approach using B-splines (BS) is implemented to model the time-dependent effects of a binary time-dependent covariate. Simulation is then to evaluate the performance of the BS model compared to different parametric functions of the time-dependent effect as proposed by Choi et al. (2021). In addition, the proposed methods are applied to data on HBOC families recruited through Breast Cancer Family Registries (BCFR) (John et al., 2004) to evaluate the effect of RRSO on BC under the different TDE models.

To address objective (2), the performance of the proposed BS model is then compared to models with different parametric functions of the time-dependent effect by applying the models to HBOC families. The existing measure of goodness of fit known as the concordance index, C-index, is adjusted to account for time-dependent effects of time-dependent covariates within clustered competing risk model and applied to evaluate the predictive ability of the proposed model. We further provide an estimation of the variance of the proposed C-index. In addition, other measures of prediction accuracy, the Akaike information criterion (AIC) and Brier score, are used to further evaluate the efficiency of the BS model.

1.6 Organization of the thesis

The remainder of the thesis is structured as follows. Chapter 2 presents a literature review on the correlated frailty model and time-dependent covariates/coefficients. The correlated competing risks model incorporating both parametric and flexible time-dependent effects of the time-dependent covariates is presented in Chapter 3. The simulation study evaluating the proposed model for estimating the parameters and penetrances is conducted in Chapter 4. Chapter 5 presents the different model performance measures such as Brier score and C-index and provides formulas of the adjusted C-index with its variance estimation. In Chapter 6, an application of our proposed model with the proposed C-index to the data from BRCA1 mutation families is presented. Finally, some discussion and limitations of the research are presented in Chapter 7.

Chapter 2 Literature Review

This chapter reviews the literature on different survival models that account for competing risks, time-dependent covariates, and time-dependent effects with family-based or clustered data to address the statistical challenges presented in Chapter 1. We focus on modelling the correlated frailty competing risk model with time-dependent covariates.

2.1 Competing risk models

Competing risks frequently occur in survival data, where the presence of other causes (competing risks) precludes or alters the probability of the occurrence of a specific cause of failure (event of interest). Conventional survival models assume competing risks as non-informative censoring results in overestimating the risk of experiencing the event of interest. Competing risk models are designed to extend conventional survival models by considering all events to address this problem. There are various methods for modelling competing risks data in the literature. In particular, the cause-specific hazard and subdistribution hazard regression models are widely used for analyzing competing risks data.

The cause-specific hazard approach, proposed by Prentice et al. (1978), models the instantaneous rate of a specific event in currently event-free subjects. The corresponding risk set only includes those who have not experienced the specific event. The effect measure to account for competing risk is the absolute risk of an event of interest up to time point t, known as the cumulative incidence at time t. In contrast to the standard survival models, cause-specific cumulative incidence can be obtained by modelling hazard functions for each event separately. The cause-specific hazard is estimated by treating competing events as censored or equivalently fitting a standard Cox proportional hazard function for each event while treating all other events censored.

Then, the cumulative incidence function is obtained as the integral of the multiplication between the cause-specific hazard of the event of interest and the overall survival function. The overall survival function is obtained as the exponential of the sum of the negative cumulative hazard function for all events. As a result, estimating the cumulative incidence for a specific event requires all the hazards for all the events. This approach can be considered as the generalization of the Cox model. Thus, the cause-specific hazards do not have a direct interpretation with respect to the cause-specific cumulative incidence as all other hazard functions must be considered.

Covariate effects on cause-specific hazards are, however, directly interpretable. Still, the effect of a covariate on the cause-specific hazard function of a particular event may not be the same as the effect of the covariate on the corresponding cumulative incidence function, leading each cause-specific hazard to have its unique interpretation of the effect of covariates (Gray, 1988).

Alternatively, Fine and Gray (1999) proposed a subdistribution hazard, which models the instantaneous rate of an event of interest in event-free subjects or previously experienced competing events. The subdistribution hazard differs from the cause-specific hazard by the definition of the risk set. The risk set of the Fine and Gray model consists of those who have not experienced the event of interest and those who have experienced the competing events. That is, individuals who experience competing events remain at risk for the event of interest despite no longer being able to experience it. In contrast to the cause-specific hazard approach, the cumulative subdistribution hazard only requires the subdistribution of a specific event as there is a direct link between the effect of covariates and the cause-specific cumulative incidence under the proportional hazard assumption. However, the cause-specific hazard approach can provide a better understanding of the hazard function for a specific event and thus provide a more straightforward interpretation of the covariate effects on a particular event (Hinchliffe and Lambert, 2013).

As this thesis aims to evaluate the effect of RRSO on BC alone, Prentice et al.'s (1978) cause-specific approach is used owing to its straightforward interpretation of the

cause-specific relative risk or cause-specific hazard ratio. The cause-specific hazard function $h_j(t)$ at time t is the instantaneous rate of occurrence of event j in the short time interval $[t, t+\Delta t]$ conditional on the subjects surviving until time t or later. The observed event time in the presence of competing risks is defined as $T = \min(T^o, C)$, where T^o and C denote the time to the event and the censoring time, respectively. Only the first event time is considered because any event after the first event is not evaluated. Let $\delta = 1, \dots, J$ be the type of the first event among J competing events and $\delta = 0$ if censored. Conditional on a vector of covariates $\boldsymbol{X}$, the cause-specific hazard for event j is given by

$$\begin{aligned} h_j(t|\boldsymbol{X}) &= \lim_{\Delta t \to 0} \frac{P(t \leq T < t+\Delta t, \delta = j | T \geq t, \boldsymbol{X})}{dt} \\ &= h_{0j}(t)\exp\{\boldsymbol{\beta}_j^T \boldsymbol{X}\} \end{aligned}$$

where $\boldsymbol{\beta}_j$ is the vector of the regression coefficients for j event, and $h_{0j}(t)$ describes the cause-specific baseline hazard function for event j. The corresponding cause-specific cumulative hazard function at time t, $H_j(t|\boldsymbol{X})$, is the integral over the cause-specific hazard from time 0 to t, defined as

$$H_j(t|\boldsymbol{X}) = \int_0^t h_j(u|\boldsymbol{X})du,$$

and the probability of being free from any event up to time t, known as the overall survival function, is defined as

$$S(t|\boldsymbol{X}) = \exp\left\{-\sum\nolimits_{j=1}^{J} H_j(t|\boldsymbol{X})\right\}.$$

Then, the probability of developing event *j* by age *t* in the presence of competing risks is defined as the cause-specific cumulative incidence function in the following form:

$$F_j(t|\boldsymbol{X}) = \int_0^t h_j(u|\boldsymbol{X})S(u|\boldsymbol{X})du = \int_0^t h_j(u|\boldsymbol{X}) \exp\left\{-\sum\nolimits_{j=1}^{J} H_j(u|\boldsymbol{X})\right\} du$$

which represents the age-specific cumulative risk of event j and is also referred to as the cause-specific penetrance function. The penetrance, i.e., cumulative risk, for event j depends on the cause-specific hazards for all J types of events, indicating that the risks of all events affect the probability of the event j occurring by time t. Hence, it is impossible to obtain the cause-specific penetrance for event j unless cause-specific hazards for all J events are obtained. Since there is no one-to-one correspondence between cause-specific penetrance for event j and cause-specific hazard for event j, the positive/negative effect of a covariate on the cause-specific hazard for a specific event j does not necessarily indicate the same effect on the cause-specific cumulative incidence of that event (Putter et al., 2007).

2.2 Frailty model in non-competing risk setting

Clustered failure time data are often encountered when multiple subjects are sampled from the same family or cluster. A correlation or unobserved random cluster effect among members of the same family may be induced by the shared common environments or characteristics such as genes. Ignoring the cluster effect can lead to bias when estimating the hazard. For example, based on the Cox model with independent failure time data, a subject with a high risk score is expected to experience the event earlier than one with a low risk score. However, in clustered data, the subject with low risk score could have a higher risk of the event earlier due to the large cluster effects. Henderson and Oman (1999) demonstrated that ignoring the cluster effect in the analysis of clustered data results in biased coefficient estimates towards zero. Hence, it is necessary to accommodate the cluster effect correctly to handle clustered data. A natural way of modelling the dependence of clustered data is by introducing a cluster-specific effect. Vaupel et al. (1979) first introduced the term frailty to account for the random effects and association in the survival models by applying the concept of frailty to population mortality data. The frailty model is an extension of the Cox proportional hazard model, including an effect for each cluster, called frailty, which acts multiplicatively on the

baseline hazard function (Hougaard, 1995). The frailty is used in the model to account for the unobserved cluster effect in the population and is assumed to be constant over time.

Conventional statistical models assume that the observations are statistically independent of each other. However, this does not hold in many applications, such as clustered data or recurrent events. To address this, the shared frailty model was introduced by Clayton (1978) without using the notion of frailty, where frailty is shared among individuals within a cluster as a means of inducing dependence among them. The frailty model is helpful in explaining the correlation within clusters. The shared frailty is a conditional independence model in which survival times are assumed to be independent given the shared frailty.

The choice of the frailty distribution is essential as it determines the correlation structure of the data. Two different distributions are commonly assumed for frailty: the log-normal distribution and gamma distribution (Clayton 1978, Vaupel et al. 1979, Yashin and Iachine 1995, Hougaard 2000, Ripatti and Palmgren 2000, Pankratz et al. 2005). Although the log-normal distribution allows for more flexible modelling of frailty correlation, the gamma distribution is mathematically convenient. The gamma distribution provides closed form expression of the log-likelihoods inference of the conditional likelihood less complicated as frailties may be integrated out. Due to computational convenience, a common choice for the distribution of frailties is a one-parameter gamma distribution with shape parameter k and scale parameter $1/k$, denoted $\text{Gamma}(k, 1/k)$ (Clayton, 1978).

2.3 Frailty model in competing risk settings

In the shared frailty model, the event times are correlated within families, and the dependence is induced by single frailty shared within a cluster. However, in the presence of competing risks, event times of each event type could be correlated within the same cluster (Zhou et al., 2012). Using one frailty for each cluster acting on all different event types might not be plausible in a competing risk setting. To handle the correlations

between competing events, Gorfine and Hsu (2011) extended the competing risk model proposed by Prentice et al. (1978) to incorporate frailty variables within the cause-specific hazards model by combining frailty variables multiplicatively while assuming a proportional hazard frailty model for each event. The flexible dependence structure among competing events within a cluster is provided by using the multivariate normal distribution between frailty variables to induce the association between cause-specific failure times. The survival times are assumed to be conditionally independent with respect to the frailties. Suppose there are J competing risk events and Z_{f_j} is the unobserved shared frailty for the jth event in cluster f. Then, the jth cause-specific hazard function conditional on the jth event frailty in cluster f is defined as

$$h_{f_i,j}\left(t\middle|\boldsymbol{X}_{f_i}, Z_{f_j}\right) = h_{oj}(t)\exp\left(\boldsymbol{\beta}_j^T \boldsymbol{X}_{f_i} + Z_{f_j}\right)$$

where $h_{oj}(t)$ is the baseline cause-specific hazard function for event j and $\boldsymbol{\beta}_j$ is the vector of regression coefficient for event j. Furthermore, suppose $\boldsymbol{Z}_f = \{Z_{f_1}, \ldots, Z_{f_J}\}$ is the vector of frailty variables for all J competing events in cluster f. Gorfine and Hsu (2011) defined the dependence structure of frailty variables as

$$\boldsymbol{Z}_f = \left\{Z_{f_1}, \ldots, Z_{f_J}\right\} \sim N(\boldsymbol{\mu}, \boldsymbol{\Sigma})$$

where $N(\boldsymbol{\mu}, \boldsymbol{\Sigma})$ is the multivariate normal distribution with J-dimensional mean vector $\boldsymbol{\mu}$ and $J \times J$ covariance matrix $\boldsymbol{\Sigma}$.

Although the method of Gorfine and Hsu (2011) can easily incorporate the frailty model in competing risk settings, it requires computationally demanding numerical integration via the expectation-maximization algorithm for inference on model parameters. Alternatively, the frailty variables are decomposed into a sum of gamma components, allowing for derivations of closed form expressions for the log-likelihood, thereby avoiding computationally demanding integration. Yashin et al. (1995) introduced a correlated gamma frailty model to analyze the survival data of twins. They decomposed the frailty variable for twins into two variables where only one variable is shared. Thus, the frailties of twins are correlated. In competing risk settings, Rueten-Budde et al. (2018)

used a gamma decomposition to model dependence between the competing events, owing to its simplicity in construction and estimation and Choi et al. (2021) extended the correlated gamma frailty model by incorporating TDC using different parametric forms of TDE.

2.4 Time-dependent covariate model and time-dependent coefficient model

The Cox proportional hazard model is one of the most widely used models in survival data modelling (Cox, 1972, Therneau and Grambsch, 2000). However, the Cox model is dependent on the proportional hazard assumption, which might not hold when covariates or their effects are time-dependent. For instance, when evaluating the effect of a treatment on the cancer risks, the treatment status could change during the follow-up time. This illustrates a binary TDC taking the value 0 before treatment and 1 afterwards. Crowley and Hu (1977) accommodated a binary time-dependent covariate as a multiplicative factor in the Cox proportional hazard model to analyze the Stanford heart transplant data by treating the transplant status as a time-dependent covariate. The Cox model with a time-dependent covariate has the form such as

$$h(t|X(t)) = h_0(t)\exp\{\beta X(t)\}$$

where $X(t)$ is the time-dependent covariate, which takes a value 0 before transplant and 1 afterward, and β is the time-invariant effect of time-dependent covariate $X(t)$ (Crowley and Hu, 1977, Kalbfleisch and Prentice, 2002).

In a comparable situation, the effect of the time-dependent covariate on the event may not be constant over time. For instance, the effect of a treatment can be strong immediately after treatment but becomes weaker over time, which exemplifies the time-dependent effect, $\beta(t)$. Incorporating the time-dependent effects of covariates into the Cox PH model, Hastie and Tibshirani (1993) proposed general time-dependent effect models, and Nan et al. (2005) accommodated the time-dependent effect of time-dependent covariate as a multiplicative factor in the Cox proportional hazard model as

$$h(t|X(t)) = h_0(t)\exp\{\beta(t)X(t)\}$$

where $\beta(t)$ is a smoothed function of time that is the time-dependent effect of the time-dependent covariate, $X(t)$.

2.4.1 Parametric models

To investigate how the effect of a TDC changes over time, Choi et al. (2021) has implemented different parametric models, such as permanent exposure (PE), exponential decay and Cox and Oakes (CO), in a correlated frailty model for clustered competing risks data.

Suppose the binary TDC, $X(t, t_x)$, is defined as 0 at $t \leq t_x$ and 1 at $t > t_x$, where t_x is the intervention time at which the TDC's value changed and its time-dependent effect as $g\big(t, X(t, t_x)\big)$. If the effect of the TDC is assumed to be constant after t_x, which can be denoted as $g\big(t, X(t, t_x)\big) = \beta X(t, t_x)$, it is referred to as the permanent exposure, since its effect stays constant over time from the treatment (Keown-Stoneman et al., 2018). To incorporate the effect decaying over time, Cox and Oakes (1984) formulated exponentially decaying time-dependent effect in the following form,

$$g\big(t, X(t, t_x)\big) = \begin{cases} 0 & \text{if } t \leq t_x \\ \eta_0 + \beta e^{-\eta(t-t_x)} & \text{if } t > t_x \end{cases}$$

where the effect of the TDC decreases over time with the rate of η, converges to η_0, and this is referred to as the CO model.

2.4.2 Flexible model using B-spline

Although it is easy to describe the effect of TDC in different parametric models, such an approach requires some clinical knowledge to specify the functional form for effect behaviour over time. Finding the appropriate function might be challenging, or the

functional for may even be unknown. In contrast to the parametric approach, incorporating splines into the Cox model may better represent the time-dependent effect of TDCs (Sleeper and Harrington, 1990). A spline function is a series of polynomials of degree D joined smoothly at breakpoints referred to as knots. The B-spline, originally introduced by De Boor et al. (1998), is one type of spline functions that is widely used due to its convenient numerical properties. The smoothness of the B-spline function depends on the number of interior knots and degree, which should be fixed in advance. Then the construction of the B-spline begins by choosing K interior knots, which partition the interval $[a, b]$ into several subintervals. The choice of the number and location of the interior knots is often arbitrary, where too few or too many knots resulting in under- or overfitting of the data. The interior knots are often selected based on the quantiles of the data, where the equal number of the observations lie in each interval. In addition, there are $D + 1$ augmented knots on each side of the interval $[a, b]$, where we have appended the lower and upper boundary knots. Such augmented knots are needed due to the recursive nature of the B-spline. Then, with K interior knots and a polynomial degree D, there are $K + D + 1$ piecewise B-splines of degree D.

Given a variable $x \in [a, b]$ with K interior knots and degree D, each spline basis $B_{k,d}(x)$ is defined recursively, where $k = 0, \dots, K + D$, and $d = 0, \dots, D$, as

$$B_{k,0}(x) = \begin{cases} 1, & \text{if } t_k \le x < t_{k+1} \\ 0, & \text{otherwise} \end{cases}$$

and

$$B_{k,d}(x) = \frac{x - t_k}{t_{k+d} - t_k} B_{k,d-1}(x) + \frac{t_{k+d+1} - x}{t_{k+d+1} - t_{k+1}} B_{k+1,d-1}(x)$$

where the locations of knots are placed at $a = t_0 = \cdots = t_D \le t_{D+1} \le \cdots \le t_{D+K} = \cdots = t_{K+2D+1} = b$.

The B-spline function of degree D with K interior knots can be expressed as

$$f(x) = \sum_{k=0}^{K+D} \beta_k B_{k,D}(x)$$

where β_k are the coefficients of the basis functions.

Figure 2.1 illustrates a) linear and b) quadratic B-spline basis functions created using two interior knots at 3.3 and 6.6 between 0 and 10. Two magenta-coloured vertical dotted lines indicate two interior knots. The linear B-spline consists of two linear pieces for each basis function joined at one interior knot, where four linear spline basis functions are denoted as $B_{0,1}, B_{1,1}, B_{2,1}$ and $B_{3,1}$. Similarly, the quadratic B-spline consists of three quadratic pieces joined at two interior knots, where five quadratic spline basis functions are denoted as $B_{0,2}, B_{1,2}, B_{2,2}, B_{3,2}$ and $B_{4,2}$. The degree of the B-spline controls the smoothness and size of the curve.

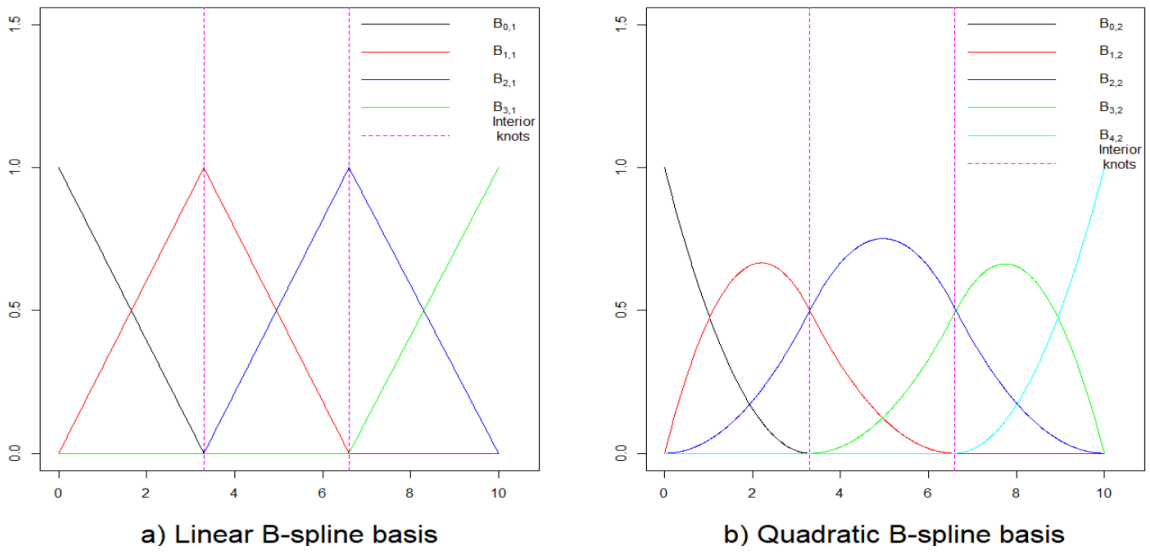

Figure 2.1: Basis functions for the linear B-spline (a) and quadratic B-spline (b) using equally spaced knots at 3.3 and 6.6 between 0 and 10.

The B-spline model flexibly estimates the effects of TDC using basis functions $B_{k,D}(t - t_x), k = 0, \dots, K + D$, such as

$$g\big(t, X(t, t_x)\big) = \begin{cases} 0 & \text{if } t \leq t_x \\ \sum_{k=0}^{K+D} \beta_k B_{k,D}(t - t_x) & \text{if } t > t_x \end{cases}$$

The B-spline provides a smooth curve as it consists of piecewise polynomials connected at the interior knots. Thus, once the B-spline is incorporated into the Cox model, the coefficient of each basis function is not interpretable, but the effect of a covariate should be interpreted as a combination of B-spline basis functions and their effects (Eilers, 1996).

Chapter 3 Proposed Statistical Models

This chapter describes the correlated frailty competing risk model with different functions for TDEs of binary TDCs for clustered competing risk data. This chapter is divided into six sections. Section 3.1 describes the competing risk model with TDCs. Section 3.2 describes the within-cluster correlation between frailties for different events. Likelihood construction for the cause-specific model to estimate the parameters is shown in Section 3.3. In Section 3.4, the cause-specific penetrance function with TDCs is provided. The variance estimation procedures for parameters and cause-specific penetrance are described in Section 3.5.

3.1 Frailty competing risk model with time-dependent covariates and coefficients

Following the general framework of the correlated gamma frailty competing risk model proposed by Choi et al. (2021), we incorporate BS for more flexible modelling of the time-dependent effect of binary time-dependent covariate using BS.

Consider the data arise from F independent families, each family consists of n_f members. Let f_i be the subject i, $i = 1, \dots, n_f$, of the family f, $f = 1, \dots, F$. We denote by $T_{f_i}^O$ and C_{f_i} the time to the first event time and the censoring time, respectively, and by $\delta_{f_i} = 1, \dots, J$ be the type of first event among J competing events and $\delta_{f_i} = 0$ if censored. Define $T_{f_i} = \min\left(T_{f_i}^O\ C_{f_i}\right)$. Let Z_{f_j} denote the unobserved frailty shared within the family f for event j, $j = 1, \dots, J$, which is a family-specific random effect assigned for each event, and $\boldsymbol{X}_{f_i,j}$ denote the vector of covariate for individual i in family f. Conditional on $\boldsymbol{X}_{f_i,j}$ and Z_{f_j}, the cause-specific hazard function for event j for individual i in family f is defined as

$$h_{f_i,j}\left(t|\boldsymbol{X}_{f_i,j}, Z_{f_j}\right) = \lim_{\Delta t \to 0} \frac{P\left(t \leq T_{f_i} < t + \Delta t, \delta_{f_i} = j | T_{f_i} \geq t, \boldsymbol{X}_{f_i,j}, Z_{f_j}\right)}{\Delta t}$$

$$= h_{0,j}(t) Z_{f_j} \exp\{\boldsymbol{\beta}_j^T \boldsymbol{X}_{f_i,j}\} \tag{3.1}$$

where $h_{0,j}(t)$ is the baseline hazard function for event j and $\boldsymbol{\beta_j}$ is the vector of coefficients which corresponds to event j. The corresponding cause-specific cumulative hazard function is written as

$$H_{f_i,j}\left(t|\boldsymbol{X}_{f_i,j}, Z_{f_j}\right) = \int_0^t h_{f_i,j}\left(u|\boldsymbol{X}_{f_i,j}, Z_{f_j}\right) du$$
$$= H_{0,j}(t) Z_{f_j} \exp\{\boldsymbol{\beta}_j^T \boldsymbol{X}_{f_i,j}\}$$

where $H_{0,j}(t)$ is the baseline cumulative hazard function for event j.

Then, the overall survival function conditional on the covariates and frailty is obtained using the cause-specific hazards for all J events as

$$S_{f_i}\left(t|\boldsymbol{X}_{f_i,j}, Z_{f_1}, \ldots, Z_{f_J}\right) = \exp\left\{-\sum_{j=1}^{J} H_{0,j}(t) Z_{f_j} \exp\{\boldsymbol{\beta}_j^T \boldsymbol{X}_{f_i,j}\}\right\} \tag{3.2}$$

where the frailties Z_{f_j} for event j are assumed to be independent across families, but the frailties between events are assumed to be correlated within families. We present the details of formulating the correlated frailties and the dependencies induced by the frailties are described in Section 3.2.

For the covariates, $\boldsymbol{X}_{f_i,j}$, they could be either a TIC, W_{f_i}, or a binary TDC, $X_{f_i,j}(t, t_x)$. We further assume that $X_{f_i,j}(t, t_x) = 0$ at $t \leq t_x$ and 1 at $t > t_x$ where t_x is the time that change in value of TDC occurred. Then, we propose to use the B-spline for flexible modelling of the TDE of TDC denoted by $g(t, X_{f_i,j}(t, t_x))$, as follows,

$$g(t, X_{f_i,j}(t, t_x)) = \begin{cases} 0 & \text{if } t \leq t_x \\ \sum_{k=0}^{K+D} \beta_{j,k} B_{k,D}(t - t_x) & \text{if } t > t_x \end{cases}$$

which gives a smoothing curve with spline basis $B_{k,D}(t-t_x), k=0,\dots,K+D$, where K represents the number of interior knots, D is the degree of basis function, and $B_{0,D}(x)$ is referred to as the intercept. Then, given the cause-specific familial frailty Z_{f_j}, the jth cause-specific hazard function and cumulative hazard function with TDE of TDC and TIC are expressed as

$$h_{f_i,j}\left(t|\boldsymbol{X}_{f_i,j}, Z_{f_j}\right) = h_{0,j}(t)Z_{f_j}\exp\{\gamma_j W_{f_i} + g(t, X_{f_i,j}(t,t_x))\}$$

and

$$H_{f_i,j}\left(t|\boldsymbol{X}_{f_i,j}, Z_{f_j}\right) = \int_0^t h_{0,j}(u)Z_{f_j}\exp\{\gamma_j W_{f_i} + g(u, X_{f_i,j}(u,t_x))\}\,du$$

where W_{f_i} is the TIC and γ_j is the corresponding cause-specific coefficient of event j. Then, the cause-specific hazard and cumulative hazard with the BS can be obtained as

$$h_{f_i,j}\left(t|\boldsymbol{X}_{f_i,j}, Z_{f_j}\right) = \begin{cases} h_{0,j}(t)Z_{f_j}\exp\{\gamma_j W_{f_i}\} & \text{if } t \le t_x \\ h_{0,j}(t)Z_{f_j}\exp\left\{\gamma_j W_{f_i} + \sum_{k=0}^{K+D}\beta_{j,k}B_{k,D}(t-t_x)\right\} & \text{if } t > t_x \end{cases}$$

and

$$H_{f_i,j}\left(t|\boldsymbol{X}_{f_i,j}, Z_{f_j}\right) = \begin{cases} H_{0,j}(t)Z_{f_j}\exp\{\gamma_j W_{f_i}\} & \text{if } t \le t_x \\ \left[\int_0^{t_x} h_{0,j}(u)Z_{f_j}\exp\{\gamma_j W_{f_i}\}\,du + \right. & \\ \left. \int_{t_x}^{t} h_{0,j}(u)Z_{f_j}\exp\left\{\gamma_j W_{f_i} + \sum_{k=0}^{K+D}\beta_{j,k}B_{k,D}(u-t_x)\right\}du\right] & \text{if } t > t_x \end{cases}$$

where the BS function provides a smooth approximation of the effect of TDC over time for $t > t_x$. Then, the corresponding survival function can be obtained by following Equation (3.2).

3.2 Dependence induced by frailties

In the frailty competing risk model, a family-specific random effect, Z_{f_j}, is assigned to each competing event and shared within families, thus inducing dependence among event times of specific event within families. In addition, we allow the frailties for different events to be correlated. To describe the correlation between frailties for different events, each frailty variable, Z_{f_j}, for event j in cluster f is constructed as the sum of two independent random variables: Y_{f_0} and Y_{f_j}, where Y_{f_0} represents the common frailty and Y_{f_j} represents an event-specific frailty that shared by members in the same cluster. The common frailty Y_{f_0} is shared regardless of events, allowing frailties for different events in the same cluster to be correlated.

In particular, the cause-specific frailties within family f are defined as

$$Z_{f_j} = \frac{k_0}{k_0 + k_j} Y_{f_0} + Y_{f_j}$$

where Y_{f_0} and Y_{f_j} are gamma distributed random variables with $Y_{f_0} \sim \text{Gamma}\left(k_0, \frac{1}{k_0}\right)$ and $Y_{f_j} \sim \text{Gamma}\left(k_j, \frac{1}{k_0 + k_j}\right)$, for k_0 and $k_j > 0$. This results in following frailty distribution

$$Z_{f_j} \sim \text{Gamma}\left(k_0 + k_j, \frac{1}{k_0 + k_j}\right)$$

with mean of 1 and variance $\frac{1}{k_0 + k_j}$. The variance of Z_{f_j} indexes the between-cluster variability for event *j*, thus provides the level of within-cluster dependence or correlation. Since larger the variance leads to stronger within-cluster dependence, smaller $k_0 + k_j$ indicates the stronger within-cluster dependence. Furthermore, the association between any two times of event j within families can be expressed by Kendall's tau (Hougaard, 2000, Munda et al., 2012), such as

$$\tau_j = \frac{1}{1 + 2(k_0 + k_j)}$$

where the value of τ_j close to 1 indicate higher dependence of event j within a family.

The covariance and correlation between the frailties of two events, Z_{f_j} and $Z_{f_{j'}}$, $j \neq j'$, in family f are given by

$$\operatorname{cov}\left(Z_{f_j}, Z_{f_{j'}}\right) = \frac{k_0}{(k_0 + k_j)(k_0 + k_{j'})}$$

and

$$\rho = \frac{k_0}{\sqrt{(k_0 + k_j)(k_0 + k_{j'})}}$$

where the value of ρ is between 0 and 1 as k_0, k_j and $k_{j'}$ are larger than 0. Furthermore, $k_0 = 0$ corresponds to the independent frailty variables for the competing events.

3.3 Likelihood construction with ascertainment correction

Based on the cause-specific hazard model conditional on the covariates and familial frailties, the conditional likelihood for family f can be written as

$$L_f^C(\boldsymbol{\theta}) = \prod_{i=1}^{n_f} \prod_{j=1}^{J} h_{f_i,j}\left(t_{f_i} | \boldsymbol{X}_{f_i,j}, Z_{f_j}\right)^{\mathrm{I}\left(\delta_{f_i}=j\right)} S_{f_i}\left(t_{f_i} | \boldsymbol{X}_{f_i,j}, \boldsymbol{Z_f}\right)$$

where $\boldsymbol{Z_f} = (Z_{f_1}, \ldots, Z_{f_J})$ and $\boldsymbol{\theta}$ is a vector of parameters involved in the model, consisting of the baseline parameters and a vector of parameters related to regression coefficients of TIC and TDC, and frailty parameters related to the frailty distribution.

Since the frailties are unobserved, we obtain the marginal likelihood for family f by integrating out the frailties over their distributions (Choi et al., 2021), such as

$$L_f(\boldsymbol{\theta}) = \prod_{i=1}^{n_f} \int_0^\infty \cdots \int_0^\infty \left\{ \prod_{j=1}^{J} h_{f_i,j}\left(t_{f_i}|\boldsymbol{X}_{f_i,j}, Z_{f_j}\right)^{\mathrm{I}\left(\delta_{f_i}=j\right)} \right\} S_{f_i}\left(t_{f_i}|\boldsymbol{X}_{f_i,j}, \boldsymbol{Z_f}\right) g_z\left(Z_{f_1}, \ldots, Z_{f_J}\right) dZ_{f_1} \ldots dZ_{f_1}.$$

By plugging the cause-specific hazard and survival functions in Equations (3.1) and (3.2), respectively, into the marginal likelihood for family *f*, we can first rewrite the marginal likelihood by taking out the terms that do not involve the frailty variables from the integrals to solve the integrals by using the Laplace transformations as follows:

$$\begin{aligned}
L_f(\boldsymbol{\theta}) &= \prod_{i=1}^{n_f} \int_0^\infty \cdots \int_0^\infty \left\{ \prod_{j=1}^{J} h_{f_i,j}\left(t_{f_i}|\boldsymbol{X}_{f_i,j}, Y_{f_0}, Y_{f_j}\right)^{\mathrm{I}\left(\delta_{f_i}=j\right)} \right\} S_{f_i}\left(t_{f_i}|\boldsymbol{X}_{f_i,j}, \boldsymbol{Y_f}\right) \times \\
&\quad g_0\left(Y_{f_0}\right) \ldots g_J\left(Y_{f_J}\right) dY_{f_0} \ldots dY_{f_J} \\
&= \prod_{i=1}^{n_f} \int_0^\infty \cdots \int_0^\infty \prod_{j=1}^{J} \left\{ \left(\frac{w_0}{w_j} Y_{f_0} + Y_{f_j}\right) h_{f_i,j}\left(t_{f_i}|\boldsymbol{X}_{f_i,j}\right) \right\}^{\mathrm{I}\left(\delta_{f_i}=j\right)} \times \\
&\quad \exp\left\{ -\sum_{j=1}^{J} \left(\frac{w_0}{w_j} Y_{f_0} + Y_{f_j}\right) \dot{H}_{f,J} \right\} g_0\left(Y_{f_0}\right) \ldots g_J\left(Y_{f_J}\right) dY_{f_0} \ldots dY_{f_J} \\
&= \left\{ \prod_{i=1}^{n_f} \prod_{j=1}^{J} h_{f_i,j}\left(t_{f_i}|\boldsymbol{X}_{f_i,j}\right)^{\mathrm{I}\left(\delta_{f_i}=j\right)} \right\} \int_0^\infty \cdots \int_0^\infty \prod_{j=1}^{J} \left(\frac{w_0}{w_j} Y_{f_0} + Y_{f_j}\right)^{d_{f_j}} \times \\
&\quad \exp\left\{ -Y_{f_0} \left(\sum_{j=1}^{J} \frac{w_0}{w_j} \dot{H}_{f,j} \right) - \sum_{j=1}^{J} \left(Y_{f_j} \dot{H}_{f,j} \right) \right\} g_0\left(Y_{f_0}\right) \ldots g_J\left(Y_{f_J}\right) dY_{f_0} \ldots dY_{f_J}
\end{aligned} \tag{3.3}$$

where $\boldsymbol{Y_f} = (Y_{f_0}, \ldots, Y_{f_J}), d_{f_j} = \sum_{i=1}^{n_f} I(\delta_{f_i} = j)$ is the number of event j experienced in family f and $\dot{H}_{f,j} = \sum_{i=1}^{n_f} H_{f_i,j}\left(t_{f_i}|\boldsymbol{X}_{f_i,j}\right)$ for simplicity.

The Laplace transform $\phi_j(\cdot)$ and their dth derivative $\phi_j(\cdot)^{(d)}$ for the frailty distribution can be employed in Equation (3.3), where the Laplace transform of the frailties and their dth derivative have the following forms

$$\phi_j(s) = \int_0^\infty e^{-sz} g_j(z) dz$$

$$\phi_j(s)^{(d)} = (-1)^d \int_0^\infty z^d e^{-sz} g_j(z) dz$$

where $g_j(z)$ is the density function of the random variable Y_{f_j}. Given that $w_0 = k_0, w_j = k_0 + k_j, j = 1, \dots, J$, we assume that each random variable Y_{f_j} for event j follows a gamma distribution with shape k_j and scale $\frac{1}{w_j}$. Then, the closed form expressions of the Laplace transform $\phi_j(\cdot)$ and their dth derivative $\phi_j(\cdot)^d$ can be expressed as

$$\phi_j(s) = \left(1 + \frac{s}{w_j}\right)^{-k_j} \tag{3.4}$$

$$\phi_j(s)^{(d)} = (-1)^d \frac{\Gamma(k_j + d)}{\Gamma(k_j) w_j^d} \left(1 + \frac{s}{w_j}\right)^{-k_j - d} \tag{3.5}$$

In addition, the product of the binomials can be expressed as a form of summations by using binomial theorem such as

$$\prod_{j=1}^{J} \left(\frac{w_0}{w_j} Y_{f_0} + Y_{f_j}\right)^{d_{f_j}} = \sum_{b_1=0}^{d_{f_1}} \cdots \sum_{b_J=0}^{d_{f_J}} \binom{d_{f_1}}{b_1} \left(\frac{w_0}{w_1} Y_{f_0}\right)^{b_1} Y_{f_1}^{d_{f_1} - b_1} \cdots \binom{d_{f_J}}{b_J} \left(\frac{w_0}{w_J} Y_{f_0}\right)^{b_J} Y_{f_J}^{d_{f_J} - b_J}$$

$$= \sum_{b_1=0}^{d_{f_1}} \cdots \sum_{b_J=0}^{d_{f_J}} Y_{f_0}^B \left\{ \prod_{j=1}^{J} \binom{d_{f_j}}{b_j} \left(\frac{w_0}{w_j}\right)^{b_j} Y_{f_j}^{d_{f_j} - b_j} \right\}$$

where $B = \sum_{j=1}^{J} b_j$.

Then, with the binomial theorem and Laplace transform, the Equation (3.3) can be further expressed as

$$
\begin{aligned}
L_f(\boldsymbol{\theta}) &= \left\{\prod_{i=1}^{n_f}\prod_{j=1}^{J} h_{f_i,j}\left(t_{f_i}|\boldsymbol{X}_{f_i,j}\right)^{\mathrm{I}\left(\delta_{f_i}=j\right)}\right\}\int_0^{\infty} Y_{f_0}^{B}\exp\left\{-Y_{f_0}\left(\sum_{j=1}^{J}\frac{w_0}{w_j}\dot{H}_{f,j}\right)\right\} g_0\left(Y_{f_0}\right)\times \\
&\quad\left[\sum_{b_1=0}^{d_{f_1}}\cdots\sum_{b_J=0}^{d_{f_J}}\left\{\prod_{j=1}^{J}\int_0^{\infty}\binom{d_{f_j}}{b_j}\left(\frac{w_0}{w_j}\right)^{b_j} Y_{f_j}^{d_{f_j}-b_j}\exp\left\{-Y_{f_j}\dot{H}_{f,j}\right\} g_j\left(Y_{f_j}\right) dY_{f_j}\right\}\right] \\
&= \left\{\prod_{i=1}^{n_f}\prod_{j=1}^{J} h_{f_i,j}\left(t_{f_i}|\boldsymbol{X}_{f_i,j}\right)^{\mathrm{I}\left(\delta_{f_i}=j\right)}\right\}(-1)^{B}\phi_0^{(B)}\left(\sum_{j=1}^{J}\frac{w_0}{w_j}\dot{H}_{f,j}\right)\times \\
&\quad\left[\sum_{b_1=0}^{d_{f_1}}\cdots\sum_{b_J=0}^{d_{f_J}}\left\{\prod_{j=1}^{J}\binom{d_{f_j}}{b_j}\left(\frac{w_0}{w_j}\right)^{b_j}(-1)^{d_{f_j}-b_j}\phi_j^{\left(d_{f_j}-b_j\right)}\left(\dot{H}_{f,j}\right)\right\}\right] \\
&= \left\{\prod_{i=1}^{n_f}\prod_{j=1}^{J} h_{f_i,j}\left(t_{f_i}|\boldsymbol{X}_{f_i,j}\right)^{\mathrm{I}\left(\delta_{f_i}=j\right)}\right\}\frac{\Gamma(w_0+B)}{\Gamma(w_0)w_0^{B}}\left(1+\sum_{j=1}^{J}\frac{\dot{H}_{f,j}}{w_j}\right)^{-w_0-B}\times \\
&\quad\left[\sum_{b_1=0}^{d_{f_1}}\cdots\sum_{b_J=0}^{d_{f_J}}\left\{\prod_{j=1}^{J}\binom{d_{f_j}}{b_j}\left(\frac{w_0}{w_j}\right)^{b_j}\frac{\Gamma\left(k_j+d_{f_j}-b_j\right)}{\Gamma\left(k_j\right)w_j^{\,d_{f_j}-b_j}}\left(1+\frac{\dot{H}_{f,j}}{w_j}\right)^{-k_j-d_{f_j}+b_j}\right\}\right] \\
&= \left\{\prod_{i=1}^{n_f}\prod_{j=1}^{J} h_{f_i,j}\left(t_{f_i}|\boldsymbol{X}_{f_i,j}\right)^{\mathrm{I}\left(\delta_{f_i}=j\right)}\right\}\frac{\Gamma(w_0+B)}{\Gamma(w_0)}\left(1+\sum_{j=1}^{J}\frac{\dot{H}_{f,j}}{w_j}\right)^{-k_0-B}\times \\
&\quad\left[\sum_{b_1=0}^{d_{f_1}}\cdots\sum_{b_J=0}^{d_{f_J}}\left\{\prod_{j=1}^{J}\binom{d_{f_j}}{b_j}\frac{\Gamma\left(k_j+d_{f_j}-b_j\right)}{\Gamma\left(k_j\right)w_j^{\,d_{f_j}}}\left(1+\frac{\dot{H}_{f,j}}{w_j}\right)^{-k_j-d_{f_j}+b_j}\right\}\right]
\end{aligned}
\tag{3.6}
$$

For the data obtained based on the affected probands, an ascertainment corrected likelihood approach should be used to adjust for ascertainment bias (Choi et al., 2021). This correction is done by weighting the $L_f(\boldsymbol{\theta})$ by the inverse probability of a proband being ascertained before age at examination a_{f_p}, which is $A_f(\boldsymbol{\theta}) = P(T_{f_p} < a_{f_p}|\boldsymbol{X}_{f_p,j})$.

Using the Laplace transform of the frailty distribution, the ascertainment probability for family f can be written as follows

$$
\begin{aligned}
A_f(\boldsymbol{\theta}) &= 1 - S_{f_p}\left(a_{f_p}\middle|\boldsymbol{X}_{f_p,j}\right) \\
&= 1 - \int \cdots \int \exp\left\{-\sum_{j=1}^{J} Z_{f_j} H_{f_p,j}\left(a_{f_p}|\boldsymbol{X}_{f_p,j}\right)\right\} g_z\left(Z_{f_1}, \ldots, Z_{f_J}\right) dZ_{f_1} \ldots dZ_{f_J} \\
&= 1 - \int \cdots \int \exp\left\{-\sum_{j=1}^{J} \left(\frac{w_0}{w_j} Y_{f_0} + Y_{f_j}\right) H_{f_p,j}\left(a_{f_p}|\boldsymbol{X}_{f_p,j}\right)\right\} \times \\
&\quad g_0\left(Y_{f_0}\right) \ldots g_J\left(Y_{f_J}\right) dY_{f_0} \ldots dY_{f_J} \\
&= 1 - \int \cdots \int \exp\left\{-Y_{f_0}\left(\sum_{j=1}^{J} \frac{w_0}{w_j} H_{f_p,j}\left(a_{f_p}|\boldsymbol{X}_{f_p,j}\right)\right) - \right. \\
&\quad \left. \sum_{j=1}^{J} Y_{f_j} H_{f_p,j}\left(a_{f_p}|\boldsymbol{X}_{f_p,j}\right)\right\} g_0\left(Y_{f_0}\right) \ldots g_J\left(Y_{f_J}\right) dY_{f_0} \ldots dY_{f_J} \\
&= 1 - \left\{1 + \sum_{j=1}^{J} \frac{H_{f_p,j}\left(a_{f_p}|\boldsymbol{X}_{f_p,j}\right)}{w_j}\right\}^{-k_0} \prod_{j=1}^{J} \left\{1 + \frac{H_{f_p,j}\left(a_{f_p}|\boldsymbol{X}_{f_p,j}\right)}{w_j}\right\}^{-k_j}
\end{aligned}
\tag{3.7}
$$

Then, putting Equations (3.5) and (3.6) together, the general form of ascertainment corrected likelihood for F families can be obtained by dividing each family's likelihood contribution by its ascertainment probability, which can be expressed as

$$L(\boldsymbol{\theta}) = \prod_{f=1}^{F} \frac{L_f(\boldsymbol{\theta})}{A_f(\boldsymbol{\theta})}$$

The regression coefficients of the cause-specific hazard model can be obtained by maximizing the corresponding ascertainment corrected log-likelihood given by

$$\ell(\boldsymbol{\theta}) = \log L(\boldsymbol{\theta}) = \sum_{f=1}^{F} \log L_f(\boldsymbol{\theta}) - \sum_{f=1}^{F} \log A_f(\boldsymbol{\theta}) \tag{3.8}$$

3.4 Cause-specific penetrance function with time-dependent covariates/coefficients

Conditional on the frailties $\boldsymbol{Z_f}$ and the covariates $\boldsymbol{X}_{f_i,j}$, the jth conditional cause-specific cumulative incidence, also called penetrance, for subject i in family f is defined as

$$\begin{aligned} F_{f_i,j}\left(t|\boldsymbol{X}_{f_i,j}, \boldsymbol{Z_f}\right) &= P\left(T_{f_i} \le t, \delta_{f_i} = j|\boldsymbol{X}_{f_i,j}, \boldsymbol{Z_f}\right) \\ &= \int_0^t h_{f_i,j}\left(u|\boldsymbol{X}_{f_i,j}, Z_{f_j}\right) S_{f_i}\left(u|\boldsymbol{X}_{f_i,j}, \boldsymbol{Z_f}\right) du \\ &= \int_0^t h_{f_i,j}\left(u|\boldsymbol{X}_{f_i,j}, Z_{f_j}\right) \exp\left\{-\sum\nolimits_{j=1}^{J} H_{f_i,j}\left(t|\boldsymbol{X}_{f_i,j}, Z_{f_j}\right)\right\} du. \end{aligned}$$

Since the family-specific frailties Z_{f_j} are unobservable, the marginal cause-specific penetrance function for event j can be obtained by integrating out the distribution of frailties Z_{f_j} using the Laplace transform as follows:

$$\begin{aligned} F_{f_i,j}\left(t|\boldsymbol{X}_{f_i,j}\right) &= \int_0^\infty \cdots \int_0^\infty \int_0^t h_{f_i,j}\left(u|\boldsymbol{X}_{f_i,j}, Z_{f_j}\right) S_{f_i}\left(u|\boldsymbol{X}_{f_i,j}, \boldsymbol{Z_f}\right) g_z\left(Z_{f_1}, \dots, Z_{f_J}\right) du dZ_{f_1} \dots dZ_{f_1} \\ &= \int_0^t \int_0^\infty \cdots \int_0^\infty \left(\frac{w_0}{w_j} Y_{f_0} + Y_{f_j}\right) h_{f_i,j}\left(u|\boldsymbol{X}_{f_i,j}\right) \times \\ &\quad \exp\left\{-\sum\nolimits_{j=1}^{J} \left(\frac{w_0}{w_j} Y_{f_0} + Y_{f_j}\right) H_{f_i,j}\left(u|\boldsymbol{X}_{f_i,j}\right)\right\} g_0\left(Y_{f_0}\right) \dots g_J\left(Y_{f_J}\right) dY_{f_0} \dots dY_{f_J} du \\ &= \int_0^t h_{f_i,j}\left(u|\boldsymbol{X}_{f_i,j}\right) \prod_{l \ne j} \int_0^\infty e^{-Y_{f_l} H_{f_i,l}\left(u|\boldsymbol{X}_{f_i}\right)} g_l\left(Y_{f_l}\right) dY_{f_l} \times \\ &\quad \left[\frac{w_0}{w_j} \int_0^\infty Y_{f_0} e^{-\sum_{l=1}^{J} \frac{w_0}{w_l} Y_{f_0} H_{f_i,l}\left(u|\boldsymbol{X}_{f_i,j}\right)} g_0\left(Y_{f_0}\right) dY_{f_0} \int_0^\infty e^{-Y_{f_j} H_{f_i,j}\left(u|\boldsymbol{X}_{f_i,j}\right)} g_j\left(Y_{f_j}\right) dY_{f_j}\right. \end{aligned}$$

$$+\int_0^{\infty} e^{-\sum_{l=1}^{J}\frac{w_0}{w_l}Y_{f_0}H_{f_i,l}\left(u|\boldsymbol{X}_{f_i,j}\right)} g_0\left(Y_{f_0}\right)dY_{f_0} \int_0^{\infty} Y_{f_j} e^{-Y_{f_j}H_{f_i,j}\left(u|\boldsymbol{X}_{f_i,j}\right)} g_j\left(Y_{f_j}\right)dY_{f_j}\Bigg] du$$

$$= \int_0^t h_{f_i,j}\left(u|\boldsymbol{X}_{f_i,j}\right)\prod_{l\neq j}\phi_l\left\{H_{f_i,l}\left(u|\boldsymbol{X}_{f_i,j}\right)\right\} \times$$

$$\left[\frac{w_0}{w_j}(-1)\phi_0^{(1)}\left\{\sum_{l=1}^{J}\frac{w_0}{w_l}H_{f_i,l}\left(u|\boldsymbol{X}_{f_i,j}\right)\right\}\phi_j\left\{H_{f_i,j}\left(u|\boldsymbol{X}_{f_i,j}\right)\right\}\right.$$

$$\left. + \phi_0\left\{\sum_{l=1}^{J}\frac{w_0}{w_l}H_{f_i,l}\left(u|\boldsymbol{X}_{f_i,j}\right)\right\}(-1)\phi_j^{(1)}\left\{H_{f_i,j}\left(u|\boldsymbol{X}_{f_i,j}\right)\right\}\right] du$$

$$= \int_0^t h_{f_i,j}\left(u|\boldsymbol{X}_{f_i,j}\right)\prod_{l\neq j}\left\{1+\frac{H_{f_i,l}\left(u|\boldsymbol{X}_{f_i,j}\right)}{w_l}\right\}^{-k_l} \times$$

$$\left[\frac{w_0}{w_j}\left\{1+\sum_{l=1}^{J}\frac{H_{f_i,l}\left(u|\boldsymbol{X}_{f_i,j}\right)}{w_l}\right\}^{-k_0-1}\left\{1+\frac{H_{f_i,j}\left(u|\boldsymbol{X}_{f_i,j}\right)}{w_j}\right\}^{-k_j}\right.$$

$$\left. + \left\{1+\sum_{l=1}^{J}\frac{H_{f_i,l}\left(u|\boldsymbol{X}_{f_i,j}\right)}{w_l}\right\}^{-k_0}\frac{k_j}{w_j}\left\{1+\frac{H_{f_i,j}\left(u|\boldsymbol{X}_{f_i,j}\right)}{w_j}\right\}^{-k_j-1}\right] du$$

$$= \int_0^t h_{f_i,j}\left(u|\boldsymbol{X}_{f_i,j}\right)\prod_{l\neq j}\left\{1+\frac{H_{f_i,l}\left(u|\boldsymbol{X}_{f_i,j}\right)}{w_l}\right\}^{-k_l}\left\{1+\frac{H_{f_i,j}\left(u|\boldsymbol{X}_{f_i,j}\right)}{w_j}\right\}^{-k_j} \times$$

$$\left\{1+\sum_{l=1}^{J}\frac{H_{f_i,l}\left(u|\boldsymbol{X}_{f_i,j}\right)}{w_l}\right\}^{-k_0} \times$$

$$\left[\frac{k_0}{w_j}\left\{1+\sum_{l=1}^{J}\frac{H_{f_i,l}\left(u|\boldsymbol{X}_{f_i,j}\right)}{w_l}\right\}^{-1} + \frac{k_j}{w_j}\left\{1+\frac{H_{f_i,j}\left(u|\boldsymbol{X}_{f_i,j}\right)}{w_j}\right\}^{-1}\right] du \tag{3.9}$$

where the Laplace transform of the frailty distribution and its dth derivative are applied as shown in Equations (3.4) and (3.5)

We further incorporate TDC and TDE into the cause-specific penetrance function, which is based on the correlated frailty competing risk model presented in Equation (3.8). For simplicity, omitting the terms related to TIC, the marginal cause-specific penetrance function for is

$$F_{f_i,j}\left(t|X_{f_i,j}(t,t_x)\right) = \int_0^t h_{f_i,j}\left(u|X_{f_i,j}(u,t_x)\right) \prod_{l\neq j}\left\{1+\frac{H_{f_i,l}\left(u|X_{f_i,j}(u,t_x)\right)}{w_l}\right\}^{-k_l} \times$$
$$\left\{1+\frac{H_{f_i,j}\left(u|X_{f_i,j}(u,t_x)\right)}{w_j}\right\}^{-k_j} \left\{1+\sum\nolimits_{l=1}^{J}\frac{H_{f_i,l}\left(u|X_{f_i,j}(u,t_x)\right)}{w_l}\right\}^{-k_0} \times$$
$$\left[\frac{w_0}{w_j}\left\{1+\sum\nolimits_{l=1}^{J}\frac{H_{f_i,l}\left(u|X_{f_i,j}(u,t_x)\right)}{w_l}\right\}^{-1}+\frac{k_j}{w_j}\left\{1+\frac{H_{f_i,j}\left(u|X_{f_i,j}(u,t_x)\right)}{w_j}\right\}^{-1}\right]du$$

For $t \leq t_x$, we assume that $X_{f_i,j}(u,t_x) = 0$, where t_x is the time that change in value of TDC. Then, the penetrance function can be obtained without considering the TDE of TDC such as

$$F_{f_ij}\left(t|X_{f_i,j}(t,t_x)\right) = \int_0^t h_{0,j}(u) \prod_{l\neq j}\left\{1+\frac{H_{0,l}(u)}{w_l}\right\}^{-k_l} \times$$
$$\left\{1+\frac{H_{0,j}(u)}{w_j}\right\}^{-k_j} \left\{1+\sum\nolimits_{l=1}^{J}\frac{H_{0,l}(u)}{w_l}\right\}^{-k_0} \times$$
$$\left[\frac{w_0}{w_j}\left\{1+\sum\nolimits_{l=1}^{J}\frac{H_{0,l}(u)}{w_l}\right\}^{-1}+\frac{k_j}{w_j}\left\{1+\frac{H_{0,j}(u)}{w_j}\right\}^{-1}\right]du$$

where $h_{0,j}(u)$ and $H_{0,j}(u)$ are the baseline hazard function and cumulative baseline hazard function, respectively.

In contrast, if $t > t_x$, we have $X_{f_i,j}(u,t_x) = 1$. Then, the penetrance at time t can be decomposed into the sum of two functions, where one without TDC/TDE ($t \leq t_x$) and the other with TDC/TDE ($t > t_x$) that the change in the effect of TDC is described by using the BS model. Then, the penetrance at time t with $t > t_x$ is expressed as

$$F_{f_ij}\left(t|\boldsymbol{X}_{f_i,j}, Z_{f_j}\right) = \int_0^{t_x} h_{0,j}(u) \prod_{l\neq j}\left\{1+\frac{H_{0,l}(u)}{w_l}\right\}^{-k_l} \times$$
$$\left\{1+\frac{H_{0,j}(u)}{w_j}\right\}^{-k_j} \left\{1+\sum\nolimits_{l=1}^{J}\frac{H_{0,l}(u)}{w_l}\right\}^{-k_0} \times$$
$$\left[\frac{w_0}{w_j}\left\{1+\sum\nolimits_{l=1}^{J}\frac{H_{0,l}(u)}{w_l}\right\}^{-1}+\frac{k_j}{w_j}\left\{1+\frac{H_{0,j}(u)}{w_j}\right\}^{-1}\right]du +$$

$$\int_{t_x}^{t} h_{0,j}(u)\exp\left\{\sum_{k=0}^{K+D}\beta_{j,k}B_{k,D}(u-t_x)\right\}du \times$$

$$\prod_{l\neq j}\left\{1+\frac{H_{0,l}(t_x)+\int_{t_x}^{u}h_{0,l}(s)\exp\left\{\sum_{k=0}^{K+D}\beta_{l,k}B_{k,D}(s-t_x)\right\}ds}{w_l}\right\}\times$$

$$\left\{1+\frac{H_{0,j}(t_x)+\int_{t_x}^{u}h_{0,j}(s)\exp\left\{\sum_{k=0}^{K+D}\beta_{j,k}B_{k,D}(s-t_x)\right\}ds}{w_j}\right\}^{-k_j}\times$$

$$\left\{1+\sum_{l=1}^{J}\frac{H_{0,l}(t_x)+\int_{t_x}^{u}h_{0,l}(s)\exp\left\{\sum_{k=0}^{K+D}\beta_{l,k}B_{k,D}(s-t_x)\right\}ds}{w_l}\right\}^{-k_0}\times$$

$$\left[\frac{w_0}{w_j}\left\{1+\sum_{l=1}^{J}\frac{H_{0,l}(t_x)+\int_{t_x}^{u}h_{0,l}(s)\exp\left\{\sum_{k=0}^{K+D}\beta_{l,k}B_{k,D}(s-t_x)\right\}ds}{w_l}\right\}^{-1}+\right.$$

$$\left.\frac{k_j}{w_j}\left\{1+\frac{H_{0,j}(t_x)+\int_{t_x}^{u}h_{0,j}(s)\exp\left\{\sum_{k=0}^{K+D}\beta_{j,k}B_{k,D}(s-t_x)\right\}ds}{w_j}\right\}^{-1}\right]du$$

where $\beta_{j,k}, k = 0, \dots, K+D$, are the regression coefficients for BS basis for event j.

3.5 Variance estimation of regression coefficients

Consider the vector of the parameters $\boldsymbol{\theta}$ consisting of parameters for baseline hazard functions, regression coefficients, parameters for TDEs, and frailty parameters. Let $\widehat{\boldsymbol{\theta}}$ be maximum likelihood estimates of the parameters $\boldsymbol{\theta}$**.** Then, the variance-covariance matrix of $\widehat{\boldsymbol{\theta}}$ is obtained using a robust sandwich variance estimator such as

$$\mathrm{Var}\left(\widehat{\boldsymbol{\theta}}\right) = I_o(\boldsymbol{\theta})^{-1}J(\boldsymbol{\theta})I_o(\boldsymbol{\theta})^{-1}$$

where $I_o(\boldsymbol{\theta})$ is the observed information matrix consisting of the second derivative of the log-likelihood function from Equation (3.6), and $J(\boldsymbol{\theta})$ is an expected information matrix. These can be obtained as

$$I_o\left(\widehat{\boldsymbol{\theta}}\right) = -\frac{\partial^2 \ell_C(\boldsymbol{\theta})}{\partial \boldsymbol{\theta}^T \partial \boldsymbol{\theta}}$$

$$J(\widehat{\boldsymbol{\theta}}) = \sum_{f} U_f^T(\boldsymbol{\theta}) U_f(\boldsymbol{\theta})$$

$$U_f(\widehat{\boldsymbol{\theta}}) = \frac{\partial \log L_f(\boldsymbol{\theta})}{\partial \boldsymbol{\theta}} - \frac{\partial \log A_f(\boldsymbol{\theta})}{\partial \boldsymbol{\theta}}$$

where $L_f(\boldsymbol{\theta})$ is the likelihood of family f from Equation (3.5), $A_f(\boldsymbol{\theta})$ is the ascertainment probability for family f from Equation (3.6), and $\ell_C(\boldsymbol{\theta})$ is the ascertainment corrected log-likelihood from Equation (3.7).

Therefore, the robust variance estimates of the estimated parameters $\widehat{\boldsymbol{\theta}}$ can be obtained by evaluating $I_o(\widehat{\boldsymbol{\theta}})$, $J(\widehat{\boldsymbol{\theta}})$ and $\widehat{\boldsymbol{\theta}}$. Then, the robust variance of the cause-specific penetrance function, $\mathrm{Var}\left(F_j(t|\widehat{\boldsymbol{\theta}})\right)$, is obtained by using Delta method, such as

$$\mathrm{Var}\left(F_j(t|\widehat{\boldsymbol{\theta}})\right) = D_{\boldsymbol{\theta}}^T(t)\mathrm{Var}(\widehat{\boldsymbol{\theta}})D_{\boldsymbol{\theta}}(t)$$

where $D_{\boldsymbol{\theta}}(t)$ is the vector of partial derivatives of $F_j(t|\widehat{\boldsymbol{\theta}})$ with respect to each parameter.

Chapter 4 Simulation study

The results in Chapter 3 are derived under the assumption of large samples. We thus conduct simulation studies in the chapter based on the correlated frailty competing risk model with a binary TDC. We evaluate the performance of different TDE functions (PE, CO, BS) of TDC in terms of the parameter estimates, penetrance estimates and AIC under different settings. Detailed objectives of this simulation study are provided in Section 4.1. Section 4.2 describes the simulation design, which includes 12 different simulation scenarios that are considered. The values of the parameters used in the simulation are presented in Section 4.3. In Section 4.4, the data generation process is described. The simulation evaluation criteria are provided in Section 4.5. Finally, the simulation results are summarized in Section 4.6.

4.1 Objectives

Our simulation study aims to evaluate our proposed modelling of the time-dependent effect of a binary time-dependent covariate using the BS and compare its performance with other parametric models (PE, CO) under different scenarios in terms of bias and precision of the parameter estimates in the correlated competing risks model, and the penetrance estimates of developing the event of interest with different intervention time points.

The two main objectives of the simulation study are:

1. To evaluate the performance of the correlated competing risks model with TDC using the BS model in terms of parameter estimates and penetrance estimates.

2. To evaluate the impact of misspecified TDE functions (PE, CO, BS) in the correlated frailty competing risk model on the following:

    i. Precision of the TDE function estimates at different time points

ii. Bias and precision of model parameter estimates and penetrance estimates

iii. Goodness of fit of the model

4.2 Simulation setting

The simulation study is designed to evaluate the performance of the proposed time-dependent effect model in the correlated frailty competing risks with a binary TDC introduced in Chapter 3 under the different settings depending on the shape of TDE, strength of correlation between competing events, and size of mutation effect.

We consider two shapes of TDE, where the first shape is a decreasing curve that exponentially decays over time converges to a certain value, and the second shape is a right-skewed curve that drastically increases right at the beginning and slowly decreases over time. The CO and BS models are used to depict those shapes. The effect staying above 0 indicates a positive effect, which dramatically increases the penetrance of the event of interest. In contrast, the negative TDEs only take values below 0, which gradually increase the penetrance of the event of interest. Then, we have a total of $2 \times 2 = 4$ different shapes of TDEs, denoted by CO+, CO-, BS+, BS-, arising from the CO and BS models, each with positive and negative TDE. These four shapes of TDE used in the simulations are graphically presented in Figure 4.1.

In addition, we examine how the strength of correlation (low and high) between competing events and the size of the mutation effect (low and high) would affect the performance of the proposed model in terms of parameter and penetrance estimation. A total of 12 simulation scenarios are considered, as presented in Table 4.1. The scenarios can be broken down into four groups by the shape of TDE: first three scenarios generated from the BS+, next three scenarios from the BS-, following three from the CO+, and last three from the CO-. Within each group, the first two scenarios are designed to evaluate the effect of correlation between competing events when the mutation effect is fixed, and

the last two scenarios are to evaluate the effect of mutation effect when the correlation is fixed.

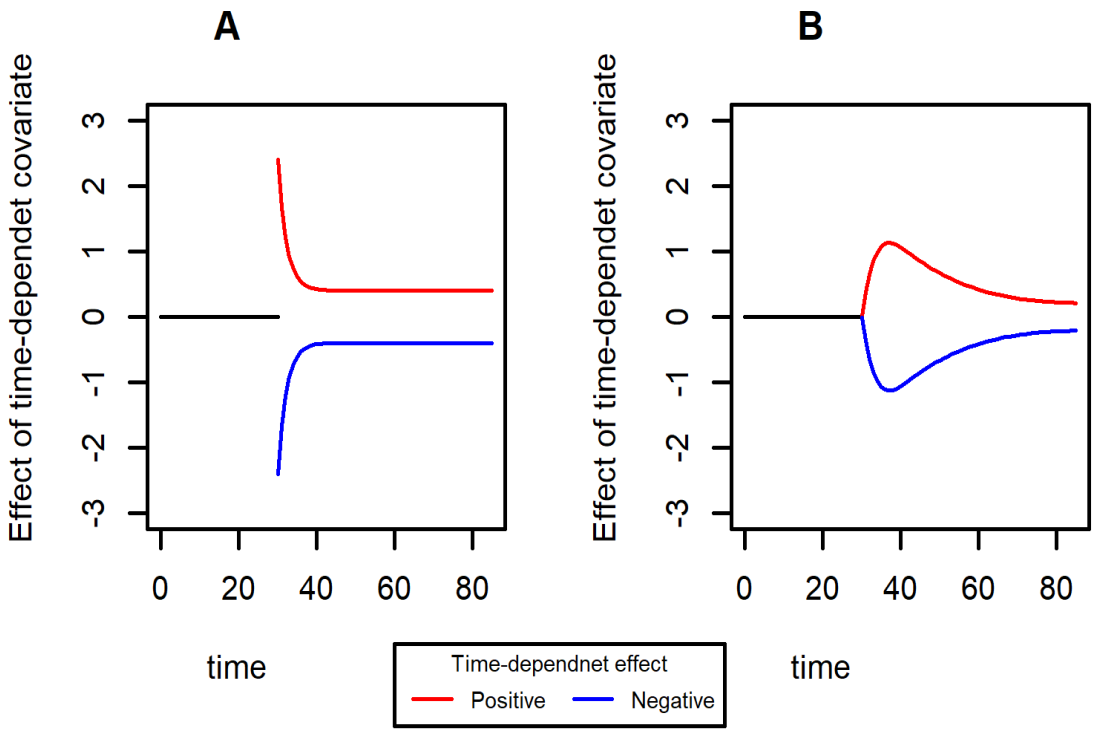

Figure 4.1: Two shapes of time-dependent effects under the Cox and Oakes (left panel) and B-spline (right panel) models. The intervention time is 30, and the black line indicates no effect before the intervention. The red and blue lines represent the time-dependent effects following the intervention time, with the red lines representing positive effects and the blue lines representing negative effects.

For the first objective, we evaluate the performance of our proposed model based on the BS in terms of parameter and penetrance estimates. We use the first 6 scenarios in which the data are generated from the BS models with different mutation effects and correlations between two competing events. For each scenario, the BS model is applied to fit the data and estimate the parameters in the model. Then, the penetrances at time 70 with intervention occurred at age 30, 40, 50 and 70 (no intervention) by plugging in the estimated parameters. The accuracy and precisions of those estimates are further evaluated via bias and coverage percentage of the confidence interval.

Table 4.1: Simulation study scenarios

Scenario	TDE Model	TDE	Mutation effect	Correlation between competing events
1	B-spline	Positive	$\gamma_{1g} = 1.50$	$\rho = 0.14$
2	B-spline	Positive	$\gamma_{1g} = 1.50$	$\rho = 0.51$
3	B-spline	Positive	$\gamma_{1g} = 2.25$	$\rho = 0.51$
4	B-spline	Negative	$\gamma_{1g} = 1.50$	$\rho = 0.14$
5	B-spline	Negative	$\gamma_{1g} = 1.50$	$\rho = 0.51$
6	B-spline	Negative	$\gamma_{1g} = 2.25$	$\rho = 0.51$
7	Cox and Oakes	Positive	$\gamma_{1g} = 1.50$	$\rho = 0.14$
8	Cox and Oakes	Positive	$\gamma_{1g} = 1.50$	$\rho = 0.51$
9	Cox and Oakes	Positive	$\gamma_{1g} = 2.25$	$\rho = 0.51$
10	Cox and Oakes	Negative	$\gamma_{1g} = 1.50$	$\rho = 0.14$
11	Cox and Oakes	Negative	$\gamma_{1g} = 1.50$	$\rho = 0.51$
12	Cox and Oakes	Negative	$\gamma_{1g} = 2.25$	$\rho = 0.51$

For the second objective, we evaluate the impact of different TDE models (PE, CO, BS) under different scenarios (see Table 4.1) by applying the PE, CO, two BS models to each scenario. The two BS models are denoted as BS2 and BS3 with degrees of 3, boundary knots $(0, 55)$ and having 2 interior knots and 3 interior knots, respectively, where the interior knots are obtained from the data based on 33% and 66% and 25%, 50% and 75% quantiles of the time difference between the surgery time and the last observed time, respectively. We first (1) assess the precision of the TDE function $g(t, X(t, t_s))$ estimates at different time points after an intervention under all scenarios 1-12, then (2) assess the bias and precision of parameter estimates and penetrance estimates under BS+,BS-, CO+, CO- when $\rho = 0.51$ and $\gamma = 2.25$, finally (3) compare the goodness of fit of the models via AICs.

For each scenario, 500 simulation replications are conducted, each with 500 families consisting of three generations of family members, for an average of 5835 individuals. The simulations of clustered correlated competing risk data with TDC are carried out by

modifying the **simfam** function from the R package **FamEvent** (Choi et al., 2021). The detailed data generation procedures are described in Section 4.4. Data generation and analyses were performed using R version 4.0.4 (R Core Team, 2021).

4.3 Selection of parameter values

For each simulation, the datasets are generated with two competing events based on the cause-specific hazard models with the true parameters obtained by fitting our model to the real data, presented in Tables 4.2 and 4.3, to mimic the data used in the application. For simplicity, the model includes one binary TDC and one binary TIC, representing intervention status and mutation status, respectively, defined as:

1. $X(t, t_s)$: Intervention status is considered as a binary TDC, such that the intervention status change at the time t_s that intervention occurred, i.e., $X(t, t_s) = I(t > t_s)$. Only the cause-specific hazard model for event 1 is affected by this variable.

2. G: mutation status is TIC, which takes value 1 for mutation carriers and 0 for non-carriers. The cause-specific hazard models for both events are affected by this variable.

Then, the cause-specific hazard functions for event 1 and event 2 are expressed as follows:

$$h_{f,1}\left(t\middle|X(t,t_s),G,Z_{f_1}\right) = h_{01}(t)Z_{f_1}\exp\left\{\gamma_{1g}G + g\left(t,X(t,t_s)\right)\right\}$$

$$h_{f,2}\left(t\middle|G,Z_{f_2}\right) = h_{02}(t)Z_{f_2}\exp\left\{\gamma_{2g}G\right\}$$

where $h_{01}(t) = \lambda_1\rho_1(\lambda_1 t)^{\rho_1-1}$ and $h_{02}(t) = \lambda_2\rho_2(\lambda_2 t)^{\rho_2-1}$ are Weibull baseline hazard functions, Z_{f_1} and Z_{f_2} are event specific frailties, γ_{1g} and γ_{2g} are the effect of mutation status for event 1 and 2, respectively. The correlated frailties are constructed by each

event-specific frailty $Z_{f_j} = \frac{k_0}{k_0+k_j} Y_{f_0} + Y_{f_j}$, where Y_{f_0} and Y_{f_j} are independently generated from gamma distributions.

For the TDE, the following $g\big(t, X(t, t_s)\big)$ functions for PE, CO and BS models are considered:

$$g\big(t, X(t, t_s)\big) = \begin{cases} 0 & \text{if } t \leq t_s \text{ (PE, CO, BS)} \\ \beta_s & \text{if } t > t_s \text{ (PE)} \\ \beta_s e^{-\eta(t-t_s)} + \eta_0 & \text{if } t > t_s \text{ (CO)} \\ \sum_{k=0}^{K+D} \beta_{s,k} B_{k,D}(t - t_s) & \text{if } t > t_s \text{ (BS)} \end{cases}$$

The numbers of parameters involved in TDE are different across the models. For the PE model, only one parameter, which is β_s, is involved in TDE, whereas the parameters involved in the CO model are $\{\beta_s, \eta, \eta_0\}$ and the number of parameters in the BS model depend on the polynomial degree D and the number of interior knots K, where the total number of parameters is $K + D + 1$ including the intercept. In addition, the BS model is constrained to be linear beyond the boundary knots (t_{min}, t_{max}).

The parameters used in the simulations are specified as:

1. Baseline hazard functions follow Weibull distributions with scale parameter: λ_1 and shape parameter ρ_1 for event 1, with λ_2 and ρ_2 for event 2. Their values are set as $\log(\lambda_1) = -4.83, \log(\rho_1) = 0.83, \log(\lambda_2) = -4.50, \log(\rho_2) = 1.07$.

2. Mutation effects are described by regression coefficient: γ_{1g} and γ_{2g} of gene mutation status for event 1 and event 2, respectively. The value of γ_{1g} is considered as 1.5 and 2.25 and that for γ_{2g} is set as 0.5.

3. Time-dependent effect of an intervention is described by β_s, η and η_0 for CO model, and $\beta_{s,k}, k = 0, \ldots, K + D$ for BS model. Referring to the shape in Figure 4.1, the true values of these parameters for CO are set as $\beta_s = 2, \log(\eta) = -0.79$ and $\eta_0 = 0.4$ for positive effect, and $\beta_s = -2, \log(\eta) = -0.79$ and $\eta_0 = -0.4$ for negative effect. For BS model, a degree of 3 and 2 interior knots at time

points 7.5 and 12.5 years with boundary knots at 0 and 55 years are considered. The true parameters related to the positive TDE are set as $\beta_{s,0} = 0.012, \beta_{s,1} = 1.024, \beta_{s,2} = 1.231, \beta_{s,3} = 0.338, \beta_{s,4} = 0.231$, and $\beta_{s,5} = 0.212$. Similarly, the values of the parameters related to negative TDE are considered as $\beta_{s,0} = -0.012, \beta_{s,1} = -1.024, \beta_{s,2} = -1.231, \beta_{s,3} = -0.338, \beta_{s,4} = -0.231$, and $\beta_{s,5} = -0.212$.

4. Frailty parameters: k_0, k_1 and k_2. The value of $\log(k_0)$ is considered to be -1.5 or 0.4, while the values of $\log(k_1)$ and $\log(k_2)$ are to be 0.4 and 0.6, respectively. These parameters influence the familial dependence and correlation between two competing events. With $\log(k_1)$ = 0.4 and $\log(k_2)$ = 0.6, $\log(k_0) = -1.5$ and 0.4 corresponds to $\tau = 0.12$ and 0.47, and $\rho = 0.14$ and 0.51.

4.4 Data generation

The family data are generated through three steps.

1. The family structure is constructed by selecting the number of siblings for each generation in the family and their current age, similar to the real data, while generating other variables, such as mutation status, proband, intervention time, and frailties for each event type.

2. The event times and event status are generated.

3. Ascertainment condition for the family is applied to mimic the population-based design of the family studies.

The detailed data generation procedures for each step are as follows:

Step 1: Family structure

1. We generate the family structure for each dataset consisting of three generations of family members with two fixed members for the first generation, two to five for the second generation, and zero to two in the third generation.

2. The current age of the proband, a_{f_p}, is generated by using the normal distribution with a mean of 55 and a standard deviation (SD) of 5. The current ages of other family members in the second generation $a_{f_i}, i = 1, \dots, n_f$, are generated from a normal distribution with mean 55 and SD 2.5. The current ages of the first generation are generated with the mean of $a_{f_p} + 20$ and SD of 2.5. The current ages third generation are generated with the mean age subtracted by 20 years from the minimum age of their parents and SD of 2.5.

3. For TDC status, we generate the intervention times, t_{s,f_i}, for all individuals from a normal distribution with a mean of 47.5 minus the minimum age of all individuals, which is 16, and SD of 2.5. Only those with current age larger than t_s undergo the intervention.

4. Two family-specific frailties, Z_{f_1} and Z_{f_2}, for two competing events are generated from three independent random variables, $Y_{f_0} \sim \text{Gamma}\left(k_0, \frac{1}{k_0}\right)$ and $Y_{f_j} \sim \text{Gamma}\left(k_j, \frac{1}{k_0+k_j}\right)$. Then Z_{f_j} are constructed as $Z_{f_j} = \left(\frac{k_0}{k_0+k_j}\right) Y_{f_0} + Y_{f_j}, j =$ 1 for event 1 and 2 for event 2,

5. For the mutation status, we first generate the proband's mutation status, G_{f_p}, under a dominant model with mutation allele frequency of 0.0021, conditional on their current age, event status, TDC time and frailties. Then, we generate the mutation status of the rest of the family members conditional on the proband's mutation status.

Step 2: Event time and event status

1. We generate the age of onset, t_{f_i}, by setting the survival function $P\left(T_{f_i} > t_{f_i} \middle| G_{f_i}, Z_{f_1}, Z_{f_2}, t_{s,f_i}\right) = u_{f_i}$, where $u_{f_i} \sim U[0,1]$ is generated from the uniform distribution, and solve for t_{f_i} from the equation. We assume the minimum age of onset is 16.

2. The event status among two competing events is determined by comparing the age of onset with the current age. If the age of onset is smaller than the current age, then the event status of a family member is selected by using a Bernoulli distribution with a probability of event 1 as $\frac{h_1\left(t \middle| X(t,t_s), G, Z_1\right)}{h_1\left(t \middle| X(t,t_s), G, Z_1\right) + h_2(t|G, Z_2)}$. Those with the current age larger than the age of onset are considered as censored.

Step 3: Ascertainment condition

1. To mimic the family-based study that families are recruited through affected individuals, called probands, we generate the families until the proband being affected (the proband's current age, a_{f_p}, larger than age of onset, t_{f_p}) and keep such family with affected proband into study.

4.5 Evaluation criteria

We evaluate via 500 simulations the performance of the parameter and penetrance estimators, the precision of the TDE functions (PE, CO, BS) at different time points, and compare the goodness of fit of models with different TDE functions. The parameter estimator is evaluated by bias (average estimate minus true parameter value), Empirical Standard Error (ESE), Average Standard Error (ASE) and Empirical Coverage Percentage (ECP). Similarly, the penetrance estimators are evaluated by Percentage Bias (PBIAS), ASE, ESE and ECP. In addition, the precision of the TDE functions (PE, CO,

BS) is measured by the Mean Squared Error (MSE) at different time points, and the goodness of fit of the model is measured by the AIC.

In the following, we describe how the evaluation criteria are obtained in our simulations.

The bias measures accuracy of the parameter estimator. It is obtained as the difference between the average parameter estimate over the $B = 500$ simulations, $\overline{\hat{\beta}} = \sum_{i=1}^{B} \hat{\beta}_i / B$, and the true value, β, as bias $= \overline{\hat{\beta}} - \beta$. Instead of relying on the difference, the percentage bias is used for the penetrance estimator, which is estimated as PBIAS $= \left(\overline{\hat{\beta}} - \beta\right)/\beta \times 100$.

The accuracy of an estimator from simulations can be obtained from the ESE, obtained by the sample standard deviation of estimates from all simulations, and it can be expressed as ESE $= \sqrt{\{1/(B-1)\}\sum_{i=1}^{B}\left(\hat{\beta}_i - \overline{\hat{\beta}}\right)^2}$. The average of the standard errors is obtained from all simulations as ASE = $\sum_{i=1}^{B} SE(\hat{\beta}_i)/B$. If the ASE is correctly estimated, it should be closed to the ESE (Burton et al., 2006).

The ECP is the percentage of times the 95% confidence interval, $\hat{\beta}_i \pm 1.96 \times SE(\hat{\beta}_i)$, include the true value, β, for $i = 1, \ldots, B$. The ECP should be close to 95%, where 5% of confidence intervals do not contain the true value. Over-coverage occurs when the coverage percentages are above 95%, which suggests that the results are too conservative since simulations would accept the null hypothesis that is actually false. This leads to a loss of power with too many type II errors. In contrast, the under-coverage occurs when the coverage percentages are lower than 95%, which is not acceptable according to Burton et al. (2006). One possible criterion of the acceptability of the coverage is that the acceptability of the coverage, that can be obtained as $SE(p) = \sqrt{p(1-p)/B}$, where p is the nominal coverage percentage (Burton et al., 2006). With $B = 500$ simulations, the acceptable range for the ECP with 95% confidence is between 93.1% and 96.9%.

The MSE evaluates the precision of the TDE functions. Given $g\big(t, X(t, t_s)\big)$ and $\hat{g}\big(t, X(t, t_s)\big)$ are the true and estimated TDE of TDC for a specific time point $t - t_s$, where t is the observed time and t_s is the time that change in intervention status occurs, the MSE is calculated as $\text{MSE} = \sum_{i=1}^{B} \left\{ \hat{g}\left(t, X_{f_i}(t, t_s)\right) - g\left(t, X_{f_i}(t, t_s)\right) \right\}^2 / B$, which is the sum of squared bias and variance at time t.

The AIC allows the comparisons between the competing risks models with different TDE functions by explaining how well the model fits the data and is obtained as $\text{AIC} = -2\log(L) + 2 \times v$, where L denotes the likelihood value of the fitted model and v is the number of parameters involved in the model. We obtain the AICs from each simulation and report the average AIC over the B simulations, that is $\overline{\text{AIC}} = \sum_{i=1}^{B} \text{AIC}_i \, / B$, where AIC_i is the AIC obtained from simulation i and the best performed model would have the smallest value of AIC.

4.6 Simulation results

We first summarize the simulation results of our evaluation of the performance of the parameter and penetrance estimators of the BS models with the positive and negative effects of TDE in Tables 4.2 and 4.3. Then the results for the impact of misspecified TDE functions on parameter and penetrance estimates are summarized in Tables 4.4 to 4.7 and Tables 4.8 to 4.11, respectively. The bias and precision of the corresponding penetrance estimators are graphically visualized in Figures 4.2 to 4.4. Tables 4.12 and 4.13 present the precision of the TDE functions (PE, CO, BS) at different time points after intervention (5, 10, 15, 20 years) under the misspecified TDE function. The performance of the correlated competing risks models with different TDE functions in terms of the average AIC is summarized in Table 4.14.

4.6.1 Correlated competing risk model with B-spline function

Table 4.2 summarizes the results of the simulation studies for the parameter estimates under the true BS model with bias, ESE, ASE and ECP, which corresponds to the first six scenarios presented in Table 4.1. Regardless of the sign of TDE, the biases of the parameter estimates related to the baseline hazard function, mutation status and frailties for two events are negligible. However, since there are not many treated individuals with time after intervention larger than 30, two parameter estimates $\beta_{s,4}$ and $\beta_{s,5}$ related to the BS model are biased. As the B-spline is a linear combination of the basis functions with its effects, such biases would affect the accuracy of estimate for the hazard function and thus bias the penetrance estimates. The ASEs and ESEs of the parameter estimates for the baseline and mutation status for two events agree with each other for all the simulation scenarios. However, the ASEs of the frailty parameters and parameters related to the TDE tend to be larger than corresponding ESEs. As a result, the ECPs higher than the nominal 95% and are not mostly within the acceptable range between 93.1% and 96.9%, indicating that the confidence intervals are conservative. Based on six different scenarios, the confidence interval for the parameters related to frailties (k_0, k_1, k_2) and TDE functions ($\beta_{s,0}, \beta_{s,1}, \beta_{s,2}, \beta_{s,3}, \beta_{s,4}, \beta_{s,5}$) are ranged from 92.6% to 99.0% and 93.6% to 99.8%, respectively.

The simulation results of the penetrance estimates at time 70 with intervention occurred at age 30, 40, 50 and 70 (no intervention) under the cubic BS model with two interior knots (7.5, 12.5), boundary knots $(0, 55)$, and positive/negative effects are presented in Table 4.3. The biases of the penetrance estimates with the BS model are mostly negligible, with PBIAS less than 3.4%. The ASEs and ESEs of the penetrance estimates for mutation noncarrier for the BS models mostly agreed well except with low event correlation. However, the ASEs of the penetrance estimates for mutation carriers are higher than the ESEs, and the ASEs increased as the event correlation decreased. In addition, most of the ASEs and ESEs of penetrance estimates for mutation carriers are larger than the ASEs and ESEs obtained for mutation noncarriers. This caused the ECPs to be above 95% nominal level, indicating the confidence intervals are conservative. Since the acceptable range of the ECP is between 93.1% and 96.9%, about 43.8% of the

results for the mutation carriers obtained the ECPs greater than 96.9%. This leads to a loss of power which produces a large number of errors of omission.

Table 4.2: Accuracy and precision of parameter estimates from the correlated frailty competing risks model with time-dependent effect modelled with cubic B-spline with 2 interior knots (7.5, 12.5) under BS+ and BS- scenarios with different correlations between competing events ($\rho = 0.14$ and 0.51) and different mutation effects ($\gamma_{1g} = 1.5$ and 2.25) based on 500 simulations each with 500 families.

BS Positive time-dependent effects (BS+)															
	True	$\rho = 0.14, \gamma_{1g} = 1.5$				True	$\rho = 0.51, \gamma_{1g} = 1.5$				True	$\rho = 0.51, \gamma_{1g} = 2.25$			
	value	Bias	ESE	ASE	ECP	value	Bias	ESE	ASE	ECP	value	Bias	ESE	ASE	ECP
$\log(\lambda_1)$	-4.83	-0.02	0.04	0.08	98.8	-4.83	-0.02	0.04	0.08	99.0	-4.83	-0.01	0.04	0.06	99.2
$\log(\rho_1)$	0.83	-0.01	0.03	0.04	98.0	0.83	-0.01	0.03	0.05	98.4	0.83	-0.00	0.02	0.03	98.6
$\log(\lambda_2)$	-4.50	0.00	0.03	0.04	97.2	-4.50	0.00	0.03	0.03	96.6	-4.50	-0.00	0.03	0.04	97.8
$\log(\rho_2)$	1.07	0.00	0.03	0.04	96.6	1.07	0.00	0.03	0.04	96.2	1.07	-0.01	0.03	0.04	96.8
γ_{1g}	1.5	0.00	0.07	0.07	96.0	1.5	0.00	0.06	0.08	96.2	2.25	0.01	0.07	0.07	96.4
γ_{2g}	0.50	0.00	0.08	0.11	96.8	0.50	0.00	0.08	0.11	96.2	0.50	0.00	0.10	0.10	95.4
$\log(k_0)$	0.40	-0.08	0.62	1.85	92.6	0.40	0.01	0.31	0.51	97.0	0.40	0.00	0.34	0.45	96.8
$\log(k_1)$	0.60	0.02	0.20	0.49	98.2	0.60	-0.03	0.43	0.56	97.2	0.60	-0.05	0.43	0.55	96.8
$\log(k_2)$	0.10	0.02	0.25	0.60	96.0	0.10	-0.02	0.55	3.26	98.2	0.10	-0.02	0.57	0.77	98.4
$\beta_{s,0}$	0.01	0.07	0.19	0.25	95.0	0.01	-0.01	0.19	0.38	97.4	0.01	-0.02	0.17	0.20	97.0
$\beta_{s,1}$	1.02	0.01	0.16	0.27	96.8	1.02	0.03	0.16	0.31	97.4	1.02	0.02	0.16	0.22	97.4
$\beta_{s,2}$	1.23	0.02	0.13	0.24	98.0	1.23	0.01	0.12	0.29	98.4	1.23	-0.01	0.13	0.20	98.0
$\beta_{s,3}$	0.34	0.07	0.36	0.78	97.4	0.34	0.07	0.30	1.03	98.6	0.34	0.08	0.34	0.68	98.8
$\beta_{s,4}$	0.23	-0.11	0.82	2.50	97.6	0.23	0.08	0.72	3.27	99.2	0.23	-0.11	0.87	2.24	99.0
$\beta_{s,5}$	0.21	0.34	1.28	6.55	98.8	0.21	0.29	1.11	8.84	99.8	0.21	0.19	1.41	6.60	99.8
BS Negative time-dependent effects (BS-)															
	True	$\rho = 0.14, \gamma_{1g} = 1.5$				True	$\rho = 0.51, \gamma_{1g} = 1.5$				True	$\rho = 0.51, \gamma_{1g} = 2.25$			
	value	Bias	ESE	ASE	ECP	value	Bias	ESE	ASE	ECP	value	Bias	ESE	ASE	ECP
$\log(\lambda_1)$	-4.83	-0.01	0.05	0.07	97.2	-4.83	-0.01	0.05	0.07	98.8	-4.83	-0.01	0.05	0.06	97.4
$\log(\rho_1)$	0.83	-0.01	0.03	0.04	96.0	0.83	-0.01	0.03	0.04	98.2	0.83	-0.01	0.02	0.03	96.4
$\log(\lambda_2)$	-4.50	0.00	0.03	0.04	96.0	-4.50	0.00	0.03	0.03	94.4	-4.50	0.00	0.03	0.03	95.8
$\log(\rho_2)$	1.07	0.00	0.03	0.03	96.6	1.07	0.00	0.03	0.03	94.8	1.07	0.00	0.03	0.03	97.0
γ_{1g}	1.5	0.01	0.08	0.09	96.2	1.5	0.00	0.08	0.09	97.6	2.25	0.01	0.07	0.09	97.8
γ_{2g}	0.50	0.00	0.08	0.09	96.4	0.50	0.00	0.08	0.08	96.4	0.50	0.01	0.08	0.09	95.8
$\log(k_0)$	0.40	-0.15	0.58	2.34	94.6	0.40	0.04	0.34	0.48	96.8	0.40	0.02	0.36	0.48	96.8
$\log(k_1)$	0.60	0.07	0.24	0.39	96.8	0.60	0.04	0.49	0.64	99.0	0.60	-0.01	0.48	0.82	97.0
$\log(k_2)$	0.10	0.03	0.21	0.39	96.4	0.10	-0.11	0.80	1.17	95.4	0.10	-0.06	0.67	0.95	97.0
$\beta_{s,0}$	-0.01	0.03	0.27	0.29	93.6	-0.01	-0.04	0.24	0.31	97.6	-0.01	-0.06	0.23	0.30	95.4
$\beta_{s,1}$	-1.02	-0.02	0.36	0.46	96.0	-1.02	0.04	0.33	0.56	96.4	-1.02	0.04	0.30	0.47	95.8
$\beta_{s,2}$	-1.23	0.00	0.26	0.41	97.6	-1.23	0.00	0.26	0.59	98.6	-1.23	-0.01	0.22	0.43	99.0
$\beta_{s,3}$	-0.34	0.07	0.53	1.11	98.2	-0.34	0.09	0.45	1.77	98.8	-0.34	0.07	0.43	1.27	99.4
$\beta_{s,4}$	-0.23	-0.10	0.92	2.90	99.6	-0.23	-0.08	0.84	4.88	99.6	-0.23	-0.07	0.93	3.60	99.2
$\beta_{s,5}$	-0.21	0.20	1.36	6.88	99.8	-0.21	0.28	1.40	11.05	99.8	-0.21	0.20	1.48	8.79	99.4

For each scenario, the mean bias, empirical standard error (ESE), average standard error (ASE), and estimated 95% coverage percentage (ECP) are obtained from 500 simulations each with 500 families. λ_j and ρ_j are the baseline hazard parameters for event $j = 1$ and 2; γ_{1g} and γ_{2g} are the regression coefficients of the time-invariant covariate for event 1 and 2, respectively; k_0, k_1 and k_2 are the frailty parameters; $\beta_{s,k}, k = 0, \dots, K + D$, describes the TDE, where K is the number of interior knots and D is the degree of the B-spline basis function; The permanent exposure (PE), Cox and Oakes (CO) and B-spline (BS) are the TDE functions.

Table 4.3: Empirical penetrance estimates at time 70 from the correlated frailty competing risks model with time-dependent effect (TDE) modelled with cubic B-spline with 2 interior knots (7.5, 12.5) under BS+ and BS- scenarios with different correlations between competing events ($\rho = 0.14$ and 0.51) and different mutation effects ($\gamma_{1g} = 1.5$ and 2.25).

BS Positive time-dependent effects (BS+)															
	True	$\rho = 0.14, \gamma_{1g} = 1.5$				True	$\rho = 0.51, \gamma_{1g} = 1.5$				True	$\rho = 0.51, \gamma_{1g} = 2.25$			
	value	PBIAS	ESE	ASE	ECP	value	PBIAS	ESE	ASE	ECP	value	PBIAS	ESE	ASE	ECP
Mutation status $G = 0$															
$F_1(70\|t_s = \infty)$	0.119	-1.15	0.008	0.014	98.0	0.119	-1.41	0.008	0.013	97.8	0.119	-0.76	0.008	0.010	98.2
$F_1(70\|t_s$=30)	0.200	2.07	0.018	0.026	98.8	0.202	1.65	0.017	0.027	98.0	0.202	1.37	0.019	0.026	97.0
$F_1(70\|t_s$=40)	0.213	1.07	0.013	0.018	97.4	0.215	0.63	0.013	0.016	96.0	0.215	0.62	0.013	0.014	97.2
$F_1(70\|t_s$=50)	0.209	0.68	0.012	0.019	96.8	0.211	0.14	0.012	0.016	96.8	0.211	0.19	0.011	0.012	96.0
Mutation status $G = 1$															
$F_1(70\|t_s = \infty)$	0.380	-0.67	0.019	0.033	97.6	0.390	-0.89	0.018	0.029	98.4	0.612	-0.13	0.021	0.024	97.4
$F_1(70\|t_s$=30)	0.547	1.33	0.029	0.045	97.2	0.569	1.05	0.026	0.045	98.4	0.783	0.47	0.022	0.033	98.2
$F_1(70\|t_s$=40)	0.561	0.81	0.022	0.033	95.6	0.584	0.49	0.020	0.026	97.0	0.788	0.30	0.016	0.019	97.2
$F_1(70\|t_s$=50)	0.546	0.55	0.020	0.033	96.8	0.567	0.17	0.019	0.026	96.8	0.768	0.17	0.016	0.017	96.2
BS Negative time-dependent effects (BS-)															
	True	$\rho = 0.14, \gamma_{1g} = 1.5$				True	$\rho = 0.51, \gamma_{1g} = 1.5$				True	$\rho = 0.51, \gamma_{1g} = 2.25$			
	value	PBIAS	ESE	ASE	ECP	value	PBIAS	ESE	ASE	ECP	value	PBIAS	ESE	ASE	ECP
Mutation status $G = 0$															
$F_1(70\|t_s = \infty)$	0.119	-0.26	0.010	0.013	97.8	0.119	-1.05	0.010	0.012	97.8	0.119	-0.57	0.009	0.011	97.4
$F_1(70\|t_s$=30)	0.074	2.84	0.011	0.014	98.2	0.074	3.37	0.011	0.015	98.6	0.074	2.53	0.009	0.015	97.6
$F_1(70\|t_s$=40)	0.072	1.50	0.006	0.008	96.8	0.072	1.31	0.007	0.008	96.6	0.072	0.93	0.006	0.007	98.4
$F_1(70\|t_s$=50)	0.079	0.80	0.006	0.008	97.4	0.079	0.13	0.006	0.008	97.2	0.079	0.10	0.006	0.007	97.0
Mutation status $G = 1$															
$F_1(70\|t_s = \infty)$	0.380	0.38	0.022	0.030	96.6	0.390	-0.52	0.021	0.027	98.4	0.612	0.25	0.024	0.028	95.8
$F_1(70\|t_s$=30)	0.260	2.62	0.028	0.038	97.6	0.263	2.73	0.028	0.040	97.8	0.454	1.95	0.034	0.054	98.2
$F_1(70\|t_s$=40)	0.25	1.75	0.016	0.021	97.0	0.260	1.26	0.016	0.020	96.8	0.452	1.25	0.021	0.027	96.2
$F_1(70\|t_s$=50)	0.280	1.21	0.016	0.021	97.4	0.285	0.34	0.015	0.020	98.0	0.487	0.74	0.021	0.024	96.0

ESE represents empirical standard error, ASE average standard error, ECP empirical coverage percentage

$F_1(70|t_s = \infty)$ denotes the cause-specific penetrance by age 70 for event 1 without intervention.

4.6.2 Impact of misspecified time-dependent effect functions

We evaluate the impact of different TDE models (PE, CO, BS) under the CO and BS models, high correlation between competing events, high mutation effect and positive/negative TDE, which correspond to scenarios 3, 6, 9, and 12. Section 4.6.2.1 summarizes the precision of TDE function estimates at different time points after an intervention. Section 4.6.2.2 evaluates the bias and precision of parameter estimates under different settings. Section 4.6.2.3 assesses the penetrance estimates under different settings. Section 4.6.2.3 compares the goodness of fit of the models through average AICs.

4.6.2.1 Precision of the time-dependent effect function

Tables 4.4 and 4.5 summarize the changes in the MSE of the TDE functions (PE, CO, BS) across the different time points after intervention (5, 10, 15, 20 years) under misspecified TDE functions. Under the CO+, the CO model has the smallest MSEs, followed by the BS models and PE model as expected. However, the PE model sometimes yields the smallest MSEs of the TDE at 5 years after the intervention with the dataset generated under the CO-. Although the MSEs of the BS models are larger than those of the CO models, they are close to the MSEs of the CO model, which shows how flexible the BS model is. With datasets generated under both BS+ and BS-, the BS models provide the smallest MSEs as expected, while the MSEs of PE and CO models are similar. However, the MSEs of the BS models got larger as the time after intervention increased, and eventually, the MSEs of the PE or CO models became smaller than those of the BS models.

Table 4.4: Mean Squared Error (MSE) of the time-dependent effect (TDE) functions at $5, 10, 15$ and 20 years after intervention under CO+ and CO- scenarios based on 500 simulations each with 500 families.

		CO Positive TDE (CO+)				CO Negative TDE (CO-)			
	t^*	PE	CO	BS2	BS3	PE	CO	BS2	BS3
$\rho = 0.14$	5	0.306	**0.006**	0.007	0.017	**0.008**	0.012	0.017	0.017
$\gamma_{1g} = 1.5$	10	0.542	**0.005**	0.009	0.011	0.048	**0.008**	0.015	0.016
	15	0.570	**0.006**	0.012	0.010	0.056	**0.009**	0.014	0.015
	20	0.573	**0.006**	0.013	0.015	0.056	**0.009**	0.018	0.021
$\rho = 0.51$	5	0.237	**0.006**	0.007	0.010	**0.010**	0.012	0.017	0.017
$\gamma_{1g} = 1.5$	10	0.447	**0.006**	0.008	0.014	0.053	**0.009**	0.016	0.017
	15	0.473	**0.007**	0.013	0.014	0.062	**0.010**	0.015	0.018
	20	0.475	**0.007**	0.015	0.016	0.063	**0.010**	0.018	0.020
$\rho = 0.51$	5	0.308	**0.006**	0.007	0.010	**0.009**	**0.009**	0.014	0.015
$\gamma_{1g} = 2.25$	10	0.544	**0.005**	0.008	0.015	0.058	**0.006**	0.012	0.015
	15	0.573	**0.006**	0.012	0.011	0.067	**0.006**	0.011	0.013
	20	0.576	**0.006**	0.015	0.015	0.068	**0.007**	0.013	0.015

PE stands for the permanent exposure model, CO for the Cox and Oakes model, BS2 for cubic B-spline with 2 interior knots, BS3 for cubic B-spline with 3 interior knots. ρ is the correlation between two competing events; γ_{1g} is the regression coefficient for the time-invariant covariate for event 1. t^*represents the time since the intervention.

Table 4.5: Mean Squared Error (MSE) of the time-dependent effect (TDE) functions at $5, 10, 15$ and 20 years after intervention under BS+ and BS- scenarios based on 500 simulations each with 500 families.

		BS Positive TDE (BS+)					BS Negative TDE (BS-)				
	t^*	PE	CO	TBS2	BS2	BS3	PE	CO	TBS2	BS2	BS3
$\rho = 0.14$	5	0.153	0.149	0.026	0.027	**0.023**	0.255	0.224	**0.043**	0.046	0.062
$\gamma_{1g} = 1.5$	10	0.153	0.158	0.028	**0.027**	0.032	0.253	0.227	**0.056**	0.057	**0.056**
	15	0.153	0.167	0.131	0.134	**0.130**	0.253	0.236	0.184	0.183	**0.169**
	20	**0.153**	0.177	0.295	0.292	0.288	0.253	**0.248**	0.368	0.371	0.392
$\rho = 0.51$	5	0.156	0.156	0.026	0.026	**0.023**	0.249	0.230	**0.050**	0.051	0.062
$\gamma_{1g} = 1.5$	10	0.156	0.164	**0.028**	**0.028**	0.032	0.247	0.236	0.056	**0.055**	0.059
	15	0.156	0.174	0.134	0.134	**0.129**	0.247	0.246	0.190	0.193	**0.186**
	20	**0.156**	0.184	0.293	0.293	0.284	**0.247**	0.257	0.378	0.386	0.393
$\rho = 0.51$	5	0.179	0.180	0.029	0.028	**0.025**	0.234	0.207	0.045	**0.044**	0.055
$\gamma_{1g} = 2.25$	10	0.179	0.177	0.033	**0.031**	0.036	0.232	0.214	**0.050**	**0.050**	0.054
	15	0.179	0.175	0.139	0.139	**0.131**	0.232	0.224	0.176	0.174	**0.170**
	20	0.179	**0.174**	0.302	0.299	0.289	**0.232**	0.235	0.358	0.357	0.369

The permanent exposure (PE) and Cox and Oakes (CO) are the TDE functions; The two cubic B-spline (BS) models, BS2 and BS3, have 2 interior knots and 3 interior knots, respectively, and TBS2 denotes the true BS model with a degree of 3 and 2 interior knots. ρ is the correlation between the frailties of two competing events j; γ_{1g} is the regression coefficient for the time-invariant covariate for event 1. t^*represents the time since the intervention.

4.6.2.2 Estimates of Model parameters

Tables 4.6 and 4.7 summarize the parameter estimates related to the baseline hazard functions, mutation status and frailties obtained by fitting the misspecified TDE models to each dataset generated under the CO+ and CO-, corresponding to scenarios 9 and 12 in Table 4.1, respectively. For all scenarios, the ASEs and ESEs of the baseline hazard function and mutation status parameters agree with each other, but the ASEs of the frailties are larger than the ESEs. Under the CO model, the ECPs for the CO and BS models are close to or above the acceptable upper range of 96.9%, leading to loss of power by including the estimates in the confidence interval that are not supposed to be. For the PE model under the CO+, the model obtained the bad ECPs below 90% most time. However, in the PE model under the CO-, the ECPs were close to 95% on average. All the TDE functions except the PE model under the CO+ worked well in terms of parameter bias, which biases are negligible. Under scenario 9, where the true model is CO+, the PE model obtained biased parameter estimates leading to the ECPs of the parameters being below 95%.

Similarly, Tables 4.8 and 4.9 are the results obtained under the BS+ and BS- with the same settings corresponding to scenarios 3 and 6. In contrast to the dataset generated under the CO+ and CO-, all the TDE functions under the BS+ and BS- performed well in terms of bias and ECP, where the biases are negligible, and the ECPs were above 95% most times. Under the negative TDE, the ECPs tended to be close to 95% compared to the ECPs under the positive TDE. Hence, in terms of bias and precision of such parameters, the parameters related to baseline hazards, TIC, and frailties are accurately estimated for the CO and BS models, even under misspecification work relatively well. However, fitting the PE model that assumes the constant TDE led to biased parameter estimates.

Few convergence issues occurred while fitting the CO model to data generated under both CO and BS models. For each simulation, the parameter estimates are obtained by maximizing the log-likelihood function using the **optim** function in R with Nelder and Mead method (Nelder and Mead, 1965). The CO model did not converge 2.4% and 1.6% of times of the total simulations under the CO model and BS model, respectively. These

issues were caused due to the degeneration of the Nelder-Mead simplex. The PE and BS model did not have any convergence issues for all the simulation scenarios. 12 out of 1500 simulations did not converge for the CO model with data under the positive CO model. Similarly, 7 out of 1500 simulations did not converge for the CO model fitting data under the positive BS model. In contrast, only 1 out of 1500 simulations did not converge for data under the negative BS model.

Table 4.6: Empirical parameter estimates from misspecified TDE models under CO+ scenario with $\rho = 0.51$ and $\gamma_{1g} = 2.25$ based on 500 simulations each with 500 families.

CO Positive time-dependent effects (CO+) with $\rho = 0.51, \gamma_{1g} = 2.25$									
	True Model (CO)					Misspecified Model (PE)			
	True value	Bias	ESE	ASE	ECP	Bias	ESE	ASE	ECP
$\log(\lambda_1)$	-4.83	0.01	0.04	0.06	97.8	-0.19	0.07	0.06	15.0
$\log(\rho_1)$	0.83	0.00	0.02	0.03	98.6	-0.07	0.03	0.03	31.6
$\log(\lambda_2)$	-4.50	0.00	0.03	0.03	98.4	-0.00	0.04	0.04	94.6
$\log(\rho_2)$	1.07	0.01	0.03	0.04	97.8	0.01	0.04	0.04	93.2
γ_{1g}	2.25	0.01	0.06	0.07	97.8	0.16	0.09	0.08	49.4
γ_{2g}	0.50	0.01	0.09	0.10	96.5	0.01	0.11	0.12	92.4
$\log(k_0)$	0.40	0.01	0.31	0.42	97.2	-0.19	0.33	0.61	94.6
$\log(k_1)$	0.60	-0.01	0.38	0.53	97.4	-0.58	0.53	0.59	80.8
$\log(k_2)$	0.10	0.01	0.50	0.69	98.4	0.18	0.48	0.70	96.4
β_s	2.00	-0.03	0.09	0.13	98.2	-	-	-	-
$\log(\eta)$	-0.79	0.10	0.18	0.27	99.6	-	-	-	-
η_0	0.40	0.00	0.08	0.13	99.2	-	-	-	-
	Misspecified Model (BS2)					Misspecified Model (BS3)			
	True value	Bias	ESE	ASE	ECP	Bias	ESE	ASE	ECP
$\log(\lambda_1)$	-4.83	0.01	0.04	0.06	97.8	0.01	0.04	0.06	98.0
$\log(\rho_1)$	0.83	0.00	0.03	0.03	98.0	0.00	0.03	0.03	97.8
$\log(\lambda_2)$	-4.50	-0.00	0.03	0.04	96.4	-0.00	0.03	0.04	95.8
$\log(\rho_2)$	1.07	-0.00	0.03	0.04	96.4	-0.00	0.03	0.04	97.2
γ_{1g}	2.25	0.00	0.07	0.07	95.8	0.00	0.07	0.07	96.6
γ_{2g}	0.50	0.00	0.10	0.10	95.2	0.00	0.10	0.10	95.8
$\log(k_0)$	0.40	0.00	0.37	0.47	95.6	0.01	0.37	0.49	96.0
$\log(k_1)$	0.60	-0.02	0.43	0.55	95.8	-0.04	0.43	0.82	95.8
$\log(k_2)$	0.10	-0.08	0.67	0.74	96.8	-0.07	0.69	0.88	96.2

ESE represents empirical standard error, ASE average standard error, ECP estimated coverage percentage. λ_j and ρ_j are the baseline hazard parameters for event $j = 1$ and 2; γ_{1g} and γ_{2g} are the regression coefficients of the time-invariant covariate for event 1 and 2, respectively; k_0, k_1 and k_2 are the frailty parameters.PE stands for permanent exposure model, CO for Cox and Oakes model, BS2 for cubic B-spline with 2 interior knots and BS3 for cubic spline with 3 interior knots.

Table 4.7: Empirical parameter estimates from misspecified TDE models under CO- scenario with $\rho = 0.51$ and $\gamma_{1g} = 2.25$ based on 500 simulations each with 500 families.

CO Negative time-dependent effects (CO-) with $\rho = 0.51, \gamma_{1g} = 2.25$									
	True Model (CO)					Misspecified Model (PE)			
	True value	Bias	ESE	ASE	ECP	Bias	ESE	ASE	ECP
$\log(\lambda_1)$	-4.83	-0.01	0.04	0.06	98.8	0.02	0.05	0.06	93.0
$\log(\rho_1)$	0.83	-0.00	0.02	0.03	98.8	0.01	0.03	0.03	94.2
$\log(\lambda_2)$	-4.50	0.00	0.03	0.03	97.4	0.00	0.03	0.03	97.4
$\log(\rho_2)$	1.07	-0.00	0.03	0.03	95.6	-0.00	0.03	0.03	95.8
γ_{1g}	2.25	0.01	0.07	0.09	96.8	0.00	0.08	0.09	96.6
γ_{2g}	0.50	0.00	0.08	0.09	97.4	0.02	0.09	0.10	96.4
$\log(k_0)$	0.40	0.02	0.30	0.41	98.6	0.00	0.43	0.61	96.6
$\log(k_1)$	0.60	0.04	0.39	0.55	98.8	0.10	0.49	0.72	96.2
$\log(k_2)$	0.10	0.05	0.51	0.74	96.4	0.05	0.59	0.99	96.6
β_s	-2.00	-0.02	0.44	0.69	97.6	-	-	-	-
$\log(\eta)$	-0.79	0.01	0.29	0.48	96.0	-	-	-	-
η_0	-0.40	0.00	0.08	0.14	99.0	-	-	-	-
	Misspecified Model (BS2)					Misspecified Model (BS3)			
	True value	Bias	ESE	ASE	ECP	Bias	ESE	ASE	ECP
$\log(\lambda_1)$	-4.83	-0.01	0.04	0.06	98.2	-0.01	0.04	0.07	98.8
$\log(\rho_1)$	0.83	-0.01	0.02	0.03	98.6	-0.01	0.02	0.04	98.6
$\log(\lambda_2)$	-4.50	-0.00	0.03	0.03	97.2	-0.00	0.03	0.03	97.8
$\log(\rho_2)$	1.07	-0.00	0.03	0.03	94.0	-0.00	0.03	0.03	94.6
γ_{1g}	2.25	0.00	0.08	0.09	96.4	0.00	0.08	0.09	96.6
γ_{2g}	0.50	0.00	0.09	0.09	95.8	0.00	0.09	0.10	95.8
$\log(k_0)$	0.40	0.01	0.35	0.41	97.4	0.02	0.33	0.51	97.2
$\log(k_1)$	0.60	-0.02	0.49	0.54	97.0	-0.03	0.49	0.64	98.4
$\log(k_2)$	0.10	-0.05	0.63	0.84	96.8	-0.07	0.76	2.40	95.8

ESE represents empirical standard error, ASE average standard error, ECP estimated coverage percentage. λ_j and ρ_j are the baseline hazard parameters for event $j = 1$ and 2; γ_{1g} and γ_{2g} are the regression coefficients of the time-invariant covariate for event 1 and 2, respectively; k_0, k_1 and k_2 are the frailty parameters.PE stands for permanent exposure model, CO for Cox and Oakes model, BS2 for cubic B-spline with 2 interior knots and BS3 for cubic spline with 3 interior knots.

Table 4.8: Empirical parameter estimates from misspecified TDE models under BS+ scenario with $\rho = 0.51$ and $\gamma_{1g} = 2.25$ based on 500 simulations each with 500 families.

BS Positive time-dependent effects (BS+) with $\rho = 0.51, \gamma_{1g} = 2.25$													
	True Model (TBS2)					Misspecified Model (PE)				Misspecified Model (CO)			
	True value	Bias	ESE	ASE	ECP	Bias	ESE	ASE	ECP	Bias	ESE	ASE	ECP
$\log(\lambda_1)$	-4.83	-0.01	0.04	0.06	99.2	0.02	0.05	0.04	96.2	0.02	0.04	0.06	96.0
$\log(\rho_1)$	0.83	-0.00	0.02	0.03	98.6	0.01	0.03	0.02	96.4	0.01	0.02	0.04	96.4
$\log(\lambda_2)$	-4.50	-0.00	0.03	0.04	97.8	-0.01	0.04	0.03	98.0	-0.01	0.03	0.04	96.8
$\log(\rho_2)$	1.07	-0.01	0.03	0.04	96.8	-0.01	0.04	0.03	97.0	-0.01	0.03	0.04	96.4
γ_{1g}	2.25	0.01	0.07	0.07	96.4	-0.02	0.07	0.06	95.6	-0.02	0.06	0.08	96.4
γ_{2g}	0.50	0.00	0.10	0.10	95.4	-0.01	0.11	0.09	95.2	-0.01	0.09	0.11	95.4
$\log(k_0)$	0.40	0.00	0.34	0.45	96.8	0.01	0.57	0.29	97.0	0.04	0.29	0.59	95.4
$\log(k_1)$	0.60	-0.05	0.43	0.55	96.8	0.01	0.56	0.32	98.0	-0.05	0.32	0.67	97.6
$\log(k_2)$	0.10	-0.02	0.57	0.77	98.4	-0.01	1.21	0.33	99.6	-0.10	0.33	1.13	98.0
$\beta_{s,0}$	0.01	-0.02	0.17	0.20	97.0	-	-	-	-	-	-	-	-
$\beta_{s,1}$	1.02	0.02	0.16	0.22	97.4	-	-	-	-	-	-	-	-
$\beta_{s,2}$	1.23	-0.01	0.13	0.20	98.0	-	-	-	-	-	-	-	-
$\beta_{s,3}$	0.34	0.08	0.34	0.68	98.8	-	-	-	-	-	-	-	-
$\beta_{s,4}$	0.23	-0.11	0.87	2.24	99.0	-	-	-	-	-	-	-	-
$\beta_{s,5}$	0.21	0.19	1.41	6.60	99.8	-	-	-	-	-	-	-	-
	Misspecified Model (BS2)					Misspecified Model (BS3)							
	True value	Bias	ESE	ASE	ECP	Bias	ESE	ASE	ECP				
$\log(\lambda_1)$	-4.83	-0.01	0.04	0.06	99.0	-0.01	0.04	0.07	99.2				
$\log(\rho_1)$	0.83	-0.00	0.02	0.03	98.8	-0.01	0.02	0.04	98.6				
$\log(\lambda_2)$	-4.50	-0.00	0.03	0.04	97.4	-0.00	0.03	0.04	97.4				
$\log(\rho_2)$	1.07	-0.01	0.03	0.04	96.8	-0.00	0.03	0.04	97.8				
γ_{1g}	2.25	0.01	0.06	0.07	97.0	0.01	0.06	0.07	97.8				
γ_{2g}	0.50	0.00	0.09	0.10	95.0	0.00	0.10	0.10	94.4				
$\log(k_0)$	0.40	0.00	0.34	0.42	97.2	0.00	0.35	0.51	95.2				
$\log(k_1)$	0.60	-0.05	0.45	0.55	96.2	-0.05	0.45	0.56	97.4				
$\log(k_2)$	0.10	-0.02	0.58	0.77	98.4	-0.02	0.56	0.76	98.0				

ESE represents empirical standard error, ASE average standard error, ECP estimated coverage percentage. λ_j and ρ_j are the baseline hazard parameters for event $j = 1$ and 2; γ_{1g} and γ_{2g} are the regression coefficients of the time-invariant covariate for event 1 and 2, respectively; k_0, k_1 and k_2 are the frailty parameters.PE stands for permanent exposure model, CO for Cox and Oakes model, TBS2 for true cubic B-spline with 2 interior knots, BS2 for cubic B-spline with 2 interior knots and BS3 for cubic spline with 3 interior knots.

Table 4.9: Empirical parameter estimates from misspecified TDE models under BS- scenario with $\rho = 0.51$ and $\gamma_{1g} = 2.25$ based on 500 simulations each with 500 families.

BS Negative time-dependent effects (BS-) with $\rho = 0.51, \gamma_{1g} = 2.25$													
	True Model (TBS2)					Misspecified Model (PE)				Misspecified Model (CO)			
	True value	Bias	ESE	ASE	ECP	Bias	ESE	ASE	ECP	Bias	ESE	ASE	ECP
$\log(\lambda_1)$	-4.83	-0.01	0.05	0.06	97.4	-0.01	0.06	0.05	97.8	0.00	0.05	0.07	96.6
$\log(\rho_1)$	0.83	-0.01	0.02	0.03	96.4	0.00	0.03	0.03	96.6	0.00	0.03	0.03	96.4
$\log(\lambda_2)$	-4.50	0.00	0.03	0.03	95.8	0.00	0.04	0.03	96.0	0.00	0.03	0.03	95.8
$\log(\rho_2)$	1.07	0.00	0.03	0.03	97.0	0.00	0.03	0.03	97.8	0.00	0.03	0.03	95.8
γ_{1g}	2.25	0.01	0.07	0.09	97.8	0.02	0.09	0.08	96.4	0.02	0.08	0.09	94.8
γ_{2g}	0.50	0.01	0.08	0.09	95.8	0.03	0.11	0.08	97.6	0.02	0.09	0.10	96.4
$\log(k_0)$	0.40	0.02	0.36	0.48	96.8	0.02	0.69	0.38	96.6	0.00	0.42	0.54	95.8
$\log(k_1)$	0.60	-0.01	0.48	0.82	97.0	0.09	0.73	0.41	97.8	0.01	0.61	0.84	96.4
$\log(k_2)$	0.10	-0.06	0.67	0.95	97.0	0.06	1.36	0.53	98.8	-0.02	0.74	0.95	96.2
$\beta_{s,0}$	-0.01	-0.06	0.23	0.30	95.4	-	-	-	-	-	-	-	-
$\beta_{s,1}$	-1.02	0.04	0.30	0.47	95.8	-	-	-	-	-	-	-	-
$\beta_{s,2}$	-1.23	-0.01	0.22	0.43	99.0	-	-	-	-	-	-	-	-
$\beta_{s,3}$	-0.34	0.07	0.43	1.27	99.4	-	-	-	-	-	-	-	-
$\beta_{s,4}$	-0.23	-0.07	0.93	3.60	99.2	-	-	-	-	-	-	-	-
$\beta_{s,5}$	-0.21	0.20	1.48	8.79	99.4	-	-	-	-	-	-	-	-
	Misspecified Model (BS2)					Misspecified Model (BS3)							
	True value	Bias	ESE	ASE	ECP	Bias	ESE	ASE	ECP				
$\log(\lambda_1)$	-4.83	-0.01	0.05	0.06	98.0	-0.01	0.05	0.06	98.4				
$\log(\rho_1)$	0.83	-0.01	0.02	0.03	97.4	-0.01	0.02	0.03	98.0				
$\log(\lambda_2)$	-4.50	0.00	0.03	0.03	95.8	0.00	0.03	0.03	96.4				
$\log(\rho_2)$	1.07	0.00	0.03	0.03	96.8	0.00	0.03	0.03	96.6				
γ_{1g}	2.25	0.01	0.08	0.09	97.2	0.01	0.08	0.09	96.4				
γ_{2g}	0.50	0.01	0.08	0.09	96.8	0.01	0.08	0.10	96.8				
$\log(k_0)$	0.40	0.02	0.35	0.41	96.2	0.02	0.36	0.57	96.2				
$\log(k_1)$	0.60	-0.01	0.51	0.58	97.6	-0.02	0.52	0.65	97.4				
$\log(k_2)$	0.10	-0.05	0.64	0.93	97.0	-0.06	0.69	1.15	96.8				

ESE represents empirical standard error, ASE average standard error, ECP estimated coverage percentage. λ_j and ρ_j are the baseline hazard parameters for event $j = 1$ and 2; γ_{1g} and γ_{2g} are the regression coefficients of the time-invariant covariate for event 1 and 2, respectively; k_0, k_1 and k_2 are the frailty parameters.PE stands for permanent exposure model, CO for Cox and Oakes model, TBS2 for true cubic B-spline with 2 interior knots, BS2 for cubic B-spline with 2 interior knots and BS3 for cubic spline with 3 interior knots.

4.6.2.3 Cause-specific penetrance

The robustness of the TDE function is evaluated under the misspecified TDE functions with high frailty correlation and large mutation effect. Tables 4.10 and 4.11 summarize the results under the CO+ and CO- and Tables 4.12 and 4.13 under the BS+ and BS-, respectively. Under the CO+, both the CO and BS models worked well in terms of the PBIAS and ECPs, where the PBIASs are negligible. In addition, since the ASEs tend to be larger than the ESEs, the corresponding confidence intervals are conservative, leading the ECPs to be higher than 95%. However, most ECPs lie within the acceptable range from 93.1% to 96.9%. In addition, there are some minor differences between the ESEs and ASEs of the CO and BS models for mutation non-carriers than for mutation carriers. In contrast, the PE model yields biased penetrance estimates, where the PBIASs of the PE model ranged from -21.1 to 37.83%. Still, the ESEs and ASEs of the PE model agree with each other leading to the ECPs below 90%, which indicates that the penetrance estimates of the PE model are biased. The results were similar to the CO-, but the PE model yields less biased parameter estimates, where the PBIASs of the PE model ranged from -14.19 to 3.54%. Under the CO+, the average ratio between the ASEs of the mutation carriers and non-carriers under all models equals 1.87. Similarly, such average ratios under all models are 2.57, 1.71 and 2.76 under the CO-, BS+ and BS-, respectively.

Similarly, under both the BS+ and BS-, only the BS models worked well in terms of the PBIAS, whereas the PBIAs of the PE and CO models were not close to zero. Although the ASEs were also larger than the ESEs for all the TDE models, the ECPs of the BS models lay within the acceptable range most time, but the ECPs of the PE and CO models were not close to 0.95. As the CO+ and CO-, there were larger differences between the ASEs and ESEs for mutation carriers than the non-carriers.

Figures 4.2 to 4.5 visualize the bias and precision of the penetrance estimates at time 70. Four different intervention times occurred at age 30, 40, 50 and without intervention under the true model and misspecified models based on 500 simulations for each TDE model. Each small circle indicates the bias of the penetrance estimates at time 70 with different intervention times, and the error bars are mean penetrance estimates $\pm$ 1.96 $\times$ ASE. The black, green-, blue-, red- and magenta-coloured lines represent the

PE, CO, BS2, BS3 and true BS model with 2 interior knots, respectively. The results corresponding to mutation non-carriers are presented on the left side of the figures and that of mutation carriers on the right side. Regardless of the level of TDE, all the graphs provide similar results, which demonstrate that the biases of the BS models were close to zero under both true and misspecified TDE models. However, the PE and CO models were not robust to the misspecified TDE models. The figures also demonstrate that mutation carriers have wider 95% confidence intervals (CI) than mutation non-carriers because they have larger ASEs than non-carriers.

4.6.2.4 AIC

To illustrate the efficiency of the BS model, the average AICs are compared for the correlated frailty competing risk models with different TDE functions in Table 4.14. With datasets generated under the CO model, the CO model obtained the smallest AIC, which indicates that the CO model is the best fit for the data. However, with low correlation and low mutation effect, the BS models obtained the smallest average AIC even though the CO model is the true model. In contrast, with datasets generated under the cubic BS model with two interior knots, the BS models provided the smallest average AIC. Although other BS models provided the smallest AIC, this demonstrates the flexibility of the BS model with a different number of interior knots and degrees and robustness to the misspecified TDE model.

Table 4.10: Empirical penetrance estimates at time 70 for mutation carriers and non-carriers with different intervention times from the correlated frailty competing risks models with different time-dependent effect (TDE) functions when data generated under the CO model with a positive TDE, high correlation between competing events ($\rho = 0.51$) and high mutation effect ($\gamma_{1g} = 2.25$); Results are based on 500 simulations, each with 500 families.

Data generated from CO positive TDE (CO+) with $\rho = 0.51, \gamma_{1g} = 2.25$									
	True Model (CO)					Misspecified Model (PE)			
	True value	PBIAS	ESE	ASE	ECP	PBIAS	ESE	ASE	ECP
Mutation status $G = 0$									
$F_1(70\|t_s = \infty)$	0.119	1.86	0.007	0.010	99.0	-21.10	0.009	0.008	18.8
$F_1(70\|t_s$=30)	0.180	1.16	0.011	0.014	98.0	37.83	0.015	0.014	0.6
$F_1(70\|t_s$=40)	0.184	0.61	0.010	0.012	97.2	24.30	0.014	0.013	8.6
$F_1(70\|t_s$=50)	0.183	0.07	0.009	0.010	96.7	7.15	0.012	0.012	77.0
Mutation status $G = 1$									
$F_1(70\|t_s = \infty)$	0.612	0.24	0.018	0.024	97.6	-7.01	0.025	0.025	55.02
$F_1(70\|t_s$=30)	0.746	0.57	0.018	0.027	99.0	12.47	0.018	0.017	1.6
$F_1(70\|t_s$=40)	0.748	0.38	0.016	0.020	98.6	8.37	0.018	0.018	9.6
$F_1(70\|t_s$=50)	0.736	0.25	0.015	0.017	98.2	3.61	0.018	0.018	63.4
	Misspecified Model (BS2)					Misspecified Model (BS3)			
	True value	PBIAS	ESE	ASE	ECP	PBIAS	ESE	ASE	ECP
Mutation status $G = 0$									
$F_1(70\|t_s = \infty)$	0.119	1.65	0.008	0.011	97.8	1.33	0.008	0.010	98.0
$F_1(70\|t_s$=30)	0.180	1.82	0.019	0.027	98.2	1.29	0.020	0.026	97.0
$F_1(70\|t_s$=40)	0.184	0.20	0.011	0.013	96.4	0.22	0.011	0.012	96.4
$F_1(70\|t_s$=50)	0.183	0.13	0.010	0.012	96.6	-0.04	0.010	0.011	96.8
Mutation status $G = 1$									
$F_1(70\|t_s = \infty)$	0.612	1.01	0.020	0.025	97.2	0.83	0.021	0.005	95.6
$F_1(70\|t_s$=30)	0.746	0.52	0.028	0.039	97.8	0.29	0.028	0.038	97.4
$F_1(70\|t_s$=40)	0.748	0.20	0.017	0.021	97.6	0.15	0.017	0.020	98.0
$F_1(70\|t_s$=50)	0.736	0.25	0.016	0.019	97.0	0.12	0.016	0.018	96.8

For each scenario, the mean bias, empirical standard error (ESE), average standard error (ASE), and estimated 95% coverage percentage(ECP) are obtained from 500 simulations each with 500 families. $F_1(70|t_s = \infty)$ denotes the cause-specific penetrance for event 1 without intervention.

Table 4.11: Empirical penetrance estimates at time 70 for mutation carriers and non-carriers with different intervention times from the correlated frailty competing risks models with different time-dependent effect (TDE) functions when data generated under the CO model with a negative TDE, high correlation between competing events ($\rho = 0.51$) and high mutation effect ($\gamma_{1g} = 2.25$); Results are based on 500 simulations, each with 500 families.

Data generated from CO negative TDE (CO-) with $\rho = 0.51, \gamma_{1g} = 2.25$									
	True Model (CO)					Misspecified Model (PE)			
	True value	PBIAS	ESE	ASE	ECP	PBIAS	ESE	ASE	ECP
Mutation status $G = 0$									
$F_1(70\|t_s = \infty)$	0.119	-0.36	0.008	0.011	97.6	3.54	0.010	0.011	94.8
$F_1(70\|t_s$=30)	0.082	-0.11	0.006	0.009	97.2	-14.19	0.006	0.006	53.6
$F_1(70\|t_s$=40)	0.085	-0.18	0.006	0.008	97.4	-8.85	0.006	0.006	78.8
$F_1(70\|t_s$=50)	0.091	-0.27	0.006	0.007	97.2	-2.04	0.006	0.007	95.8
Mutation status $G = 1$									
$F_1(70\|t_s = \infty)$	0.612	0.30	0.020	0.027	98.2	2.20	0.023	0.026	93.6
$F_1(70\|t_s$=30)	0.489	0.43	0.022	0.029	97.4	-9.06	0.022	0.022	48.6
$F_1(70\|t_s$=40)	0.502	0.42	0.020	0.024	97.4	-4.89	0.020	0.021	79.4
$F_1(70\|t_s$=50)	0.527	0.39	0.018	0.021	96.6	-0.39	0.019	0.021	95.4
	Misspecified Model (BS2)					Misspecified Model (BS3)			
	True value	PBIAS	ESE	ASE	ECP	PBIAS	ESE	ASE	ECP
Mutation status $G = 0$									
$F_1(70\|t_s = \infty)$	0.119	-0.67	0.009	0.011	97.2	-0.84	0.009	0.013	96.6
$F_1(70\|t_s$=30)	0.082	1.87	0.009	0.015	98.6	2.32	0.009	0.015	99.0
$F_1(70\|t_s$=40)	0.085	0.71	0.006	0.008	96.8	0.78	0.006	0.009	98.2
$F_1(70\|t_s$=50)	0.091	0.04	0.007	0.008	96.8	0.04	0.007	0.009	97.6
Mutation status $G = 1$									
$F_1(70\|t_s = \infty)$	0.612	-0.41	0.023	0.027	97.0	-0.49	0.024	0.033	97.0
$F_1(70\|t_s$=30)	0.489	0.86	0.030	0.050	98.6	1.12	0.031	0.051	98.8
$F_1(70\|t_s$=40)	0.502	0.33	0.021	0.025	97.8	0.38	0.021	0.028	97.2
$F_1(70\|t_s$=50)	0.527	-0.05	0.021	0.023	96.4	-0.06	0.021	0.027	96.8

For each scenario, the mean bias, empirical standard error (ESE), average standard error (ASE), and estimated 95% coverage percentage (ECP) are obtained from 500 simulations each with 500 families. $F_1(70|t_s = \infty)$ denotes the cause-specific penetrance for event 1 without intervention.

Table 4.12: Empirical penetrance estimates at time 70 for mutation carriers and non-carriers with different intervention times from the correlated frailty competing risks models with different time-dependent effect (TDE) functions when data generated under the BS model with a positive TDE, high correlation between competing events ($\rho = 0.51$) and high mutation effect ($\gamma_{1g} = 2.25$); Results are based on 500 simulations, each with 500 families.

BS Positive time-dependent effects (BS+) with $\rho = 0.51, \gamma_{1g} = 2.25$													
	True Model (TBS2)					Misspecified Model (PE)				Misspecified Model (CO)			
	True value	PBIAS	ESE	ASE	ECP	PBIAS	ESE	ASE	ECP	PBIAS	ESE	ASE	ECP
Mutation status $G = 0$													
$F_1(70\|t_s = \infty)$	0.119	-0.76	0.008	0.010	98.2	3.02	0.007	0.009	97.4	2.49	0.008	0.011	97.8
$F_1(70\|t_s$=30)	0.202	1.37	0.019	0.026	97.0	20.58	0.012	0.014	10.2	21.87	0.019	0.024	27.3
$F_1(70\|t_s$=40)	0.215	0.62	0.013	0.014	97.2	6.77	0.011	0.013	80.6	7.22	0.013	0.016	83.0
$F_1(70\|t_s$=50)	0.211	0.19	0.011	0.012	96.0	-2.92	0.010	0.012	94.8	-3.06	0.010	0.011	92.8
Mutation status $G = 1$													
$F_1(70\|t_s = \infty)$	0.612	-0.13	0.021	0.024	97.4	0.80	0.019	0.024	97.2	0.56	0.022	0.026	95.8
$F_1(70\|t_s$=30)	0.783	0.47	0.022	0.033	98.2	4.71	0.014	0.019	38.4	4.93	0.018	0.027	49.9
$F_1(70\|t_s$=40)	0.788	0.30	0.016	0.019	97.2	1.20	0.014	0.018	93.0	1.29	0.016	0.021	92.2
$F_1(70\|t_s$=50)	0.768	0.17	0.016	0.017	96.2	-1.18	0.014	0.019	96.4	-1.22	0.016	0.018	95.4
	Misspecified Model (BS2)					Misspecified Model (BS3)							
	True value	PBIAS	ESE	ASE	ECP	PBIAS	ESE	ASE	ECP				
Mutation status $G = 0$													
$F_1(70\|t_s = \infty)$	0.119	-0.81	0.008	0.010	98.0	-1.11	0.007	0.011	98.0				
$F_1(70\|t_s$=30)	0.202	1.59	0.018	0.029	98.4	1.40	0.018	0.031	98.0				
$F_1(70\|t_s$=40)	0.215	0.73	0.012	0.016	97.6	0.75	0.012	0.015	98.0				
$F_1(70\|t_s$=50)	0.211	0.22	0.011	0.014	95.4	0.26	0.011	0.014	98.0				
Mutation status $G = 1$													
$F_1(70\|t_s = \infty)$	0.612	-0.17	0.021	0.024	97.6	-0.33	0.020	0.027	97.6				
$F_1(70\|t_s$=30)	0.783	0.54	0.022	0.037	98.8	0.48	0.022	0.038	99.2				
$F_1(70\|t_s$=40)	0.788	0.33	0.016	0.020	96.6	0.32	0.016	0.021	96.4				
$F_1(70\|t_s$=50)	0.768	0.17	0.016	0.018	95.8	0.16	0.015	0.019	96.6				

For each scenario, the mean bias, empirical standard error (ESE), average standard error (ASE), and estimated 95% coverage percentage (ECP) are obtained from 500 simulations each with 500 families. $F_1(70|t_s = \infty)$ denotes the cause-specific penetrance for event 1 without intervention.

Table 4.13: Empirical penetrance estimates at time 70 for mutation carriers and non-carriers with different intervention times from the correlated frailty competing risks models with different time-dependent effect (TDE) functions when data generated under the BS model with a negative TDE, high correlation between competing events ($\rho = 0.51$) and high mutation effect ($\gamma_{1g} = 2.25$); Results are based on 500 simulations, each with 500 families.

BS Negative time-dependent effects (BS-) with $\rho = 0.51, \gamma_{1g} = 2.25$													
	True Model (TBS2)					Misspecified Model (PE)				Misspecified Model (CO)			
	True value	PBIAS	ESE	ASE	ECP	PBIAS	ESE	ASE	ECP	PBIAS	ESE	ASE	ECP
Mutation status $G = 0$													
$F_1(70\|t_s = \infty)$	0.119	-0.57	0.009	0.011	97.4	-0.29	0.009	0.011	98.0	0.51	0.010	0.012	96.6
$F_1(70\|t_s$=30)	0.074	2.53	0.009	0.015	97.6	-16.72	0.005	0.006	40.0	-15.49	0.007	0.012	60.8
$F_1(70\|t_s$=40)	0.072	0.93	0.006	0.007	98.4	-3.58	0.005	0.006	93.6	-3.28	0.006	0.008	94.2
$F_1(70\|t_s$=50)	0.079	0.10	0.006	0.007	97.0	3.69	0.006	0.007	96.4	3.64	0.006	0.007	94.4
Mutation status $G = 1$													
$F_1(70\|t_s = \infty)$	0.612	0.25	0.024	0.028	95.8	1.10	0.021	0.028	97.2	1.02	0.025	0.031	95.4
$F_1(70\|t_s$=30)	0.454	1.95	0.034	0.054	98.2	-9.51	0.021	0.022	48.0	-9.22	0.027	0.048	64.2
$F_1(70\|t_s$=40)	0.452	1.25	0.021	0.027	96.2	-0.41	0.019	0.021	97.0	-0.81	0.021	0.028	96.0
$F_1(70\|t_s$=50)	0.487	0.74	0.021	0.024	96.0	3.78	0.018	0.022	88.8	3.21	0.020	0.023	88.6
	Misspecified Model (BS2)					Misspecified Model (BS3)							
	True value	PBIAS	ESE	ASE	ECP	PBIAS	ESE	ASE	ECP				
Mutation status $G = 0$													
$F_1(70\|t_s = \infty)$	0.119	-0.48	0.009	0.011	97.4	-0.44	0.009	0.012	97.0				
$F_1(70\|t_s$=30)	0.074	2.84	0.009	0.014	98.2	2.34	0.010	0.016	97.6				
$F_1(70\|t_s$=40)	0.072	0.92	0.006	0.007	98.4	1.17	0.006	0.007	97.8				
$F_1(70\|t_s$=50)	0.079	0.12	0.006	0.007	97.0	0.25	0.006	0.007	96.8				
Mutation status $G = 1$													
$F_1(70\|t_s = \infty)$	0.612	0.33	0.024	0.027	96.4	0.18	0.025	0.030	97.0				
$F_1(70\|t_s$=30)	0.454	2.19	0.033	0.052	98.4	1.67	0.036	0.057	98.8				
$F_1(70\|t_s$=40)	0.452	1.28	0.021	0.023	96.0	1.23	0.022	0.025	95.4				
$F_1(70\|t_s$=50)	0.487	0.80	0.020	0.022	94.6	0.67	0.021	0.024	93.4				

For each scenario, the mean bias, empirical standard error (ESE), average standard error (ASE), and estimated 95% coverage percentage (ECP) are obtained from 500 simulations each with 500 families. $F_1(70|t_s = \infty)$ denotes the cause-specific penetrance for event 1 without intervention.

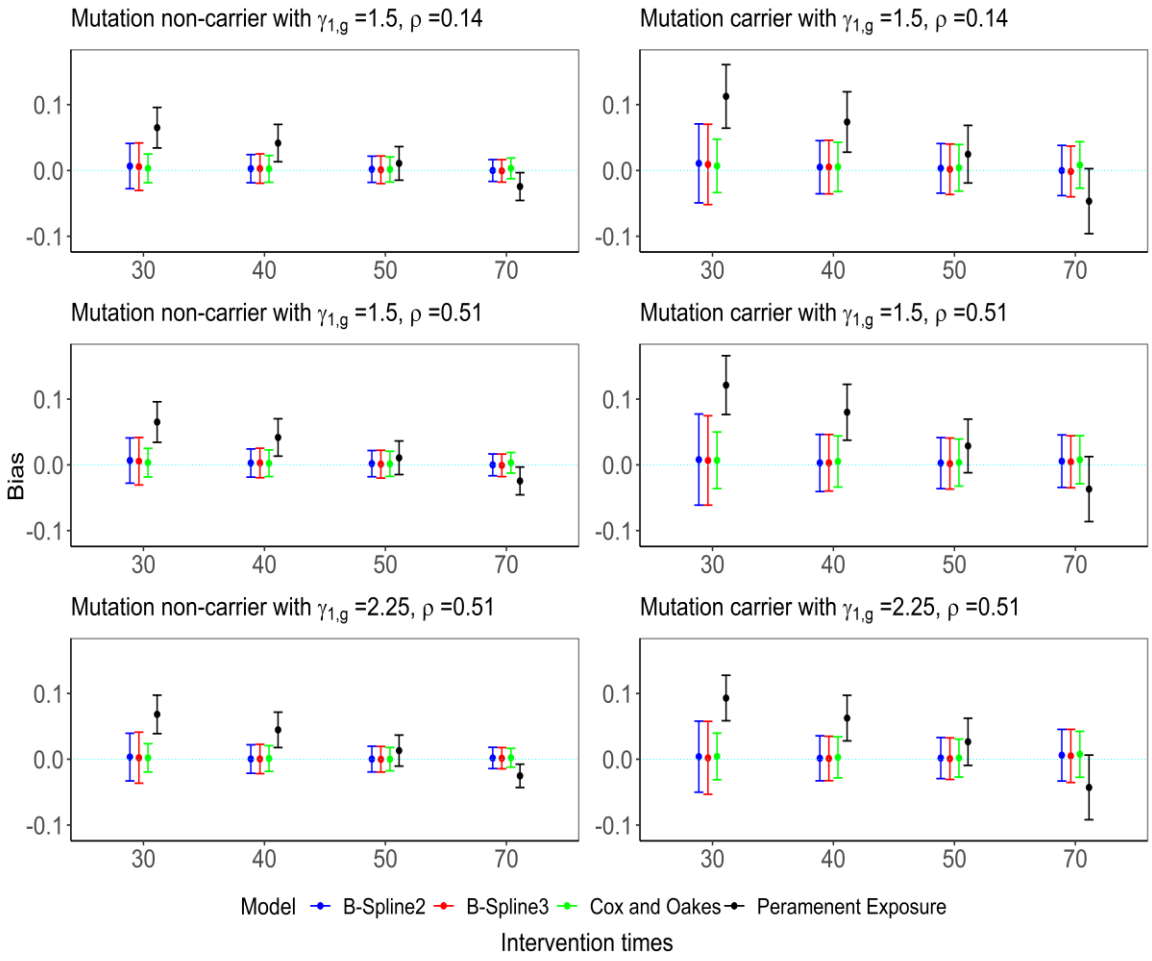

Figure 4.2: Bias and 95% confidence interval of the bias for penetrance estimations at time 70 for mutation carriers and non-carriers with different intervention times (30, 40, 50, and 70 (no intervention)) estimated from the correlated frailty competing risks models with different time-dependent effect (TDE) functions. Data generated under the CO model with a positive TDE, a high correlation between competing events ($\rho = 0.51$) a high mutation ($\gamma_{1g} = 2.25$). Results are based on 500 simulations each with 500 families.

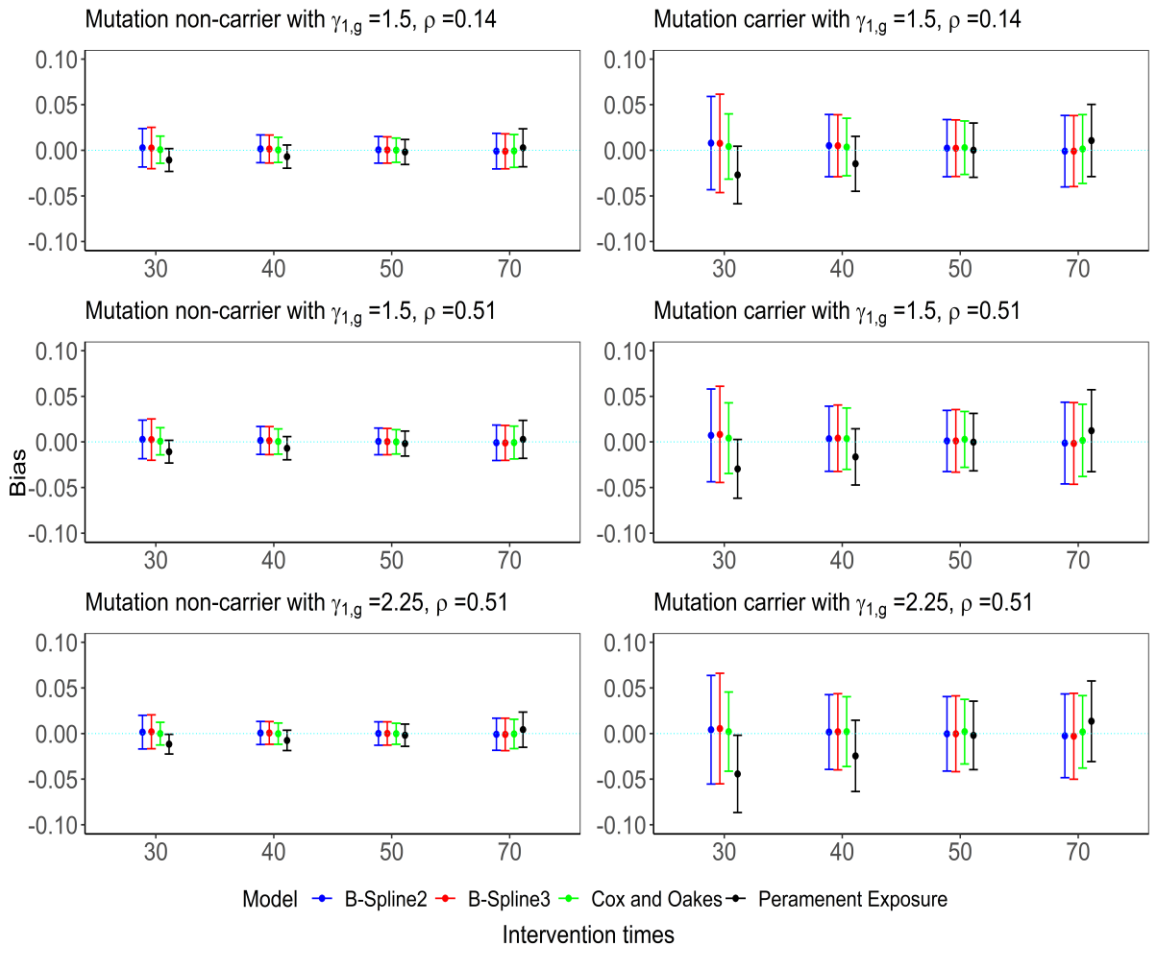

Figure 4.3: Bias and 95% confidence interval of the bias for penetrance estimations at time 70 for mutation carriers and non-carriers with different intervention times (30, 40, 50, and 70 (no intervention)) estimated from the correlated frailty competing risks models with different time-dependent effect (TDE) functions. Data generated under the CO model with a negative TDE, a high correlation between competing events ($\rho = 0.51$) a high mutation ($\gamma_{1g} = 2.25$). Results are based on 500 simulations each with 500 families.

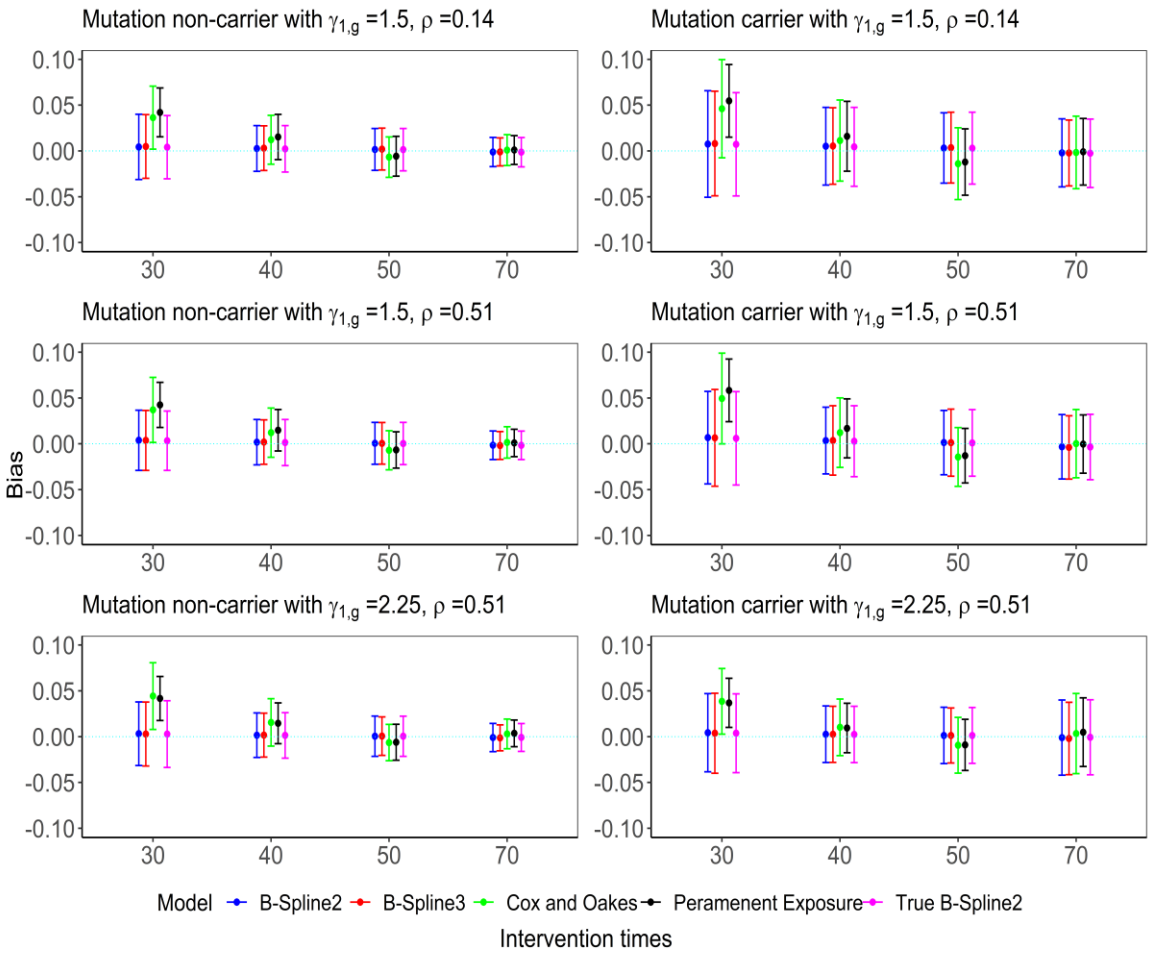

Figure 4.4: Bias and 95% confidence interval of the bias for penetrance estimations at time 70 for mutation carriers and non-carriers with different intervention times (30, 40, 50, and 70 (no intervention)) estimated from the correlated frailty competing risks models with different time-dependent effect (TDE) functions under the BS model with 2 interior knots and a positive TDE, a high correlation between competing events ($\rho = 0.51$) a high mutation ($\gamma_{1g} = 2.25$) based on 500 simulations each with 500 families.

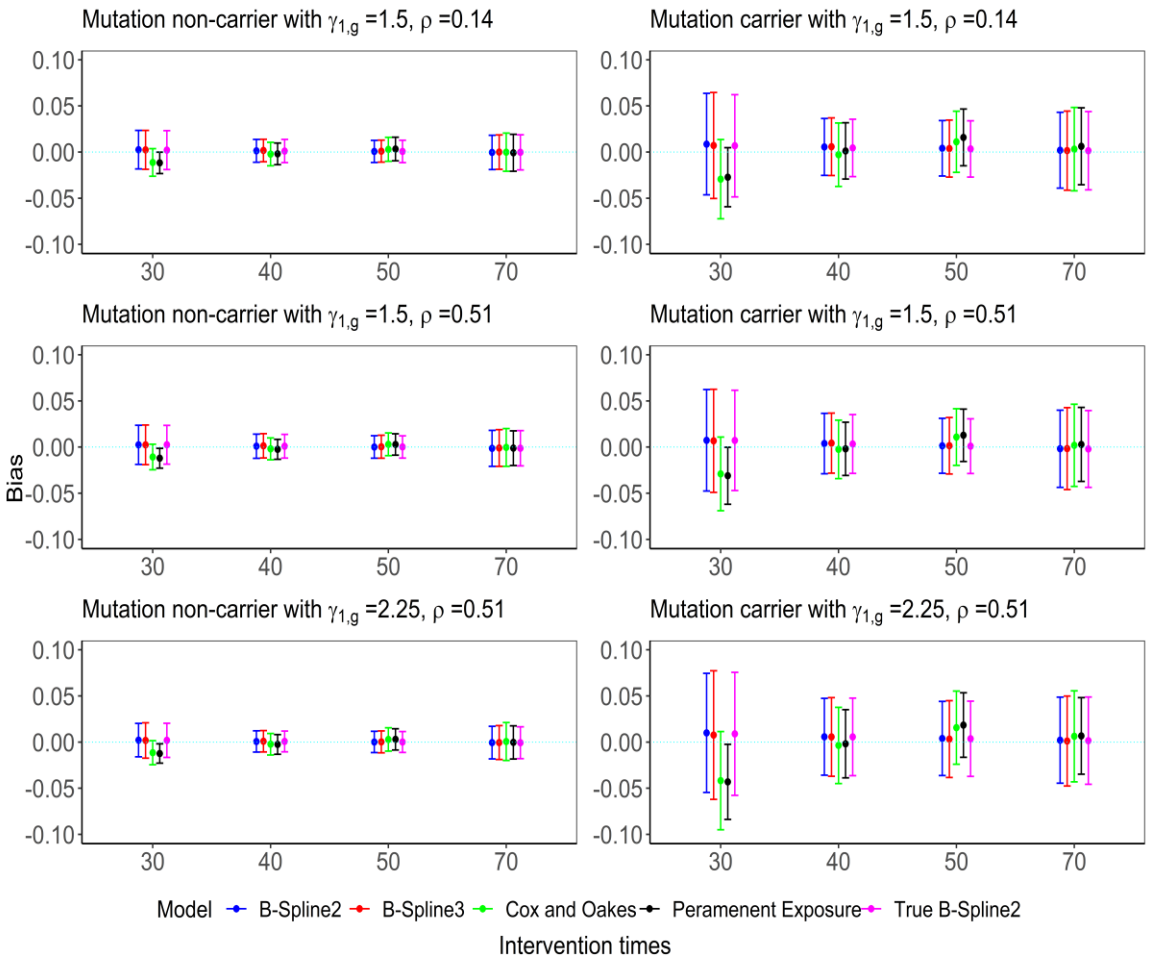

Figure 4.5: Bias and 95% confidence interval of the bias for penetrance estimations at time 70 for mutation carriers and non-carriers with different intervention times (30, 40, 50, and 70 (no intervention)) estimated from the correlated frailty competing risks models with different time-dependent effect (TDE) functions under the BS model with 2 interior knots and a negative TDE, a high correlation between competing events ($\rho = 0.51$) a high mutation ($\gamma_{1g} = 2.25$) based on 500 simulations each with 500 families.

Table 4.14: Average AIC values from the correlated frailty competing risks model with misspecified TDE model under different scenarios with $\rho = 0.51$ and $\gamma_{1g} = 2.25$ based on 500 simulations each with 500 families.

Scenario	True model	PE	CO	TBS2	BS2	BS3
1	BS+	19819.51	19821.89	19775.07	**19774.86**	19775.95
2	BS+	19711.88	19714.49	19664.12	**19664.11**	19665.17
3	BS+	20241.20	20242.68	**20189.73**	**20189.73**	20190.57
4	BS-	17458.92	17649.96	**17444.05**	17444.12	17444.95
5	BS-	17228.54	17437.10	17216.83	**17216.63**	17217.67
6	BS-	18260.01	18434.24	18244.73	**18244.68**	18245.52
7	CO+	19614.22	19389.31	-	19340.98	**19339.18**
8	CO+	19472.86	**19224.00**	-	19230.01	19229.91
9	CO+	20021.06	**19754.66**	-	19758.18	19756.87
10	CO-	17677.15	17649.96	-	**17653.38**	17654.31
11	CO-	17463.88	**17437.10**	-	17440.69	17441.81
12	CO-	18467.09	**18434.24**	-	18437.90	18438.86

For each scenario, the AICs are obtained from 500 simulations each with 500 families. The permanent exposure (PE) and Cox and Oakes (CO) are the TDE functions; The two cubic B-spline (BS) models, BS2 and BS3, have 2 interior knots and 3 interior knots, respectively, and TBS32 denotes the true BS model with a degree of 3 and 2 interior knots. ρ is the correlation between the frailties of two competing events j; γ_{1g} is the regression coefficient for the time-invariant covariate for event 1.

.

Chapter 5 Model performance

For survival analysis, several measures of quantifying the predictive ability of risk prediction models have been proposed, which are often classified as discrimination and calibration. In this chapter, we focus on the C-index and Brier score applied particularly for clustered survival data in competing risks settings to evaluate the predictive ability of the proposed model with time-dependent covariates. Based on exemplified data, we illustrate their use. This chapter is divided into two sections. Section 5.1 describes the concordance index quantifies discrimination under various settings while introducing a new approach that accounts for simultaneously clustered competing risk data with TDC/TDE. In section 5.2, the Brier score is described to assess the calibration of our proposed model.

5.1 Discrimination

5.1.1 C-index for survival data

Concordance, or c-index, is commonly used to quantify the relationship between two variables. Two subjects are called concordant if both values of one subject are larger (or smaller) than the corresponding values of the other subject. This index has commonly been used to quantify model performance, referred to as discrimination, where observations are the standard while model predictions are regarded as test value (Steyerberg et al., 2010). In the case of binary outcomes, the C-index is equivalent to the area under the receiver operating characteristic curve (AUC) (Bamber, 1975; Hanley and McNeil, 1982). For survival data, Harrell et al. (1982) proposed the C-index with the ranks of observed data as the standard and computed the concordance of the predicted survival times with the observed data. Kang et al. (2015) has proposed an inference method for survival data that has been implemented in SAS proc phreg.

Harrell's C-index quantifies the probability that of two randomly selected subjects, the one with a lower survival time will experience the event first (Harrell et al., 1982). Considering a pair of subjects (i, j) randomly selected from the data with the observed survival times (T_i, T_j) and event indicators (δ_i, δ_j) and predicted survival times $(\hat{T}_i, \hat{T}_j)$, Harrell's C-index is defined as

$$C_H = P\left(\hat{T}_i < \hat{T}_j \middle| T_i < T_j\right)$$

which can be interpreted as the proportion of the number of concordant pairs over the number of comparable pairs.

A pair is called comparable if and only if it is known which subject has the event first. For example, two subjects are considered as a comparable pair if the subject with a shorter observed survival time experiences the event regardless of the event status of the subject with a longer observed time $(T_i < T_j, \delta_i = 1)$. Even if their observed survival times are the same, they are considered comparable once their event statuses are different $(T_i = T_j, \delta_i \neq \delta_j)$. However, some pairs are not comparable if neither of the subjects experiences the event during the follow-up time regardless of their observed survival times $(\delta_i = \delta_j = 0)$, the subject with a shorter observed survival time is censored $(T_i < T_j, \delta_i = 0)$, or both have the event at the same time $(T_i = T_j, \delta_i = \delta_j = 1)$ because it is impossible to determine which one experiences the event first.

Among the comparable pairs, if the predicted survival time is longer (shorter) for the pair member with later (earlier) survival time, the pair is referred to as concordant (discordant).

It is known that a one-to-one correspondence holds between the predicted survival time, $\hat{T}_i$, and predicted survival probability, $\hat{S}_i(t|x_i)$, for any $t > 0$, when a proportional hazard model is used. That is, a comparison of the predicted survival times of any pair is equivalent to a comparison of their predicted survival probabilities for any $t > 0$ (Pencina and D'Agostino, 2004). Furthermore, comparing their predicted survival probabilities

under the proportional hazard model can be reduced to comparing their risk scores or linear predictors, $\hat{\beta}^T X$, implying the following comparisons are equivalent:

$$\hat{T}_i < \hat{T}_j \Leftrightarrow \hat{S}_i(t|X_i) < \hat{S}_j(t|X_j) \Leftrightarrow \hat{\beta}^T X_i > \hat{\beta}^T X_j$$

Thus, Harrell's C-index can be expressed in terms of the predicted survival probabilities or predicted risk scores as

$$C_H = P(\hat{T}_i < \hat{T}_j | T_i < T_j) = P(\hat{S}_i(t|X_i) < \hat{S}_j(t|X_j) | T_i < T_j) = P(\hat{\beta}^T X_i > \hat{\beta}^T X_j | T_i < T_j).$$

As a comparison measure, the C-index can take a value between 0.5 and 1. In general, the C-index of 0.5 corresponds to prediction no better than chance, 0.5 to 0.7 is considered as poor discrimination, 0.7 to 0.8 indicates considered acceptable, 0.8 to 0.9 is considered excellent, and 1 indicates perfect prediction (Hosmer et al., 2013). Thus, a value close to 0.5 represents the poor predictive performance of the model, and a value close to 1 represents good performance.

For the data with n individuals, consider t_i and t_j as the observed survival times of subjects i and j. The event indicator δ_i equals 1 if the subject experiences the event and 0 otherwise. Then, by using all comparable pairs from the data, Harrell's C-index can be calculated by

$$\hat{C}_H = \frac{\sum_{i=1}^{n} \sum_{j \neq i, j=1}^{n} Q_{ij} \{ I(t_i < t_j) + I(t_i = t_j, \delta_j = 0) \} \delta_i}{\sum_{i=1}^{n} \sum_{j \neq i, j=1}^{n} \{ I(t_i < t_j) + I(t_i = t_j, \delta_j = 0) \} \delta_i}$$

where $\{ I(t_i < t_j) + I(t_i = t_j, \delta_j = 0) \} \delta_i$ indicates if a pair is comparable or not. In addition, $Q_{ij} = I\{ (\hat{\beta}^T X_i > \hat{\beta}^T X_j) + 0.5 I(\hat{\beta}^T X_i = \hat{\beta}^T X_j) \}$ indicates the order of the predicted risk scores, which takes a value 0, 0.5, or 1, such that

$$Q_{ij} = \begin{cases} 1 & \hat{\beta}^T X_i > \hat{\beta}^T X_j \ (i\text{th risk score is larger than } j\text{th risk score}), \\ 0.5 & \hat{\beta}^T X_i = \hat{\beta}^T X_j \ (\text{tied risk scores}), \\ 0 & \hat{\beta}^T X_i < \hat{\beta}^T X_j \ (i\text{th risk score is smaller than } j\text{th risk score}). \end{cases}$$

Although Harrell's C-index is widely used, it excludes the pairs that are not comparable due to the censoring resulting in dependence on the censoring distribution (Schmid and Potapov, 2012). As a result, Harrell's C-index is upwardly biased when the amount of censoring is large. To address this limitation, Uno et al. (2011) proposed use of inverse probability of censoring weight (IPCW) applied to each pair of subjects to remove the censoring dependence in Harrell's C-index, where the weight is based on the inverse of the probability that two subjects are not censored at the lower observed time t_i. The censoring probability can be estimated from the Kaplan-Meier estimator of the censoring distribution. Furthermore, the censoring time is often shorter than that of the true failure time in survival data, resulting in few available data. Then, the estimation of the survival function with a large time would be unstable due to the small number of risk set at the tail of the survival curve. To address this problem, the discriminative ability of a model at a certain time interval can be used instead of evaluating the global prediction accuracy. Uno's C-index assesses the model performance accounting for censoring within the time interval (0, ν). Since the truncation time ν influences the interpretation of Uno's C-index, multiple truncation time points can be evaluated to compare discrimination ability.

Uno's C-index conditional on the time interval $(0, \nu)$ is defined as

$$C_U(\nu) = P\left(\hat{\beta}^T X_i > \hat{\beta}^T X_j \middle| T_i < T_j, T_i < \nu\right)$$

where ν represents the truncation time for ith subject. The major difference between Harrell's C-index and Uno's C-index is how they order the survival times in the presence of censoring. Uno's C-index is the truncated version of Harrell's C-index accounting for censoring with a condition, where the shortest observed time of a pair of subjects should be less than a prespecified time point ν.

With $\hat{G}_C(t-)$, the censoring distribution estimated by the Kaplan Meier estimator at time $t-$, which is the time point just before t, Uno's C-index can be obtained by applying the inverse probability of censoring weights into the Harrell's C-index as

$$\hat{C}_U(v) = \frac{\sum_{i=1}^{n}\sum_{j\neq i,j=1}^{n}\{\hat{G}_C(t_i-)\}^{-2}Q_{ij}\{I(t_i < t_j) + I(t_i = t_j, \delta_j = 0)\}I(t_i < v)\delta_i}{\sum_{i=1}^{n}\sum_{j\neq i,j=1}^{n}\{\hat{G}_C(t_i-)\}^{-2}\{I(t_i < t_j) + I(t_i = t_j, \delta_j = 0)\}I(t_i < v)\delta_i}$$

where $I(t_i < v)$ is the indicator of the truncation.

5.1.2 Time-dependent C-index

Generally, the C-index in survival analysis only depends on the ordering of the predictions while assuming a one-to-one correspondence between the predicted survival probability and observed survival time. In other words, the orderings of the predicted survival times and observed times are assumed to be the same. However, the one-to-one relationship may not be plausible when TDC or TDE is involved in the model, where the ordering of the survival probabilities may change over time. Since Harrell's C-index is based on the one-to-one assumption, using the original Harrell's C-index is not plausible once TDC or TDE is involved. To overcome this limitation, Antolini et al. (2005) extended the standard C-index by using the predicted survival probabilities at the minimum observed time from the pairs of two subjects instead of the risk scores. Such a measure is referred to as the time-dependent C-index, where each pair of two subjects uses the different observed times to estimate the survival probabilities. In other words, all possible pairs of two subjects use different time points to estimate the predicted survival probabilities. Then, the time-dependent C-index is defined as

$$C^{td} = P\big(\hat{S}_i(T_i|x_i) < \hat{S}_j(T_i|x_j)\big|T_i < T_j\big)$$

which is based on the property that the predicted survival probability at the time, when ith subject experience the event, would be greater for the jth subject than the ith subject. The time-dependent C-index has the benefit of providing a single value measuring the model performance instead of the function of time t and is equivalent to Harrel's C-index if the proportional hazard assumption holds, where the orders of the survival probabilities stay constant.

5.1.3 C-index in competing risk setting

In a non-competing risk setting, the risk set includes the subjects who experience the event or subjects who are censored until the event or censoring time. However, in the presence of the competing risks, the risk set can be defined in two different ways. The first definition of risk set treats individuals who experience the event of interest or are censored are at risk until the event or the censoring time while censoring individuals who experience the competing risk events (Wolbers et al., 2014). Alternatively, since competing risks can potentially influence the occurrence of the event of interest, the second definition of the risk set further retains those who have failed from the competing events at any time instead of censoring them (Wolbers et al., 2009).

The use of these definitions depends on the purpose of the study (Wolbers et al., 2014). The first definition was motivated by a situation where a specific treatment affects all the events, including the event of interest and the competing events. Then, it might be less suitable if the main goal is to assess the effect of treatment on a specific event. For example, suppose smoking status affects lung cancer and bowel cancer simultaneously. In this case, the amount of the effect of smoking on two subjects, one experiencing lung cancer and the other experiencing bowel cancer, would not be comparable. In contrast, when a specific treatment reduces the risk of an event of interest but does not affect the competing events, the subjects experiencing competing events can be at risk all time. This study is based on the second definition as our interest lies in the effect of surgery on breast cancer, which does not affect competing events that are ovarian cancer or death caused by other reasons.

Harrell's C-index for competing risks data, which is presented by Wolbers et al. (2009), is based on the penetrance $F_{i,k}(t|x_i)$ for the event of interest k instead of the survival probability. Let δ_i be the event type for individual i where $\delta_i = 1$ for the event of interest, 2 for any competing risks and 0 if censored. Harrell's C-index for event 1 based on the second definition is defined as

$$C_{H,1} = P\big(F_{i,1}(t|x_i) > F_{j,1}(t|x_j) | (T_i < T_j \; or \; \delta_j = 2), \delta_i = 1\big) \text{ for any } t > 0$$

where the rank of two penetrances for event 1 is not subjected to time.

Wolbers et al. (2014) further adapted Uno's C-index to competing risks setting by applying IPCW to each pair of subjects to remove the censoring dependency. Then, Uno's C-index for competing risks is defined as

$$C_{U,1}(\nu) = P\big(F_{i,1}(\nu|x_i) > F_{j,1}(\nu|x_j)|(T_i < T_j \; or \; \delta_j = 2), \delta_i = 1, T_i < \nu\big)$$

where ν represents the truncation time for ith subject.

Suppose we have two weights $W_{ij1} = \{\hat{G}_C(t_i -)\}^{-2}$ and $W_{ij2} = \{\hat{G}_C(t_i -)\hat{G}_C(t_j -)\}^{-1}$. We also define $A_{ij} = I(t_i < t_j) + I(t_i = t_j, \delta_j = 0)$ and $B_{ij} = I(t_i \geq t_j, \delta_j = 2)$, where B_{ij} indicates that the subjects with competing risks stay in risk set for all time. Harrell's C-index and Uno's C-index for event 1 at time ν accounting for competing risks are obtained as

$$\hat{C}_{H,1} = \frac{\sum_{i=1}^{n}\sum_{j\neq i,j=1}^{n} Q_{ij1}(\nu)\{A_{ij} + B_{ij}\} I(\delta_i = 1)}{\sum_{i=1}^{n}\sum_{j\neq i,j=1}^{n}\{A_{ij} + B_{ij}\} I(\delta_i = 1)} \text{ for any } \nu > 0$$

and

$$\hat{C}_{U,1}(\nu) = \frac{\sum_{i=1}^{n}\sum_{j\neq i,j=1}^{n} Q_{ij1}(\nu)\{W_{ij1}A_{ij} + W_{ij2}B_{ij}\} I(t_i < \nu, \delta_i = 1)}{\sum_{i=1}^{n}\sum_{j\neq i,j=1}^{n}\{W_{ij1}A_{ij} + W_{ij2}B_{ij}\} I(t_i < \nu, \delta_i = 1)}$$

where $Q_{ij1}(\nu) = I\{\hat{F}_{i,1}(\nu|x_i) > \hat{F}_{j,1}(\nu|x_j)\} + 0.5I\{\hat{F}_{i,1}(\nu|x_i) = \hat{F}_{j,1}(\nu|x_j)\}$ takes a value 1 if concordance, 0 if discordance, or 0.5 if tied.

5.1.4 Time-dependent Uno's C-index for clustered competing risk

As presented in previous sections, several authors introduced various types of concordance measures to account for TDE/TDC (Antolini et al., 2005) and competing risk (Wolbers et al., 2009; Wolbers et al., 2014). Building on their work, we propose an

extended C-index to evaluate the discriminative ability of our proposed model, which includes time-dependent covariates having time-dependent effects in the analysis of clustered competing risk data. We proposed time-dependent Uno's C-index (TDUC) that extends Uno's approach to the case of time-dependent C-index while accounting for the presence of competing risks.

Consider the data arise from F independent families, each family consist of n_f members. Let f_i be the subject $i, i = 1, \dots, n_f$, of the family $f, f = 1, \dots, F$. To consider pairs consisting of individuals from different families, we denote by g_j the subject $j, j = 1, \dots, n_g$, of the family g, where $g = 1, \dots, F$. Let δ_{f_i} be the event type for individual i in cluster f where $\delta_{f_i} = 1$ for the event of interest, 2 for any competing risks and 0 if censored. The marginal cause-specific penetrance function for event 1, $F_{f_i,1}\left(t_{f_i}\middle|x_{f_i}\right)$, is used as the frailties are not observed. Conditional on the time interval $(0, v)$, the TDUC is defined as

$$C_{td,U,1}(v) = P\left(F_{f_i,1}(t_{f_i}|\boldsymbol{X}_{f_i}) > F_{g_j,1}(t_{f_i}|\boldsymbol{X}_{g_j})|(T_{f_i} < T_{g_j}\ or\ \delta_{g_j} = 2), \delta_{f_i} = 1, T_{f_i} < v\right)$$

where f and g can be the same ($f = g$) or different families ($f \neq g$).

Given that $\hat{G}_C(t)$, which is the Kaplan Meier estimator of the censoring distribution at time t, we have two weights $W_{f_i1} = \left\{\hat{G}_C\left(t_{f_i} -\right)\right\}^{-2}$ and $W_{f_ig_j2} = \left\{\hat{G}_C\left(t_{f_i} -\right)\hat{G}_C\left(t_{g_j} -\right)\right\}^{-1}$, where $t_{f_i} -$ is the time point just before t_{f_i}. We also define $A_{f_ig_j} = I(t_{f_i} < t_{g_j}) + I(t_{f_i} = t_{g_j}\ \delta_{g_j} = 0)$, where $A_{f_ig_j}$ identifies the pairs that the first subject experiences the event first, and $B_{f_ig_j} = I(t_{f_i} \geq t_{g_j}, \delta_{g_j} = 2)$, where $B_{f_if_j}$ indicates that the subjects with competing risks stay in risk set for all time. Given the penetrance $F_{f_i1}(t|\boldsymbol{X}_{f_i})$ for the event of interest 1, the TDUC with TDC/TDE for clustered competing risk data can be obtained as

$$\hat{C}_{td,U,1}(v) = \frac{\sum_{f=1}^{F}\sum_{g=1}^{F}\left[\sum_{i=1}^{n_f}\sum_{j\neq i,j=1}^{n_g} Q_{f_ig_j1}\left\{W_{f_i1}A_{f_ig_j} + W_{f_ig_j2}B_{f_ig_j}\right\} I\left(t_{f_i} < v, \delta_{f_i} = 1\right)\right]}{\sum_{f=1}^{F}\sum_{g=1}^{F}\left[\sum_{i=1}^{n_f}\sum_{j\neq i,j=1}^{n_g}\left\{W_{f_i1}A_{f_ig_j} + W_{f_ig_j2}B_{f_ig_j}\right\} I\left(t_{f_i} < v, \delta_{f_i} = 1\right)\right]}$$

where $Q_{f_i g_j 1} = I\left\{\hat{F}_{f_i 1}\left(t_{f_i}|\boldsymbol{X}_{f_i}\right) > \hat{F}_{g_j 1}\left(t_{f_i}|\boldsymbol{X}_{g_j}\right)\right\} + 0.5I\left\{\hat{F}_{f_i 1}\left(t_{f_i}|\boldsymbol{X}_{f_i}\right) = \hat{F}_{g_j 1}\left(t_{f_i}|\boldsymbol{X}_{g_j}\right)\right\}$ indicates the order of predicted penetrances according to the shorter observed time among two subjects, and pairs with tied predicted penetrances are counted as 0.5.

5.1.5 C-index and Kendall's Tau

Alternatively, the proposed TDUC can be estimated using the inference of Kendall's tau, which measures the association between two variables by quantifying the difference between concordance and discordance. Given $t_m = \min(t_{f_i}, t_{g_j})$, we introduce two indicator functions for a pair of two subjects (f_i, g_j), $i \neq j$ for $f = g$ or $f \neq g$, that accounts for competing risks such as

$$sign\left(\hat{F}_{f_i,1}(t_m|\boldsymbol{X}_{f_i}), \hat{F}_{g_j,1}\left(t_m\middle|\boldsymbol{X}_{g_j}\right)\right) = I\left\{\hat{F}_{f_i,1}(t_m|\boldsymbol{X}_{f_i}) > \hat{F}_{g_j,1}\left(t_m\middle|\boldsymbol{X}_{g_j}\right)\right\} - I\left\{\hat{F}_{f_i,1}(t_m|\boldsymbol{X}_{f_i}) < \hat{F}_{g_j,1}\left(t_m\middle|\boldsymbol{X}_{g_j}\right)\right\} \tag{5.1}$$

$$csign\left(t_{f_i}, \delta_{f_i}, t_{g_j}, \delta_{g_j}, \nu\right) = cs_1\left(t_{f_i}, \delta_{f_i}, t_{g_j}, \delta_{g_j}, \nu\right) - cs_2\left(t_{f_i}, \delta_{f_i}, t_{g_j}, \delta_{g_j}, \nu\right) \tag{5.2}$$

where

$$cs_1\left(t_{f_i}, \delta_{f_i}, t_{g_j}, \delta_{g_j}, \nu\right) = \left\{I\left(t_{f_i} \leq t_{g_j}\right) + I\left(t_{f_i} > t_{g_j}, \delta_{g_j} = 2\right)\right\} I(\delta_{f_i} = 1) I\{t_{f_i} < \nu\}$$

$$cs_2\left(t_{f_i}, \delta_{f_i}, t_{g_j}, \delta_{g_j}, \nu\right) = \left\{I\left(t_{f_i} \geq t_{g_j}\right) + I\left(t_{f_i} < t_{g_j}, \delta_{f_i} = 2\right)\right\} I\left(\delta_{g_j} = 1\right) I\left\{t_{g_j} < \nu\right\}$$

and $sign$ and $csign$ functions take value in $\{-1, 0, 1\}$. Given that one with a shorter observed time is less than ν, Equation (5.2) represents the order of two observed survival times with censoring indicators, which equals 1 if subject *i* has a shorter observed survival time or subject *j* experiences a competing event while having a shorter survival

time, -1 if subject *j* has a shorter observed survival time or *i*th subject experiences a competing event while having a shorter survival time, and 0 if two subjects are not comparable. Also, Equation (5.1) is the order of two predicted penetrances for event 1, where it has a value of 1 if subject *i* has a higher predicted penetrance, -1 if subject *j* has a higher predicted penetrance, and 0 if two predicted penetrance the same.

Since we consider the subjects with any competing events to stay at risk all time, we introduce two different weights, $W^*_{f_i g_j 1} = \left[\hat{G}_C(t_m -)\right]^{-2}$ and $W^*_{f_i g_j 2} = \left\{\hat{G}_C(t_{f_i} -)\hat{G}_C\left(t_{g_j} -\right)\right\}^{-1}$, to remove the censoring dependency, where $t_m = \min(t_{f_i}, t_{g_j})$ and $W^*_{f_i g_j 1}$ and $W^*_{f_i g_j 2}$ correspond to the weights for the pairs without and with competing events, respectively. We also define $A^*_{f_i g_j} = \left\{I\left(t_{f_i} > t_{g_j}, \delta_{g_j} = 1\right) + I\left(t_{f_i} < t_{g_j}, \delta_{f_i} = 1\right)\right\}$, where $A^*_{f_i g_j}$ represents the order of two observed survival times with censoring distribution that is the condition used for $W^*_{f_i g_j 1}$. Similarly, we introduce $B^*_{f_i g_j} = \left\{I\left(t_{f_i} \le t_{g_j}, \delta_{f_i} = 2, \delta_{g_j} = 1\right) + I\left(t_{f_i} \ge t_{g_j}, \delta_{f_i} = 1, \delta_{g_j} = 2\right)\right\}$, where $B^*_{f_i g_j}$ is the order of two observed survival times involving competing events that is the condition used for $W^*_{f_i g_j 2}$. The subject with the competing event has a shorter observed time than the one with the event of interest, as comparable pairs. These two weights are used to obtain the unified weight such as

$$W^*_{Cf_i g_j 1} = W^*_{f_i g_j 1} A^*_{f_i g_j} + W^*_{f_i g_j 2} B^*_{f_i g_j}.$$

Then, Kendall's tau for event 1 can be obtained by using following formulas

$$d_{f_i g_j cs1}(v) = sign\left(\hat{F}_{f_i,1}(t_m|\boldsymbol{X}_{f_i}), \hat{F}_{g_j,1}\left(t_m\middle|\boldsymbol{X}_{g_j}\right)\right) csign\left(t_{f_i}, D_{f_i}, t_{g_j}, D_{g_j}, v\right) W^*_{Cf_i g_j 1}$$

$$d_{f_i g_j c1}(v) = csign\left(t_{f_i}, D_{f_i}, t_{g_j}, D_{g_j}, v\right)^2 W^*_{Cf_i g_j 1}$$

where $d_{f_i g_j cs1}(v)$ identifies the concordant as 1 and discordant pair as -1, inversely weighted by censoring distribution. Similarly, $d_{f_i g_j c1}(v)$ indicates the comparable pair,

while accounting for censoring. Then, the time-dependent Kendall's tau for clustered competing risk data as

$$\hat{\tau}_{td,U,1}(v) = \frac{\sum_{f=1}^{F}\sum_{g=1}^{F}\left\{\sum_{i=1}^{n_f}\sum_{j\neq i,j=1}^{n_g} d_{f_i g_j cs1}(v)\right\}}{\sum_{f=1}^{F}\sum_{g=1}^{F}\left\{\sum_{i=1}^{n_f}\sum_{j\neq i,j=1}^{n_g} d_{f_i g_j c1}(v)\right\}} = \frac{d_{cs1}(v)}{d_{c1}(v)} \tag{5.3}$$

where $d_{cs1}(v) = \sum_{f=1}^{F}\sum_{g=1}^{F}\left\{\sum_{i=1}^{n_f}\sum_{j\neq i,j=1}^{n_g} d_{f_i g_j cs1}(v)\right\}/\{n(n-1)\}$ is the difference between the weighted proportions of concordant pairs and the discordant pairs, $d_{c1}(v) = \sum_{f=1}^{F}\sum_{g=1}^{F}\left\{\sum_{i=1}^{n_f}\sum_{j\neq i,j=1}^{n_g} d_{f_i g_j c1}(v)\right\}/\{n(n-1)\}$ is the total weighted proportion of the comparable pairs across all families, and $n = \sum_{f=1}^{F} n_f$ represents the total number of subjects across all families. Thus, the TDCU is obtained using the Kendall's tau as

$$\hat{C}_{td,U,1}(v) = 0.5\left(\hat{\tau}_{td,U,1}(v) + 1\right) = 0.5\left(\frac{d_{cs1}(v)}{d_{c1}(v)} + 1\right). \tag{5.4}$$

5.1.6 Variance of C-index

To obtain the variance of the TDUC, the methodology proposed by Cliff and Charlin (1991) and Kang et al. (2015) can be adapted to our proposed C-index, where the Delta method was used to approximate the variance of Kendall's tau, and Kang et al. (2015) used the linear relationship between Harrell's C-index and Kendall's tau to estimate the variance of the C-index. Then, the variance of TDUC for event 1 is obtained as

$$\mathrm{Var}\left(C_{td,U,1}(v)\right) = \mathrm{Var}\left(\frac{1}{2}\{\tau_{td,U,1}(v) + 1\}\right) = \frac{1}{4}\mathrm{Var}\left(\tau_{td,U,1}(v)\right) = \frac{1}{4}\mathrm{Var}\left(\frac{d_{cs1}(v)}{d_{c1}(v)}\right).$$

Then, the variance of Kendall's tau can be approximated by using the Delta method such as

$$\mathrm{Var}\left(\tau_{td,U,1}(v)\right) = \mathrm{Var}\left(\frac{d_{cs1}(v)}{d_{c1}(v)}\right)$$

$$= \begin{pmatrix} \frac{1}{d_{c1}(v)} & \frac{-d_{cs1}(v)}{d_{c1}(v)^2} \end{pmatrix} \begin{bmatrix} \mathrm{Var}\big(d_{cs1}(v)\big) & \mathrm{Cov}\big(d_{c1}(v), d_{cs1}(v)\big) \\ \mathrm{Cov}\big(d_{c1}(v), d_{cs1}(v)\big) & \mathrm{Var}\big(d_{c1}(v)\big) \end{bmatrix}$$

$$\begin{pmatrix} \frac{1}{d_{c1}(v)} & \frac{-d_{cs1}(v)}{d_{c1}(v)^2} \end{pmatrix}^T$$

$$= \begin{bmatrix} \frac{\mathrm{Var}\big(d_{cs1}(v)\big)}{d_{c1}(v)} - \frac{d_{cs1}(v)\mathrm{Cov}\big(d_{c1}(v), d_{cs1}(v)\big)}{d_{c1}(v)^2} \\ \frac{\mathrm{Cov}\big(d_{c1}(v), d_{cs1}(v)\big)}{d_{c1}(v)} - \frac{d_{cs1}(v)\mathrm{Var}\big(d_{c1}(v)\big)}{d_{c1}(v)^2} \end{bmatrix}^T \begin{pmatrix} \frac{1}{d_{c1}(v)} & \frac{-d_{cs1}(v)}{d_{c1}(v)^2} \end{pmatrix}^T$$

$$= \frac{\mathrm{Var}\big(d_{cs1}(v)\big)}{d_{c1}(v)^2} - \frac{2d_{cs1}(v)\mathrm{Cov}\big(d_{c1}(v), d_{cs1}(v)\big)}{d_{c1}(v)^3} + \frac{d_{cs1}(v)^2\mathrm{Var}\big(d_{c1}(v)\big)}{d_{c1}(v)^4}.$$

(5.5)

To estimate the variances and covariances in Equation (5.5), we employ variance estimators for Kendall's tau proposed by Cliff and Charlin (1991),

$$\widehat{\mathrm{Var}}\big(d_{cs1}(v)\big) = \frac{2}{n(n-1)}\widehat{\mathrm{Var}}\left(d_{f_i g_j cs1}(v)\right) + \frac{4(n-2)}{n(n-1)}\widehat{\mathrm{Var}}\left(d_{f_i cs1}(v)\right)$$

$$\widehat{\mathrm{Var}}\big(d_{c1}(v)\big) = \frac{2}{n(n-1)}\widehat{\mathrm{Var}}\left(d_{f_i g_j c1}(v)\right) + \frac{4(n-2)}{n(n-1)}\widehat{\mathrm{Var}}\left(d_{f_i c1}(v)\right)$$

and

$$\widehat{\mathrm{COV}}\big(d_{c1}(v), d_{cs1}(v)\big) = \frac{2}{n(n-1)}\widehat{\mathrm{COV}}\left(d_{f_i g_j c1}(v), d_{f_i g_j cs1}(v)\right)$$

$$+ \frac{4(n-2)}{n(n-1)}\widehat{\mathrm{COV}}\left(d_{f_i c1}(v), d_{f_i cs1}(v)\right)$$

where $n = \sum_{f=1}^{F} n_f$ is the total number of individuals across all families, $d_{f_i cs1}(v) = \sum_{g=1}^{F}\sum_{j=1}^{n_g} d_{f_i g_j cs1}(v)/(n-1)$ and $d_{f_i c1}(v) = \sum_{g=1}^{F}\sum_{j=1}^{n_g} d_{f_i g_j c1}(v)/(n-1)$. Substitution of sample variance and covariance provides consistent estimators.

As proposed by Zou et al (2022), the variance and covariance estimators can be further simplified by ignoring the first term when sample size is not very small

$$\widehat{\mathrm{Var}}\left(d_{cs1}(v)\right) \approx \frac{4}{n}\widehat{\mathrm{Var}}\left(d_{f_i cs1}(v)\right) \tag{5.6}$$

$$\widehat{\mathrm{Var}}\left(d_{c1}(v)\right) \approx \frac{4}{n}\widehat{\mathrm{Var}}\left(d_{f_i c1}(v)\right) \tag{5.7}$$

and

$$\widehat{\mathrm{COV}}\left(d_{c1}(v), d_{cs1}(v)\right) \approx \frac{4}{n}\widehat{\mathrm{COV}}\left(d_{f_i c1}(v), d_{f_i cs1}(v)\right) \tag{5.8}$$

where the variance and covariance terms are estimated by the sample variance and covariance, respectively. Zou et al. (2022) demonstrated that these simple variance and covariance estimators performed well even with small to moderate sample size (n > 30). Note that unbiased estimators for the variance and covariance of $d_{cs1}(v)$ and $d_{c1}(v)$ were also proposed by Cliff and Charlin (1991) and Kang et al. (2015). Although they are unbiased and widely implemented, they have a drawback that they sometimes provide a negative value for the variance of Kendall's tau.

To account for clustering, the variance and covariance terms in Equations (5.6) to (5.8) are estimated by the cluster mean variance and covariance weighted by cluster sizes respectively, such as

$$\widehat{\mathrm{Var}}\left(d_{f_i cs1}(v)\right) = \frac{\sum_{f=1}^{F} n_f \left\{d_{fcs1}(v) - d_{cs1}(v)\right\}^2}{n(F-1)} \tag{5.9}$$

$$\widehat{\mathrm{Var}}\left(d_{f_i c1}(v)\right) = \frac{\sum_{f=1}^{F} n_f \left\{d_{fc1}(v) - d_{c1}(v)\right\}^2}{n(F-1)} \tag{5.10}$$

and

$$\widehat{\mathrm{COV}}\left(d_{f_i c1}(v), d_{f_i cs1}(v)\right) = \frac{\sum_{f=1}^{F}\sum_{g=1}^{F} n_f \left\{d_{fcs1}(v) - d_{cs1}(v)\right\}\left\{d_{fc1}(v) - d_{c1}(v)\right\}}{n(F-1)} \tag{5.11}$$

where $d_{fcs1}(v) = \sum_{i=1}^{n_f} d_{f_i cs1}(v)/n_f$ and $d_{fc1}(v) = \sum_{i=1}^{n_f} d_{f_i c1}(v)/n_f$ are the cluster-specific averages of $d_{f_i cs1}(v)$ and $d_{f_i c1}(v)$, respectively.

5.1.7 Illustration of time-dependent C-index and its variance calculation for clustered competing risk

We present the calculation of TDUC and its variance for clustered competing risk via Kendall's tau calculation using a small exemplary survival data provided in Table 5.1. Consider a dataset of (t, δ, x) consists of 2 different families consists of 3 and 4 subjects. We ordered them by observed time for each family and obtained their penetrance $\hat{F}_1(t|x)$ for event of interest, denote 1. Since the penetrances for two subjects at the shortest observed time among a pair of two subjects are used to compare, a binary covariate x is used to reduce the number of pairs with tied penetrances. Furthermore, the inverse of the Kaplan-Meier estimator of the censoring distribution at each observed time $\hat{G}_C(t-)^{-1}$ is obtained by using all subjects instead of estimating it for each family. We further set a time point of 50 as the truncation time.

Table 5.1: Exemplary data of 2 families to compute time-dependent Uno's C-index

Family (f_i)	**t**	**δ**	**x**	$\widehat{F}_1(t\|x=0)$	$\widehat{F}_1(t\|x=1)$	$\widehat{G}_C(t-)^{-1}$
1_1	23	0	1	0.59	0.55	1
1_2	37	1	0	0.71	0.66	1.09
1_3	63	2	1	0.46	0.39	2.36
2_1	41	1	0	0.67	0.61	1.21
2_2	49	2	0	0.51	0.45	1.41
2_3	60	0	1	0.73	0.67	1.77
2_4	69	1	1	0.55	0.52	7.07

Based on the given data, we present how to get TDUC and its variance.

Step 1: Determine the weighted proportion of comparable pairs using observed time accounting for censoring via *csign* function.

We create all possible pairs of the observed data by tabulating them regarding rows as f_i and columns as g_j where f_i indicates ith subjects in f family and g_j indicates jth subjects in g family. Table 5.2 (a) presents *csign* function that ranks the observed times with the time truncation at time 50, and Table 5.2 (b) illustrates the weights applied to each pair of subjects to remove the censoring dependence using $W^*_{Cf_ig_j1}$, where $W^*_{Cf_ig_j1} = W^*_{f_ig_j1,1} + W^*_{f_ig_j2,1}$. In addition, Table 5.2 (c) identifies the comparable pairs accounting for censoring using $d_{f_ig_jc1}(50) = csign\left(t_{f_i}, D_{f_i}, t_{g_j}, D_{g_j}, 50\right)^2 W^*_{Cf_ig_j1}$. By aggregating the table by row, the most right column in Table 5.2 (c) is obtained to estimate the weighted proportion of comparable pairs for each individual $d_{f_ic1}(50) = \sum_{g=1}^{F}\sum_{j=1}^{n_g} d_{f_ig_jc1}(v)/(n-1)$, i.e., the weighted number of comparable pairs divided by the total number of pairs, $(n-1)$, for each individual can get. Then, by averaging them over all individuals, we compute the average weighted proportion of comparable pairs by 50 years as $d_{c1}(50)$ = 0.56, indicating that out of 42 possible pairs, 56% of them are comparable, accounting for censoring.

Table 5.2: Computing the weighted number of comparable pairs accounting for censoring.

(a) csign $\left(t_{f_i}, \delta_{f_i}, t_{f_j}, \delta_{f_j}, 50\right)$

	t_{g_j}	23	37	41	49	60	63	69
t_{f_i}	δ	0	1	1	2	0	2	1
23	0	-	0	0	0	0	0	0
37	1	0	-	1	1	1	1	1
41	1	0	-1	-	1	1	1	1
49	2	0	-1	-1	-	0	0	0
60	0	0	-1	-1	0	-	0	0
63	2	0	-1	-1	0	0	-	0
69	1	0	-1	-1	0	0	0	-

(b) $W^*_{Cf_ig_j1}$

$W^*_{Cf_ig_j1}$	t_{g_j}	23	37	41	49	60	63	69
t_{f_i}	δ	0	1	1	2	0	2	1
23	0	-	0	0	0	0	0	0
37	1	0	-	1.19	1.19	1.19	1.19	1.19
41	1	0	1.19	-	1.46	1.46	1.46	1.46
49	2	0	1.19	1.46	-	0	0	9.97
60	0	0	1.19	1.46	0	-	0	0
63	2	0	1.19	1.46	0	0	-	16.69
69	1	0	1.19	1.46	9.97	0	16.69	-

(c) $d_{f_ig_jc1}(50) = csign\left(t_{f_i}, D_{f_i}, t_{g_j}, D_{g_j}, 50\right)^2 W^*_{Cf_ig_j1}$

	t_{g_j}	23	37	41	49	60	63	69	$d_{f_ic1}(50)$
t_{f_i}	δ	0	1	1	2	0	2	1	
23	0	-	0	0	0	0	0	0	0/6 = 0
37	1	0	-	1.19	1.19	1.19	1.19	1.19	5.95/6 = 0.99
41	1	0	1.19	-	1.46	1.46	1.46	1.46	7.03/6 = 1.17
49	2	0	1.19	1.46	-	0	0	0	2.65/6 = 0.44
60	0	0	1.19	1.46	0	-	0	0	2.65/6 = 0.44
63	2	0	1.19	1.46	0	0	-	0	2.65/6 = 0.44
69	1	0	1.19	1.46	0	0	0	-	2.65/6 = 0.44
									$d_{c1}(50) = 23.58/42 = 0.56$

Step 2: Estimate the variances of $d_{f_ic,1}(50)$ and $d_{c1}(50)$

By using the values of $d_{f_ic1}(50)$ and $d_{c1}(50)$ in Table 5.11 (c), we first estimate the family specific average of $d_{f_ic,1}(50)$ for family 1 and family 2 as follows:

$$d_{1c1}(50) = \sum_{i=1}^{n_1} \frac{d_{1_ic1}(50)}{n_1} = \frac{0 + 0.99 + 0.44}{3} = 0.48$$

and

$$d_{2c1}(50) = \sum_{i=1}^{n_2} \frac{d_{2_ic1}(50)}{n_2} = \frac{1.17 + 0.44 + 0.44 + 0.44}{4} = 0.63$$

By using the family specific average of $d_{f_i c,1}(50)$, the variance of family-specific averages across families is obtained using Equation (5.10) as

$$\widehat{\text{Var}}\left(d_{f_i c1}(50)\right) = \frac{\sum_{f=1}^{F} n_f \left\{d_{fc1}(50) - d_{c1}(50)\right\}^2}{n(F-1)}$$

$$= \frac{3 \times (0.48 - 0.56)^2 + 4 \times (0.63 - 0.56)^2}{7(2-1)} = 0.0055$$

Then, the variance for $d_{c1}(50)$ is obtained using Equation (5.7) as

$$\widehat{\text{Var}}\left(d_{c1}(50)\right) = \frac{4}{7} \times \widehat{\text{Var}}\left(d_{f_i c1}(50)\right) = \frac{4}{7} \times 0.0055 = 0.0030$$

Step 3: Obtain the penetrances for two subjects at the lower observed time among two subjects instead of using each subject's observed time. Table 5.3 presents the estimation of the penetrances at minimum time of a pair of two subjects for a subject with larger observed time.

Table 5.3: Estimating the penetrances at minimum time of a pair of two subjects for a subject with larger observed time.

		t_{g_j}	23	37	41	49	60	63	69
		x_{g_j}	1	0	0	0	1	1	1
t_{f_i}	x_{f_i}	$\widehat{F}_1(t_{f_i}\|x_{f_i})$	$\widehat{F}_1(\min(t_{f_i}, t_{g_j})\|x_{g_j})$						
23	1	0.55	-	0.59	0.59	0.59	0.55	0.55	0.55
37	0	0.71	0.55	-	0.71	0.71	0.66	0.66	0.66
41	0	0.67	0.55	0.71	-	0.67	0.61	0.61	0.61
49	0	0.51	0.55	0.71	0.67	-	0.45	0.45	0.45
60	1	0.67	0.55	0.71	0.67	0.45	-	0.67	0.67
63	1	0.39	0.55	0.71	0.67	0.45	0.67	-	0.39
69	1	0.52	0.55	0.71	0.67	0.45	0.67	0.39	-

Step 4: Determine the weighted proportion of concordant and discordant pairs accounting for censoring.

The orders of the predicted penetrance are determined by using *sign* function as shown in Table 5.4 (a). Table 5.4 (b) identifies the difference between the weighted number of concordant pairs and the weighted number of discordant pairs accounting for censoring using

$$d_{f_i g_j cs1}(50) = sign\left(\hat{F}_{f_i,1}(t_m|\boldsymbol{X}_{f_i}, Z_{f_1}), \hat{F}_{g_j,1}\left(t_m\middle|\boldsymbol{X}_{g_j}, Z_{g_1}\right)\right) csign\left(t_{f_i}, D_{f_i}, t_{g_j}, D_{g_j}, 50\right) W^*_{Cf_i g_j 1}$$

where $d_{f_i g_j cs1}(50) > 0$ for concordant pair, $d_{f_i g_j cs1}(50) < 0$ for discordant pair, and $d_{f_i g_j cs1}(50) = 0$ for non-comparable pair. By aggregating the table by row, the most right column in Table 5.4 (b) is obtained to estimate the proportion of the difference between the weighted number of concordant pairs and the weighted number of discordant pairs for each individual $d_{f_i cs1}(v) = \sum_{g=1}^{F}\sum_{j=1}^{n_g} d_{f_i g_j cs1}(v)/(n-1)$, i.e., the difference between the weighted number of concordant pairs and the weighted number of discordant pairs divided by the total number of pairs, $(n-1)$, for each individual can get. The value of $d_{f_i cs1}(v)$ above 0 indicates that most pairs are concordant, whereas below 0 indicates that most pairs are discordant. Then, by averaging them over all individuals, we compute the average proportion of the difference between the weighted number of concordant pairs and the weighted number of discordant pairs by 50 years as $d_{cs1}(50)$ = 0.38.

Table 5.4: Determining the order of penetrances

(a) $sign\left(\hat{F}_{f_i,1}\left(\min\left(t_{f_i}, t_{g_j}\right)\middle|X_{f_i}, Z_{f_1}\right), \hat{F}_{g_j,1}\left(\min\left(t_{f_i}, t_{g_j}\right)\middle|X_{g_j}, Z_{f_1}\right)\right)$

	$\mathbf{t_{g_j}}$	23	37	41	49	60	63	69
$\mathbf{t_{f_i}}$	$\boldsymbol{x}$	1	0	0	0	1	1	1
23	1	-	-1	-1	-1	0	0	0
37	0	1	-	0	0	1	1	1
41	0	1	0	-	0	1	1	1
49	0	1	0	0	-	1	1	1
60	1	0	-1	-1	-1	-	0	0
63	1	0	-1	-1	-1	0	-	0
69	1	0	-1	-1	-1	0	0	-

$(b) d_{f_i g_j cs1}(50) = sign\left(\hat{F}_{f_i,1}(t_m|\boldsymbol{X}_{f_i}, Z_{f_1}), \hat{F}_{g_j,1}\left(t_m\middle|\boldsymbol{X}_{g_j}, Z_{g_1}\right)\right) csign\left(t_{f_i}, D_{f_i}, t_{g_j}, D_{g_j}, 50\right) W^*_{Cf_i g_j 1}$

$\boldsymbol{f_i}$	1_1	1_2	2_1	2_2	2_3	1_3	2_4	$d_{f_i cs,1}(50)$
1_1	-	0	0	0	0	0	0	0/6 = 0
1_2	0	-	0	0	1.19	1.19	1.19	3.57/6 = 0.60
2_1	0	0	-	0	1.46	1.46	1.46	4.38/6 = 0.73
2_2	0	0	0	-	0	0	0	0/6 = 0
2_3	0	1.19	1.46	0	-	0	0	2.65/6 = 0.44
1_3	0	1.19	1.46	0	0	-	0	2.65/6 = 0.44
2_4	0	1.19	1.46	0	0	0	-	2.65/6 = 0.44
								$d_{cs1}(50) = 15.90/42 = 0.38$

Step 5: Estimate the variances of $d_{f_i cs,1}(50)$ and $d_{cs1}(50)$

By using the values of $d_{f_i cs1}(50)$ and $d_{cs1}(50)$ in Table 5.11 (c), we estimate the family specific average of $d_{f_i cs,1}(50)$ for family 1 and family 2 as follow:

$$d_{1cs1}(50) = \sum_{i=1}^{n_1} \frac{d_{1_i cs1}(50)}{n_1} = \frac{0 + 0.60 + 0.44}{3} = 0.34$$

and

$$d_{2cs1}(50) = \sum_{i=1}^{n_2} \frac{d_{2_i cs1}(50)}{n_2} = \frac{0.73 + 0 + 0.44 + 0.44}{4} = 0.40$$

By using the family specific average of $d_{f_i c,1}(50)$, the variance of family-specific averages across families is obtained using Equation (5.9) as

$$\widehat{\text{Var}}\left(d_{f_i cs1}(50)\right) = \frac{\sum_{f=1}^{F} n_f \left\{d_{f cs1}(50) - d_{cs1}(50)\right\}^2}{n(F-1)}$$

$$= \frac{3 \times (0.34 - 0.38)^2 + 4 \times (0.40 - 0.38)^2}{7(2-1)} = 0.0009$$

Then, variance for $d_{cs1}(50)$ is obtained using Equation (5.6) as

$$\widehat{\mathrm{Var}}\big(d_{cs1}(50)\big) = \frac{4}{7} \times \widehat{\mathrm{Var}}\left(d_{f_i cs1}(50)\right) = \frac{4}{7} \times 0.0009 = 0.0005$$

Step 6: Estimate the covariance between $d_{f_i c1}(50)$ and $d_{f_i cs1}(50)$ and between $d_{c1}(50)$ and $d_{cs1}(50)$

By using the family specific average of $d_{f_i c,1}(50)$ and $d_{f_i cs,1}(50)$, the covariance between family specific averages across families is obtained using Equation (5.11) as

$$\begin{aligned}\widehat{\mathrm{COV}}\left(d_{f_i c1}(50), d_{f_i cs1}(50)\right) &= \frac{\sum_{f=1}^{F}\sum_{g=1}^{F} n_f\{d_{fcs1}(50) - d_{cs1}(50)\}\{d_{fc1}(50) - d_{c1}(50)\}}{n(F-1)} \\ &= \frac{3 \times (0.48 - 0.56)(0.34 - 0.38) + 4 \times (0.63 - 0.56)(0.40 - 0.38)}{7(2-1)} \\ &= 0.0022.\end{aligned}$$

Then, the covariance between $d_{c1}(50)$ and $d_{cs1}(50)$ is obtained using Equation (5.8) as

$$\widehat{\mathrm{COV}}\big(d_{c1}(50), d_{cs1}(50)\big) = \frac{4}{7} \times \widehat{\mathrm{COV}}\left(d_{f_i c1}(50), d_{f_i cs1}(50)\right) = \frac{4}{7} \times 0.0022 = 0.0012.$$

Step 7: Compute the time-dependent Kendall's tau and its variance

As shown in Equation (5.3), the time-dependent Kendall's tau is obtained as

$$\hat{\tau}_{td,U,1}(50) = \frac{d_{cs1}(50)}{d_{c1}(50)} = \frac{0.38}{0.56} = 0.68$$

and the corresponding variance is estimated using Equation (5.5) such as

$$\widehat{\mathrm{Var}}\left(\tau_{td,U,1}(50)\right) = \frac{\widehat{\mathrm{Var}}\big(d_{cs1}(50)\big)}{d_{c1}(50)^2} - \frac{2d_{cs1}(50)\widehat{\mathrm{COV}}\big(d_{c1}(50), d_{cs1}(50)\big)}{d_{c1}(50)^3} + \frac{d_{cs1}(50)^2\widehat{\mathrm{Var}}\big(d_{c1}(50)\big)}{d_{c1}(50)^4}$$

$$= \frac{0.0005}{0.56^2} - \frac{2 \times 0.38 \times 0.0012}{0.56^3} + \frac{0.38^2 \times 0.0030}{0.56^4} = 0.0008.$$

Step 8: Determine the time-dependent C-index and its variance

By using the linear relationship between Kendall's tau and the C-index as shown in Equation (5.4), the overall TDUC is estimated as

$$\hat{C}_{td,U,1}(50) = 0.5\left(\hat{\tau}_{td,U,1}(50) + 1\right) = 0.5\left(\frac{0.38}{0.56} + 1\right) = 0.5 \times 1.68 = 0.84.$$

Similarly, the variance of overall TDUC is estimated as

$$\widehat{\mathrm{Var}}\left(C_{td,U,1}(50)\right) = \widehat{\mathrm{Var}}\left(\frac{1}{2}\{\tau_{td,U,1}(50) + 1\}\right) = \frac{1}{4}\widehat{\mathrm{Var}}\left(\tau_{td,U,1}(50)\right) = \frac{1}{4} \times 0.0008 = 0.0002.$$

Furthermore, the 95% confidence interval of the time-dependent C-index can be obtained as

$$\hat{C}_{td,U,1}(50) \pm 1.96 \times \sqrt{\widehat{\mathrm{Var}}\left(C_{td,U,1}(50)\right)} = 0.84 \pm 1.96 \times \sqrt{0.0002} = (0.81, 0.86)$$

where the lower bound is 0.81 and upper bound is 0.86. We further presented the illustration of estimating the TDUC with its variance using R in Appendix B

5.2 Calibration

5.2.1 Brier score and integrated Brier score

Alternatively, calibration quantifies how close the predicted probabilities or the predicted risks of an event are to the observed event rates given the duration of time (Harrell et al., 1996; Steyerberg et al., 2010). For example, if we predict a 10% failure probability, approximately 10 out of 100 subjects should have a disease. It can be quantified using the Brier score, which evaluates the accuracy of the survival model at a specific time point.

The Brier score was proposed by Brier (1950) and was extended by Graf et al. (1999) to survival data. Gerds and Schumacher (2006) further introduced the consistent version of the Brier score, which uses the IPCW to account for the loss of information due to censoring. With survival data, the Brier score can be used to evaluate the accuracy of a survival model at a given time t. Mathematically, it is calculated as the difference between the predicted event probabilities and the true event status at a certain prediction time point t. It ranges from 0 to 0.25, where a value closer to 0 indicates better overall performance, whereas the model that performs no better than a chance has a value of 0.25. The Brier score evaluated at time t is defined as

$$\begin{aligned} BS(t) &= \mathrm{E}[I(T > t) - S(t|\boldsymbol{X})]^2 \\ &= \frac{1}{N}\sum_{i=1}^{N}\{I(T_i > t) - S_i(t|\boldsymbol{X_i})\}^2 \end{aligned}$$

where $S_i(t|\boldsymbol{X_i})$ is the survival probability for individual i at time t conditional on the covariate vector $\boldsymbol{X}$. Schoop et al. (2011) extended the Brier score to the framework of competing risks and introduced the consistent Brier score estimator. They considered two competing events and computed the Brier score by using the penetrance of a specific event instead of the survival probability.

The Brier score only provides a snapshot of the predictive ability of a model at a specific time point t. Hence, it is difficult to evaluate the model at all available times. The integrated Brier score (IBS) can be used to remedy this problem by providing an overall measure of model performance within a time interval $[0, t]$. The IBS over the interval $[0, t]$ is defined as

$$IBS(t) = \frac{1}{t}\int_0^t BS(s)ds$$

where the IBS provides an average Brier score across a time interval.

5.2.2 Time-dependent Brier score for competing risk data

Conditional on a vector of covariates $\boldsymbol{X}$, the Brier score for event j at time point t in the presence of competing risks is defined as

$$BS_j(t) = E\{I(T < t, \delta = j) - F_j(t|\boldsymbol{X})\}^2.$$

Then, the consistent estimator of $BS_j(t)$ was proposed by Schoop et al. (2011) to remove dependence on the censoring distribution by applying an IPCW. Then, the Brier score for event j at time t can be estimated as

$$\widehat{IBS}_j(t) = \frac{1}{n}\sum_{f=1}^{F}\sum_{i=1}^{n_f}\left\{I\left(t_{f_i} \le t, \delta_{f_i} = j\right) - F_{f_i j}\left(t|\boldsymbol{X}_{f_i}, Z_{f_j}\right)\right\}^2 w\left(t_{f_i}, t, \delta_{f_i}\right)$$

where

$$w\left(t_{f_i}, t, \delta_{f_i}\right) = \frac{I\left(t_{f_i} \le t, \delta_{f_i} \neq 0\right)}{\hat{G}_c(t_{f_i}-)} + \frac{I\left(t_{f_i} > t\right)}{\hat{G}_c(t)}$$

$\hat{G}_c(t)$ represents Kaplan-Meier estimator of the censoring distribution and $t_{f_i} -$ is a time point just before t_{f_i}.

Then, the IBS for event j over the interval $[0, t]$ can be estimated as

$$\widehat{IBS}_j(t) = \frac{1}{t}\int_0^t \widehat{BS}_j(s)ds.$$

Chapter 6 Application to Hereditary Breast and Ovarian Cancer Family

This chapter describes the analysis of the HBOC family data. Our main objective is to evaluate the efficiency of using the B-spline compared to two parametric models, the permanent exposure and the Cox and Oakes models, in the context of estimating the time-dependent effect of RRSO within the cause-specific correlated frailty competing risks model. Section 6.1 presents a descriptive analysis of the BRCA 1 mutation positive family data. Section 6.2 describes the specification of the fitted model. In Section 6.3, the risk of breast cancer is estimated under three different time-dependent effect models with time-dependent covariates, and penetrance by age 70 is estimated with for various screening and surgery times. Section 6.4 summarizes the evaluation of the performance of models with different time-dependent effect functions. Section 6.5 provides a summary of the results.

6.1 HBOC family data

Hereditary breast-ovarian cancer syndrome is an inherited condition characterized by mutations in tumour suppressor genes, BRCA 1 and BRCA 2 genes, causing a significant increase in the risk of breast cancer and ovarian cancer (Petrucelli et al., 2022). Mutation carriers tend to develop either BC, OC or both of them earlier in life as well. The BRCA 1 mutation carrier family data used in this thesis was obtained from the Breast Cancer Family Registries, which recruited families from six participating sites in the United States, Canada and Australia (John et al., 2004). The HBOC is a population-based dataset featuring families at high risk of BC or OC based on family history or genetic mutation such as those in the BRCA1 genes. The BCFR dataset includes a three-generation pedigree involving the proband, the initial family member who entered the study, and second-degree relatives. Variables considered include study entry time for probands, the ages at the event (BC, OC, and death), mutation status in BRCA 1 genes, and preventive

interventions statuses such as mammographic screening, risk-reducing mastectomy, and risk-reducing salpingo-oophorectomy.

As shown in Table 6.1, the data used in this study consisted of 498 BRCA1 mutation carrier families recruited through BCFR consisting of 2650 women. Of the 2650 women, 924 (34.9%) experienced BC as the first event, 182 (6.9%) women experienced OC as the first event, and 958 (36.2%) women died before developing either BC or OC. Women who did not experience any event prior to the last observed times are considered censored.

A small portion of women underwent prophylactic surgeries. 166 (6.2%) women underwent RRSO, and 64 (2.4%) women underwent RRM. We assumed that those who underwent RRM would not experience BC, and those who underwent RRSO would not experience OC. More women opted for screening rather than surgery: 360 (13.6%) women had one screening, 101 (3.8%) had two screenings, and 108 (4.1%) had three screenings.

Table 6.2 summarizes the time distribution for three different MS, the times between screenings, and RRSO. The mean age at RRSO and first MS are 44.4 and 40.6 years, respectively, and the mean time between BC and RRSO is 11.3 years. In addition, the mean times between consecutive screening times are presented, where the mean time between first and second screenings and second and third screenings are 9.2 and 6.2 years, respectively.

Table 6.1: Characteristics of BRCA 1 mutation carrier families.

	Breast cancer	Ovarian cancer	Death	Censored	Total
Number of individuals					
N (%)	924 (34.9%)	182 (6.9%)	958 (36.2%)	586 (22.1%)	2650
Age at event diagnosis					
Mean	44.2	53.0	70.5	50.9	55.8
Min, Max	21, 86	28, 89	18.5, 102.5	18.1, 95	18.1, 102.5
BRCA 1 mutation status					
Carrier	705 (76.3%)	91 (50%)	87 (9.1%)	240 (41.0%)	1123 (42.4%)
Non-carrier	219 (23.7%)	91 (50%)	871 (90.9%)	346 (59.0%)	1527 (57.6%)
Number of screenings					
0	722 (78.1%)	158 (86.8%)	944 (98.5%)	257 (43.9%)	2081 (78.5%)
1	160 (17.3%)	19 (10.4%)	7 (0.7%)	174 (29.7%)	360 (13.6%)
2	31 (3.4%)	4 (2.2%)	3 (0.3%)	63 (10.8%)	101 (3.8%)
3	11 (1.2%)	1 (0.5%)	4 (0.4%)	92 (15.7%)	108 (4.1%)
Type of surgery					
None	896 (97.0%)	181 (99.5%)	946 (98.8%)	441 (75.3%)	2464 (93.0%)
RRSO	28 (3.0%)	0 (0.0%)	9 (0.9%)	129 (22.0%)	166 (6.2%)
RRM	0 (0.0%)	1 (0.6%)	3 (0.3%)	60 (10.2%)	64 (2.4%)

RRSO for risk-reducing salpingo-oophorectomy and RRM for risk-reducing mastectomy

Table 6.2: Characteristics of the times of mammography screening (MS) and risk-reducing salpingo oophorectomy (RRSO) for BRCA 1 mutation carrier families.

	Mean	Standard deviation
RRSO	44.4	9.1
First MS	40.6	12.4
BC - RRSO	11.3	8.4
Time between two screenings		
MS1 – MS2	9.2	7.5
MS2 – MS3	6.2	4.2

RRSO for risk-reducing salpingo-oophorectomy

MS1, MS2 and MS3 for the first, second and third mammographic screenings

BC stands for breast cancer

6.2 Model specification

The cause-specific correlated frailty competing risks model with different functions for time-dependent effects of binary time-dependent covariates discussed in Chapter 3 is fitted to the HBOC data. The model includes one binary time-invariant covariate and four time-dependent covariates, presenting mutation status, the three screening statuses and RRSO status. Formally,

1. G: mutation status, a binary time-invariant covariate taking the value 1 for mutation carriers and 0 for non-carriers. The cause-specific hazard models for all events, BC, OR, and death, are affected by this variable.

2. $X(t, t_{S_k})$: The three screening statuses are considered as binary TDCs, wherein the kth screening status change at the time t_{s_k} of the kth screening occurrence, i.e., $X(t, t_{S_k}) = I(t_{S_k} \leq t < t_{S_{k+1}})$ for $k = 1,2,3$, $t_{S_1} < t_{S_2} < t_{S_3}$ and $X(t, t_{S_3}) = 1$ for $t > t_{S_3}$.

3. $X(t, t_r)$: RRSO status is considered as a binary TDC, wherein the RRSO status change at the time t_r of RRSO occurrence, i.e., $X(t, t_r) = I(t > t_r)$.

Then, the cause-specific hazard functions for breast cancer, ovarian cancer and death are expressed respectively as

$$h_{f,1}\left(t\middle|G, Z_{f_1}, \boldsymbol{X}(\boldsymbol{t}, \boldsymbol{t_s}), X(t, t_r)\right) = h_{01}(t) Z_{f_1} \exp\left\{\gamma_{1g} G + g_{s1}\left(t, X\left(t, t_{S_1}\right)\right) + g_{s2}\left(t, X\left(t, t_{S_2}\right)\right) + g_{s3}\left(t, X\left(t, t_{S_3}\right)\right) + g_r\left(t, X(t, t_r)\right)\right\}$$

$$h_{f,2}\left(t\middle|G, Z_{f_2}\right) = h_{02}(t) Z_{f_2} \exp\{\gamma_{2g} G\}$$

$$h_{f,3}(t|G) = h_{03}(t) \exp\{\gamma_{3g} G\}$$

where $\boldsymbol{X}(\boldsymbol{t}, \boldsymbol{t_s}) = \left\{X\left(t, t_{S_1}\right), X\left(t, t_{S_2}\right), X\left(t, t_{S_3}\right)\right\}$ is the vector of TDCs for screenings, $h_{0j}(t) = \lambda_j \rho_j \left(\lambda_j t\right)^{\rho_j - 1}, j = 1,2,3$ are Weibull baseline hazard functions and γ_{jg} are the effect of mutation status for event j. Similary, Z_{f_1} and Z_{f_2} are event specific frailties for breast cancer and ovarian cancer. Since the correlation between breast cancer and death and between ovarian cancer and death are close to 0, and the frailty parameter for death is not significant, only the frailty parameters for breast cancer and ovarian cancer are considered (Choi et al., 2021).

We considered three different functions for the effect of RRSO

$$g_r\left(t, X(t, t_r)\right) = \begin{cases} 0 & \text{if } t \le t_s \text{ (PE, CO, BS)} \\ \beta_r & \text{if } t > t_s \text{ (PE)} \\ \beta_r e^{-\eta(t - t_r)} + \eta_0 & \text{if } t > t_s \text{ (CO)} \\ \sum_{k=0}^{K+D} \beta_{r,k} B_{k,D}(t - t_r) & \text{if } t > t_s \text{ (BS)} \end{cases}$$

where only one parameter, β_r, is involved as a TDE for the PE model. The parameters involved in the CO model are $\{\beta_r, \eta, \eta_0\}$ and the number of parameters involved in the BS model depends on the polynomial degree D and the number of interior knots K. The BS model features a total of parameters is $K + D + 1$ parameters including the intercept. In this study, to provide a smooth curve of the effect of RRSO, the B-spline model is constructed with a degree of 2, boundary knots (0, 57) and 2 interior knots (5.74, 12.76),

where the two interior knots represent the 33rd and 66th quantile of the time difference between RRSO event time and end of follow-up, and the second boundary knot $t = 57$ represents the maximum time difference between end of follow-up and RRSO event time.

In contrast to the effect of RRSO, Choi et al. (2021) demonstrated that the effects of the three screenings under the CO model are significant based on the likelihood ratio test comparing a model with the screenings and to one with no screenings. Thus, the CO model is used for the effect of three different screenings, where the first, second, and third screening effects are defined as

$$g_{S_1}\left(t, X\left(t, t_{S_1}\right)\right) = \begin{cases} 0 & \text{if } t \le t_{S_1} \text{ or } t > t_{S_2} \\ \beta_{S_1} e^{-\eta_{S_1}(t - t_{S_1})} + \eta_{0S_1} & \text{if } t_{S_1} < t \le t_{S_2} \end{cases}$$

$$g_{S_2}\left(t, X\left(t, t_{S_2}\right)\right) = \begin{cases} 0 & \text{if } t \le t_{S_2} \text{ or } t > t_{S_3} \\ \beta_{S_2} e^{-\eta_{S_2}(t - t_{S_2})} + \eta_{0S_2} & \text{if } t_{S_2} < t \le t_{S_3} \end{cases}$$

and

$$g_{S_3}\left(t, X\left(t, t_{S_3}\right)\right) = \begin{cases} 0 & \text{if } t \le t_{S_3} \\ \beta_{S_3} e^{-\eta_{S_3}(t - t_{S_3})} + \eta_{0S_3} & \text{if } t_{S_3} < t \end{cases}$$

where the effects of screenings exponentially decay over time at a rate of η_{S_k} before eventually converging to a certain value η_{0S_k} for $k = 1,2,3$.

6.3 Analysis of risk of breast cancer

The hazard ratio (HR), also known as the relative risk, is obtained via the exponential transformation of the modelled risk scores. The log relative risk of BRCA mutation status, mammographic screenings and RRSO on the events of breast cancer, ovarian cancer and death, along with their corresponding robust standard errors (SE) and p-values, were estimated using three different time-dependent effects models (PE, CO, BS). The results from the three models are summarized in Table 6.3, wherein similar patterns for the parameter estimates related to the baseline hazard function, mutation status and

first screening for the PE, CO and BS models were found. However, differing patterns appeared in the parameter estimates related to frailties, second and third screenings, and RRSO obtained under the PE, CO and BS models. Nevertheless, all models provided evidence that all covariates are significantly associated with the risk of developing breast cancer except for the frailties.

To better illustrate the time-dependent effects of screenings and RRSO over time associated with breast cancer, Figure 6.1 displays the hazard ratio measuring the time-dependent effect of three different screenings for the BS models, assuming the CO model for screening effects. The HRs of the first and third screenings are above 1, whereas the HR of the second screening converges to a value below 1. Similarly, Figure 6.2 presents the hazard ratio of RRSO on breast cancer for the PE, CO and BS models, respectively. Although different effects of RRSO are obtained across the models, all of them obtained a negative association between RRSO and risk of developing breast cancer in BRCA 1. The PE model has a constant effect of RRSO on breast cancer, whereas such an effect varies over time for the CO and BS models. The HR of RRSO for both CO and BS models drastically increases, but the HR for the CO model eventually converges to a particular value. In contrast, the HR for the BS model fluctuates over time as it provides a smooth curve of the effect of RRSO.

To identify the best fitting model, we used the AIC, where the lowest AIC indicates the best fit of the model to data. According to AIC, the BS model (AIC = 19076.954) fits the data better than the PE (AIC = 19080.393) and CO (AIC = 19077.433) models, although the AIC difference between BS and CO models is quite small. Then, we describe the results of the parameter and penetrance estimators based on the BS model chosen as the best fitting model.

Table 6.3: Parameter estimates and AICs based on the correlated competing risks models with frailties; the Cox and Oakes model is assumed for mammography screening (MS) and permanent exposure, Cox and Oakes and B-spline are used for risk-reducing salpingo-oophorectomy (RRSO).

	Permanent Exposure			Cox and Oakes			B-Spline			
Parameter	EST	SE	p-value	EST	SE	p-value	EST	SE	p-value	
log (λ_1)	-4.678	0.038	< 0.001	-4.692	0.039	< 0.001	-4.680	0.038	< 0.001	
log (ρ_1)	0.972	0.029	< 0.001	0.960	0.029	< 0.001	0.955	0.028	< 0.001	
log (λ_2)	-4.825	0.047	< 0.001	-4.782	0.043	< 0.001	-4.804	0.044	< 0.001	
log (ρ_2)	1.189	0.044	< 0.001	1.208	0.043	< 0.001	1.212	0.043	< 0.001	
log (λ_3)	-4.178	0.008	< 0.001	-4.176	0.008	< 0.001	-4.179	0.008	< 0.001	
log (ρ_3)	1.436	0.034	< 0.001	1.435	0.034	< 0.001	1.445	0.034	< 0.001	
Mutation Status										
γ_{1g}	2.262	0.127	< 0.001	2.254	0.126	< 0.001	2.190	0.124	< 0.001	
γ_{2g}	1.594	0.231	< 0.001	1.484	0.230	< 0.001	1.614	0.229	< 0.001	
γ_{3g}	-0.329	0.138	0.017	-0.355	0.139	0.011	-0.357	0.142	0.012	
Frailties										
log (k_0)	0.380	0.361	0.293	0.426	0.401	0.289	0.711	0.450	0.114	
log (k_1)	0.670	0.387	0.083	0.633	0.412	0.124	0.217	0.793	0.785	
log (k_2)	-0.605	0.724	0.402	-0.038	0.788	0.962	0.298	0.712	0.676	
First MS on Breast Cancer										
β_{S_1}	3.572	0.252	< 0.001	3.437	0.256	< 0.001	3.351	0.266	< 0.001	
log (η_{S_1})	1.553	0.245	< 0.001	1.544	0.238	< 0.001	1.439	0.246	< 0.001	
η_{oS_1}	0.306	0.145	0.034	0.357	0.141	0.011	0.343	0.143	0.016	
Second MS on Breast Cancer										
β_{S_2}	3.873	0.424	< 0.001	3.967	0.455	< 0.001	4.153	0.512	< 0.001	
log (η_{S_2})	1.030	0.365	0.005	0.869	0.368	0.018	0.789	0.402	0.049	
η_{oS_2}	-0.272	0.367	0.458	-0.434	0.412	0.292	-0.601	0.507	0.235	
Third MS on Breast Cancer										
β_{S_3}	4.142	0.699	< 0.001	3.949	0.972	< 0.001	3.712	0.808	< 0.001	
log (η_{S_3})	2.305	0.759	0.002	1.548	1.239	0.211	2.084	0.730	0.004	
η_{oS_3}	0.114	0.363	0.754	-0.378	0.597	0.526	0.028	0.390	0.943	
RRSO on Breast Cancer										
β_r	-0.605	0.203	0.003	-1.787	0.714	0.012	$\beta_{r,0}$	-2.513	1.012	0.013
log (η_r)	-	-	-	-0.187	0.451	0.678	$\beta_{r,1}$	0.482	0.632	0.446
η_{or}	-	-	-	-0.411	0.236	0.081	$\beta_{r,2}$	-0.987	0.451	0.029
							$\beta_{r,3}$	0.688	2.100	0.743
							$\beta_{r,4}$	-6.121	8.019	0.445
-loglik	9518.196			9514.717			9512.477			
AIC	19080.393			19077.433			19076.954			

SE represents robust standard error. λ_j and ρ_j represent the parameters related to the baseline hazard function and γ_j are the mutation status parameters for jth event. β_{sk}, η_{sk} and η_{0sk} represent the parameters related to the kth screening. k_0, k_1 and k_2 are the frailty parameters. -loglik is the negative log-likelihood value for the fitted model and AIC represents the Akaike information criterion.

6.3.1 Genetic effect

The genetic effects were estimated similarly across different models. We describe the results based on the BS model chosen as a best fit of the model. On the risk of developing breast cancer in the presence of competing risks, adjusting for the RRSO and three MSs as TDCs in the model, the effects of mutation status on all events were found to be significant with the log relative risks of $\hat{\gamma}_{1g} = 2.190$ (95% CI between 1.948 and 2.433; $p < 0.001$), $\hat{\gamma}_{2g} = 1.613$ (95% CI between 1.164 and 2.063; $p < 0.001$), and $\hat{\gamma}_{3g} = -0.357$ (95% CI between -0.635 and -0.078; $p = 0.012$) for BC, OC and death, respectively. These results indicate that being a mutation carrier increases the cause-specific hazard of developing BC and OC by 8.93 and 5.02, respectively, whereas it decreases the risk of death by 0.7 compared to non-mutation carriers.

6.3.2 Screening effect

Up to three screenings were considered and each screening as TDC. We assumed the CO model for the effects of the screenings as it was found to be the best model for screenings from the previous study (Choi et al., 2021). The effects of the first, second and third screenings on breast cancer were significant across all models. Also, the shapes of the changes in the HRs for the screenings are similar for all the models, where the time-dependent effects of the screenings can be assessed by estimating the HR given by $g_{S_k}\left(t, X\left(t, t_{S_k}\right)\right), k = 1,2,3$. Figure 6.1 presents the time-dependent HRs of each screening estimated on a continuous scale from 0.5 to 10 years under the best fitting model (BS model). As shown in Figure 6.1, the HRs of the screenings are reduced over time from HR = 2.117 (95% CI between 1.756 and 2.479) to HR = 1.409 (95% CI between 1.118 and 1.701), from HR = 2.183 (95% CI between 1.422 and 2.944) to HR = 0.548 (95% CI between -0.490, 1.586), and from HR = 1.100 (95% CI between 0.247 and 1.952) to HR = 1.029 (95% CI between 0.260 and 1.797), respectively, from 0.5 to 10 years after screenings. The HRs of the first and third screenings exponentially decayed but stayed above 1, which indicates that having a first or third screening increase the risk of developing BC. In contrast, the HR of the second screening decayed to below 1,

indicating that having a second screening eventually decreases the risk of developing BC. The results also demonstrate that the most changes in the HR occurred in the second screening among three screenings, whereas the HR of the third screening did not vary a lot over time.

6.3.3 RRSO effect

In opposition to the screenings, the time-dependent effect of RRSO was modelled under three structures (PE, CO, BS) that is given by $g_r\big(t, X(t, t_r)\big)$, where the effect of RRSO stays constant for PE and exponentially decays to a certain value for CO. In contrast, the BS model is obtained as a linear combination of the BS basis function and their coefficients, leading to the effect providing a smooth curve that fluctuates over time while having a peak and trough. By fitting the models, the results under all models showed a negative association between RRSO and breast cancer risks. We present the effect of RRSO in terms of HR changes over time graphically in Figure 6.2 and its point and interval estimates from 0.5 to 20 years after surgery in Appendix A Table A.1.

Since there is a negative association between RRSO and breast cancer risks for all models, having RRSO reduces the risk of developing breast cancer. Then, although each model obtained the different shapes of the HR of RRSO over time, the values of HR for all models stay below 1. As shown in Figure 6.2, the HR of RRSO for the PE model stays constant as the effect of RRSO stays constant. For the CO model, the HR of RRSO depicts the shape of a logarithmic growth curve, where the HR has a period of rapid increase and is followed by a period where the growth slows. In contrast to the PE and CO models, the HR of RRSO for the BS model fluctuates over time, where the HR drastically increases for the first five years. Once it reaches the peak, the HR radically decreases, but it slowly increases over time.

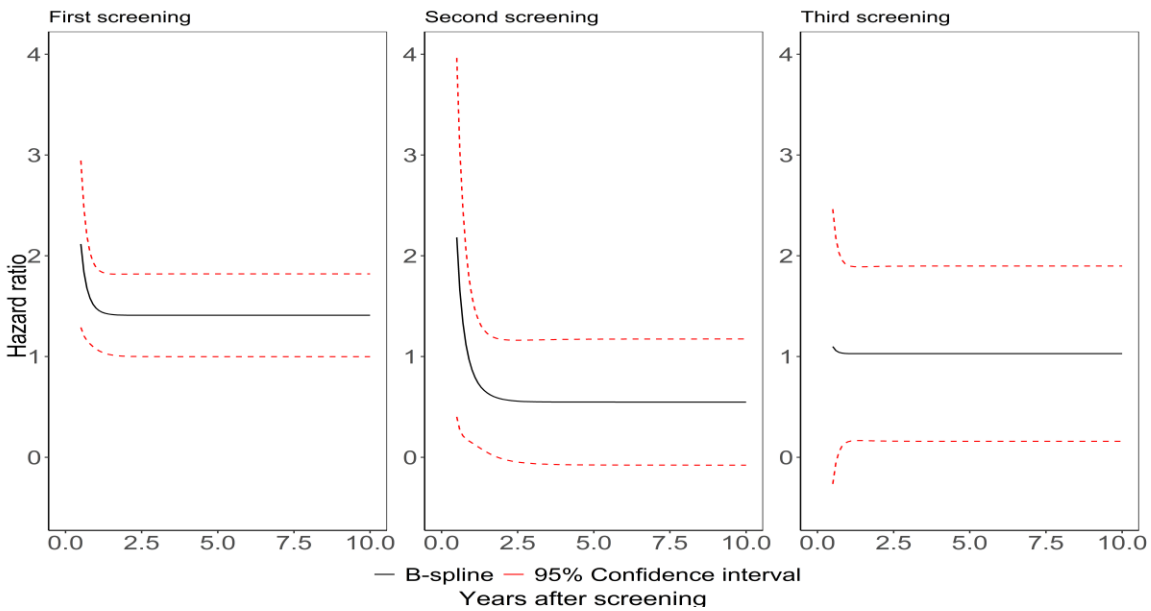

Figure 6.1: Hazard ratios (black) and their 95% confidence intervals (red) measuring the time-dependent effect of mammography screenings (MSs) on breast cancer, assuming Cox and Oakes model for the effects of MSs and B-spline model for the effects of risk-reducing salpingo-oophorectomy (RRSO) in BRCA 1 mutation families.

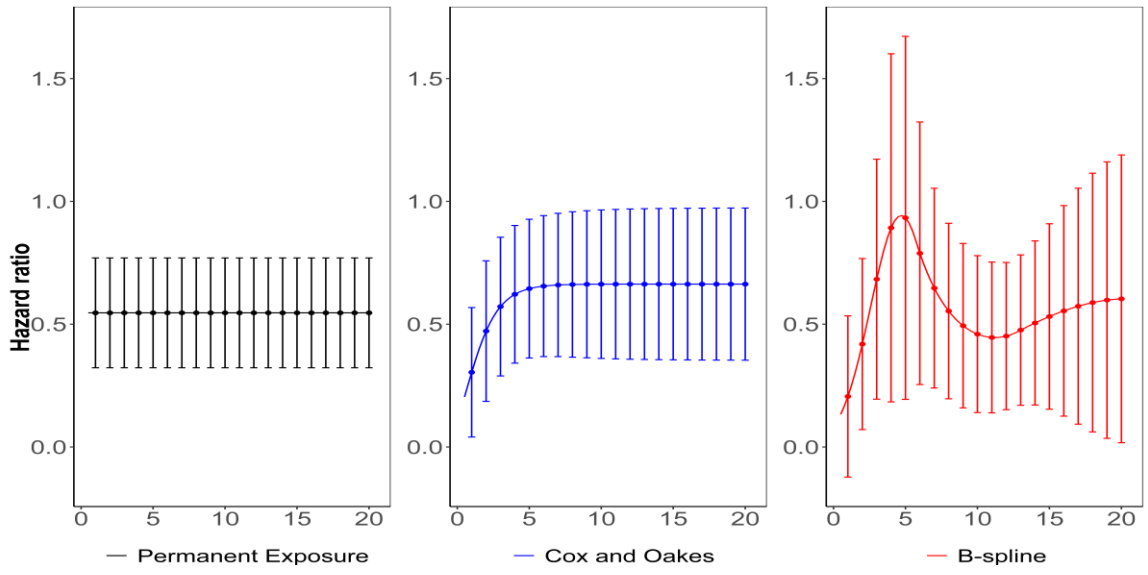

Figure 6.2: Hazard ratios and their 95% confidence intervals measuring the time-dependent effect of risk-reducing salpingo-oophorectomy on breast cancer under different time-dependent effect models (B-spline (red), Cox and Oakes (blue), permanent exposure (black)) for BRCA 1 mutation families.

Since the effect of RRSO is negatively associated with the risk of developing breast cancer, the large effect of RRSO is equivalent to the low breast cancer risks. Under the BS model, the effect of RRSO reduces from time 0.5 to 4.75 years, leading to increasing the risk of developing breast cancer that is HR = 0.206 (95% CI between -0.122 and 0.534) to HR = 0.942 (95% CI between 0.183 and 1.701), which is a trough of the effect of RRSO and a peak of HR of RRSO on breast cancer. Then, the effect of RRSO increases and reaches a trough at 11.25 years, indicating that the HR of RRSO to be decreased, that is HR = 0.446 (95% CI between 0.141 and 1.189). Again, the effect of RRSO decreases from 11.25 to 20 years, which increases the HR of RRSO to 0.603 (95% CI between 0.017 and 1.189). Then, the results demonstrate that RRSO increases the cause-specific hazard of developing breast cancer right after RRSO, eventually decreasing it. Furthermore, RRSO is highly significant based on the likelihood ratio test obtained by comparing a model with RRSO and without RRSO, where the p value equals 0.001.

6.3.4 Dependence between competing events

As described in Section 3.2, the shared frailties within families for each competing event depict dependences between events or within families for each event. The estimates of frailty parameters k_0, k_1 and k_2 obtained using the BS model are 2.037 (95% CI between 0.242 and 3.831), 1.242 (95% CI between -0.689 and 3.173) and 1.346 (95% CI between -0.532 and 3.225). Then, the estimated correlation between breast cancer and ovarian cancer is obtained as

$$\rho = \frac{k_0}{\sqrt{(k_0 + k_1)(k_0 + k_2)}} = \frac{2.037}{\sqrt{(2.037 + 1.242)(2.037 + 1.346)}} = 0.612$$

with 95% confidence interval between 0.218 and 0.874, indicating that the frailties of two events are not independent. In other words, there is a significant correlation between two events, breast cancer and ovarian cancer.

In addition, the variance of each frailty is obtained as $1/(k_0 + k_1) = 1/(2.037 + 1.242) = 0.305$ for BC and $1/(k_0 + k_2) = 1/(2.037 + 1.346) = 0.296$ for OC. The corresponding measures of familial correlation, Kendall's tau, are estimated as

$$\tau_1 = \frac{1}{1 + 2 \times (k_0 + k_1)} = \frac{1}{1 + 2 \times (2.037 + 1.242)} = 0.132$$

for BC with 95% confidence interval between 0.063 and 0.175 and

$$\tau_2 = \frac{1}{1 + 2 \times (k_0 + k_1)} = \frac{1}{1 + 2 \times (2.037 + 1.346)} = 0.129$$

for OC with 95% confidence interval between 0.057 and 0.243. Both values of 0.132 and 0.129 indicate the low within familial correlation for breast cancer and ovarian cancer, respectively. Although the estimates of frailty parameters k_0, k_1 and k_2 under the BS model are different from those under other models, the estimated measures of familial correlation are similar for all models. However, the PE model has the largest value of the estimated correlation between breast cancer and ovarian cancer, followed by the CO and BS models.

6.3.5 Penetrance estimation

Figure 6.3 presents breast cancer penetrance for a mutated woman with RRSO at different time points (30, 40, 50) and no MS while assuming the BS model for the effect of RRSO. The green, red, and blue lines represent a woman with RRSO at age 30, 40 and 50 years, respectively. The plot demonstrates that having RRSO earlier is beneficial to reduce breast cancer risks. To better illustrate the effect of RRSO and screenings on the cumulative risk of breast cancer among women with BRCA 1 mutations, Figures A.1 to A.3 in Appendix A display the breast cancer penetrance estimates with different screening and RRSO times. Figure A.1 shows the breast cancer penetrance given the screenings with no RRSO, and Figure A.2 shows the breast cancer penetrance given

RRSO without screenings. Figure A.3 presents the breast cancer penetrance given one to three screenings with RRSO.

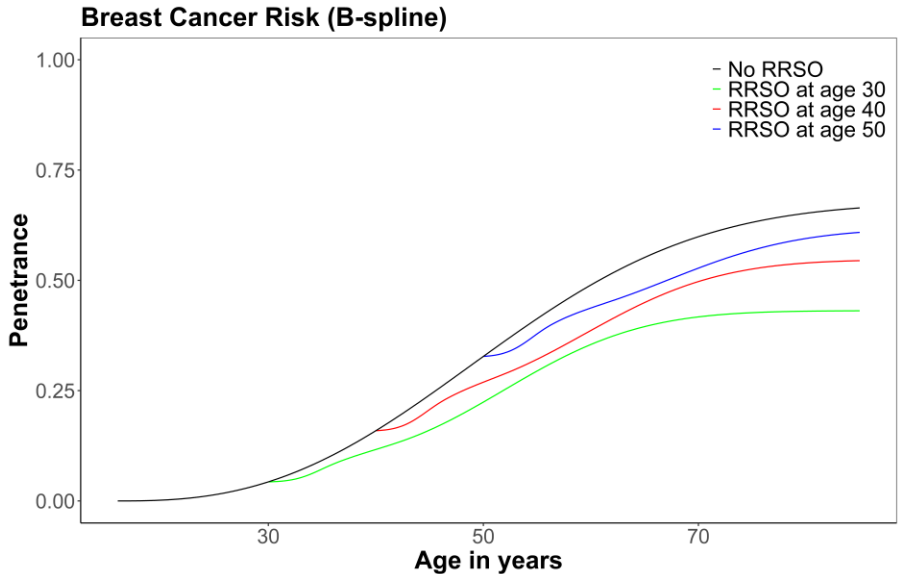

Figure 6.3: Breast cancer penetrance estimations for mutation carriers with risk-reducing salpingo-oophorectomy (RRSO). The black line represents a woman who did not have RRSO, the green line a woman who had RRSO at age 30 years, the red line a woman who had RRSO at age 40 years, and the blue line a woman who had RRSO at age 50 years.

We also present the penetrance estimates at age 70 from the correlated frailty competing risks model with different screening and RRSO times in Table 6.4. Denoting RRSO time by t_r and the kth screening time by t_{S_k}, we consider $t_{s1} = 35$, $t_{s2} = 37$ and $t_{s3} = 39$ as the first, second, and third screening times close to the mean ages from the data and three different RRSO times, $t_r = 30, 40, 50$ years, to evaluate the effect of RRSO. The following eight different breast cancer penetrances by age 70, denoted as P_1 to P_8, for mutation/non-mutation carriers are estimated:

1. P_1 = penetrance with no MS and no RRSO;

2. P_2 = penetrance with MS at ages 35, 37 and 39, no RRSO;

3. P_3 = penetrance with RRSO at age 30, no screening;

4. P_4 = penetrance with RRSO at age 40, no screening;

5. P_5 = penetrance with RRSO at age 50, no screening;

6. P_6 = penetrance with RRSO at age 40; MS at age 35;

7. P_7 = penetrance with RRSO at age 40; MS at ages 35 and 37;

8. P_8 = penetrance with RRSO at age 40; MS at ages 35, 37 and 39.

The penetrance estimates are obtained under each PE, CO and BS model. The results demonstrate that RRSO reduces the penetrance of BC for all three models, which indicates that having RRSO earlier is more beneficial. In contrast, having all three screenings increases the penetrance for both the PE and BS models, whereas it lowers the penetrance for the CO model. Similarly, having both RRSO and screenings lowers the penetrance of BC for both PE and BS models, whereas having only one screening with RRSO vaguely increases the penetrance for the CO model. Although all models obtain different penetrance estimates, changes in the trends of the penetrance estimates are similar except for the penetrances involving the screenings, where the changes in the penetrance for the CO model are in the opposite direction of the PE and BS models. Under the BS model, the penetrance at age 70 with no screenings nor RRSO is estimated at 0.125 (95% CI between 0.107 and 0.143) and 0.599 (95% CI between 0.555 and 0.643) for non-mutation carriers and mutation carriers, respectively. Since three consecutive screenings occurred at age 35, 37 and 39, the penetrances at age 70 for non-mutation carriers and mutation carriers are estimated at around 0.142 (95% CI between 0.061 and 0.223)/0.644 (95% CI between 0.474 and 0.815), respectively. The results show that having multiple screenings increases the penetrance.

For women with RRSO at 30 years, the breast cancer penetrance is 0.062 (95% CI between 0.023 and 0.101)/0.417 (95% CI between 0.233 and 0.602), while the breast cancer penetrance for women with RRSO at 50 years is 0.093 (95% CI between 0.067 and 0.119)/0.528 (95% CI between 0.447 and 0.609) for non-mutation carriers and

mutation carriers, respectively. Although there is not much change in the penetrance of the non-carriers, having RRSO earlier is beneficial to reduce the risk of breast cancer.

Similarly, the breast cancer penetrance at 70 years with RRSO at 40 years and the first screening at 35 years is 0.113 (95% CI between 0.062 and 0.164)/0.603 (95% CI between 0.465 and 0.740) while the penetrance with the same conditions and the second screening at time 37 is 0.066 (95% CI between 0.029 and 0.103)/0.429 (95% CI between 0.266 and 0.592) for non-mutation/mutation carriers, respectively. In contrast, with a third screening at 39 years, the penetrance increases to 0.099 (95% CI between 0.042 and 0.155)/0.556 (95% CI between 0.374 and 0.738) for non-mutation/mutation carriers, respectively. Since the hazard ratio of RRSO under the BS model is less than 1 as shown in Figure 6.2, the effect of RRSO has a negative association with the cause-specific hazard of breast cancer. However, since both hazard ratios of the first and third screenings are above 1, it turns out that the effects of RRSO and screenings do not affect the penetrance in the same ways.

Table 6.4: Penetrance estimates at age 70 from the correlated frailty competing risks model with time-dependent effects (TDE) of mammographic screenings (MS) and risk-reducing salpingo-oophorectomy (RRSO); Cox and Oakes model is assumed for MS; The permanent exposure, Cox and Oakes and B-spline models are considered for RRSO.

	Permanent Exposure		Cox and Oakes		B-Spline	
	Estimate	95% CI	Estimate	95% CI	Estimate	95% CI
Mutation status $G = 0$						
No MS and RRSO						
P_1	0.121	(0.104, 0.139)	0.120	(0.102, 0.137)	0.125	(0.107, 0.143)
No RRSO						
P_2	0.147	(0.066, 0.228)	0.105	(0.035, 0.175)	0.142	(0.061, 0.223)
No MS						
P_3	0.073	(0.043, 0.103)	0.085	(0.047, 0.122)	0.062	(0.023, 0.101)
P_4	0.078	(0.051, 0.106)	0.088	(0.055, 0.120)	0.082	(0.047, 0.117)
P_5	0.089	(0.066, 0.111)	0.094	(0.069, 0.119)	0.093	(0.067, 0.119)
Both MS and RRSO						
P_6	0.106	(0.067, 0.145)	0.122	(0.075, 0.170)	0.113	(0.062, 0.164)
P_7	0.076	(0.037, 0.114)	0.075	(0.035, 0.116)	0.066	(0.029, 0.103)
P_8	0.100	(0.048, 0.153)	0.082	(0.032, 0.132)	0.099	(0.042, 0.155)
Mutation status $G = 1$						
No screenings and surgery						
P_1	0.611	(0.568, 0.654)	0.608	(0.565, 0.652)	0.599	(0.555, 0.643)
No RRSO						
P_2	0.674	(0.515, 0.833)	0.572	(0.368, 0.777)	0.644	(0.474, 0.815)
No MS						
P_3	0.489	(0.366, 0.613)	0.537	(0.399, 0.675)	0.417	(0.233, 0.602)
P_4	0.507	(0.404, 0.609)	0.541	(0.429, 0.654)	0.497	(0.366, 0.629)
P_5	0.535	(0.463, 0.607)	0.552	(0.476, 0.629)	0.528	(0.447, 0.609)
Both MS and RRSO						
P_6	0.603	(0.493, 0.712)	0.649	(0.534, 0.764)	0.603	(0.465, 0.740)
P_7	0.493	(0.339, 0.647)	0.491	(0.326, 0.655)	0.429	(0.266, 0.592)
P_8	0.584	(0.422, 0.746)	0.517	(0.326, 0.709)	0.556	(0.374, 0.738)

$P_1 = F_1(70|t_r = \infty, t_{s1}{=}\infty, t_{s2} = \infty, t_{s3}{=}\infty)$; $P_2 = F_1(70|t_r = \infty, t_{s1}{=}35, t_{s2} = 37, t_{s3}{=}39)$;
$P_3 = F_1(70|t_r = 30, t_{s1}{=}\infty, t_{s2} = \infty, t_{s3}{=}\infty)$; $P_4 = F_1(70|t_r = 40, t_{s1}{=}\infty, t_{s2} = \infty, t_{s3}{=}\infty)$;
$P_5 = F_1(70|t_r = 50, t_{s1} = \infty, t_{s2} = \infty, t_{s3} = \infty)$; $P_6 = F_1(70|t_r = 40, t_{s1}{=}35, t_{s2} = \infty, t_{s3}{=}\infty)$;
$P_7 = F_1(70|t_r = 40, t_{s1}{=}35, t_{s2} = 37, t_{s3}{=}\infty)$; $P_7 = F_1(70|t_r = 40, t_{s1}{=}35, t_{s2} = 37, t_{s3}{=}39)$
CI stands for the confidence interval; t_r represents the age of RRSO and t_{sk} the age of the kth MS.

6.4 Performance measures

To examine the efficiency of the BS model, its model performance is compared with the PE and CO models via the TDUC, Brier score and IBS at various time points (55, 70, 85, 100 years). Since only 166 among 2650 individuals underwent RRSO, it caused all the models to have similar predictive abilities by obtaining the same values of the penetrance across all the models for those who did not undergo RRSO. To discern the effect of RRSO on the risk of breast cancer, we have only used 166 individuals who underwent RRSO to compute the performance measures. The results of TDUC, Brier score and IBS at different time points are presented in Tables 6.6 and 6.7.

6.4.1 Time-dependent Uno's C-index

The C-index is used to evaluate the discrimination ability of the models, where it can be seen as a proportion of the concordant pairs over the comparable pairs. Table 6.5 presents the number of the concordant, discordant and comparable pairs for all TDE models among those who underwent RRSO at different time points. All models obtained similar numbers of concordant and discordant pairs across time, which caused the models to have similar values of TDUC over time, as shown in Table 6.6. Nevertheless, the BS model has the largest number of concordant pairs with the smallest number of discordant pairs.

Table 6.6 presents the point estimates and their 95% confidence intervals at various truncation time points (55, 70, 85, 100 years) under the PE, CO and BS models. The truncation time of 100 years allows all comparable pairs to be included as the maximum observed time among 166 individuals is less than 100 years. The results in Table 6.6 show that the values of the TDUC increased with the larger truncation time points for all models. At most time points except time 55, the BS model provided the largest TDUC values ranged from 0.564 to 0.574, while the PE model provided the smallest TDUC values ranged from 0.524 to 0.555 regardless of the time points. Although these values indicate that the BS model has better prediction discrimination ability than the other model, TDUC values are similar across different models, indicating that the prediction discrimination abilities of these three models are indistinguishable.

Furthermore, the TDUC values for all models are greater than 0.5, but lower than 0.6, indicating a poor performance in terms of discrimination.

Table 6.5: Total number of the concordant, discordant and comparable pairs at different truncation times (55, 70, 85, 100) for different time-dependent effect models among 166 individuals underwent RRSO for different time-dependent effect models.

Time	Comparable pairs	Concordant pairs			Discordant Pairs		
		PE	CO	BS	PE	CO	BS
55	4070	2112	2230	2224	1948	1830	1836
70	5358	2876	2996	3000	2466	2346	2342
85	5452	2964	3084	3088	2472	2352	2348
100	5452	2964	3084	3088	2472	2352	2348

PE stands for permanent exposure model, CO for Cox and Oakes model, and BS for B-spline model

Table 6.6: Time-dependent Uno's C-index at different time points (55, 70, 85, 100 years) among 166 individuals underwent RRSO.

	Permanent Exposure		Cox and Oakes		B-Spline	
Time	EST	95% CI	EST	95% CI	EST	95% CI
55	0.524	(0.514, 0.533)	**0.549**	(0.541, 0.558)	0.547	(0.539, 0.556)
70	0.544	(0.536, 0.552)	0.563	(0.556, 0.571)	**0.564**	(0.556, 0.572)
85	0.555	(0.547, 0.563)	0.573	(0.566, 0.581)	**0.574**	(0.567, 0.582)
100	0.555	(0.547, 0.563)	0.573	(0.566, 0.581)	**0.574**	(0.567, 0.582)

EST stands for estimate, SE stands for the standard error and CI denotes the confidence interval.

6.4.2 Time-dependent Brier score

Alternatively, we examined the calibrations of different TDE models (PE, CO, BS models) via the Brier score and IBS over different time points. The changes of the Brier score and IBS values over time are graphically displayed in Figure 6.4, and the points estimates and 95% CIs at selected time points of 55, 70, 85 and 100 are presented in Table 6.7.

The Brier score is a cross-sectional measure that provides a snapshot of the predictive ability of a model at a specific time point, while the IBS gives an overall measure of model performance during a time interval $(0, t)$. Considering the Brier score and IBS as time-dependent prediction error and cumulative prediction error, respectively, smaller values indicate better performance in prediction.

As shown in Figure 6.4, the Brier scores and IBS are almost identical until age 60 across different models, and the CO model provides the smallest Brier score and IBS most of the time. We notice that although the CO model provides the smallest Brier score at time 55, the BS model provides the smallest IBS at time 55 (1.392, 95% CI=1.064, 1.675), and the CO model provides the smallest IBS afterwards, indicating that the BS model predicts better providing smallest prediction errors better until 55 then the CO model predicts better afterwards. It appears that the BS model does not predict well at later time points as the prediction of the BS model would be unstable with not enough data points available at later time points.

Table 6.7: Brier score and integrated Brier score (IBS) for 166 individuals who underwent RRSO at different truncation times (55, 70, 85, 100).

	Permanent Exposure		Cox and Oakes		B-Spline	
Time	EST	95% CI	EST	95% CI	EST	95% CI
Brier score						
$BS_1(55)$	0.114	(0.097, 0.131)	**0.111**	(0.096, 0.128)	0.112	(0.096, 0.128)
$BS_1(70)$	0.082	(0.063, 0.103)	**0.079**	(0.061, 0.102)	0.085	(0.065, 0.105)
$BS_1(85)$	0.047	(0.033, 0.070)	**0.044**	(0.030, 0.070)	0.056	(0.039, 0.071)
$BS_1(100)$	0.043	(0.030, 0.069)	**0.041**	(0.027, 0.069)	0.056	(0.038, 0.071)
Integrated Brier score						
$IBS_1(55)$	1.421	(1.073, 1.692)	1.397	(1.068, 1.674)	**1.392**	(1.064, 1.675)
$IBS_1(70)$	2.983	(2.335, 3.559)	**2.912**	(2.309, 3.516)	2.956	(2.326, 3.543)
$IBS_1(85)$	3.864	(2.983, 4.759)	**3.751**	(2.922, 4.711)	3.939	(3.036, 4.777)
$IBS_1(100)$	4.528	(3.443, 5.794)	**4.376**	(3.341, 5.746)	4.774	(3.605, 5.840)

$BS_1(t)$ is the Brier score at time t for breast cancer, denoted as 1.
$IBS_1(t)$ is the integrated Brier score within a time interval $(0, t)$ for breast cancer, denoted as 1.

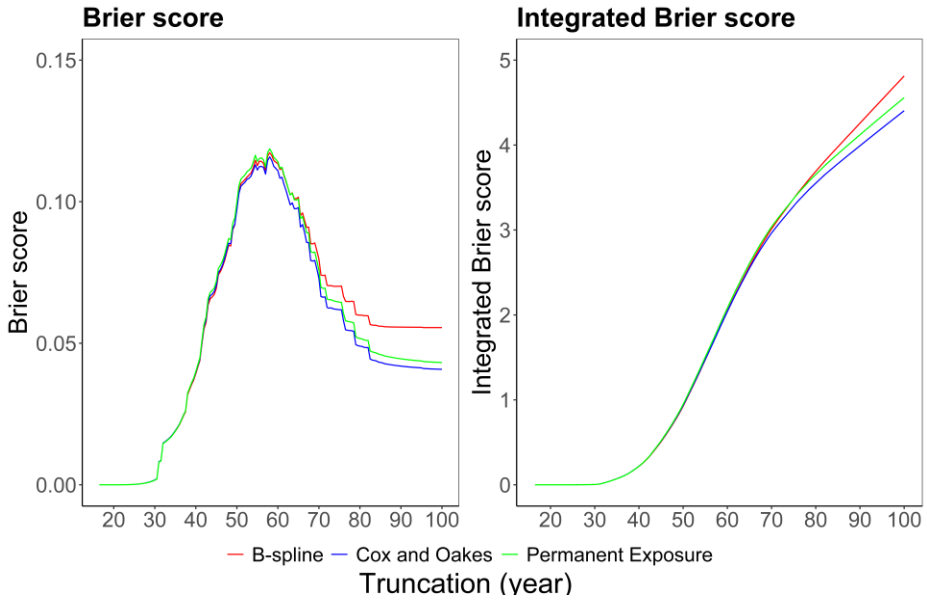

Figure 6.4: Time-dependent Brier score (left panel) and integrated Brier score (right panel) estimated from 16 to 100 years based on different time-dependent models (Permanent Exposure (green), Cox and Oakes (blue), and B-spline (red)).

6.5 Summary

We have analyzed the HBOC family data focusing on estimating the time-dependent effect of RRSO on breast cancer risks in the presence of competing events such as ovarian cancer and death. The time-dependent effect of RRSO was modelled parametrically using the PE and CO models and flexibly using the B-splines within the correlated frailty competing risks model.

Our study demonstrated that there is a significant negative association between RRSO and the risk of developing breast cancer in the presence of competing events as the hazard ratios of RRSO were estimated below 1 all the time under all TDE models. Especially the BS model enabled us to flexibly model the effect of RRSO over time, whose negative effect became weakened and provided a significant negative association after RRSO.

As the BS model provides flexible modelling of time-dependent effect, our data analysis shows the BS model fits the data well, providing the smallest AIC. In addition, we have further compared the model performance in terms of prediction ability based on discrimination (TDUC) and calibration (Brier score, IBS) at different time points. In terms of the TDUC, which assesses how well each model can distinguish between those and those without breast cancer, the BS model provided the highest discrimination overall. In terms of calibration, which quantifies how close the predicted probabilities or the predicted risks of outcomes are to the observed values, the CO model provided a better predictive ability with respect to calibration in general, even though the BS model performed slightly better before age 55. However, the three models we considered in our application appear to perform similarly, and their predictive performances were rather poor as their C-indexes were close to 0.5. Although there is no clearly better model in our study, the choice of the model often depends on the purpose of the study, and different measures can be used, where the TDUC can be used for finding a better discrimination model while the Brier score or IBS for finding a better calibration model.

Chapter 7 Discussion

7.1 Summary

This thesis aimed to incorporate B-splines to better capture the time-dependent effect of a binary time-dependent covariate in the correlated frailty competing risk model proposed by Choi et al. (2021). The performance of the BS model was evaluated via a simulation study, and the impact of misspecification of the TDE model was also examined. The simulation results demonstrate that the BS model leads to the unbiased parameter and penetrance estimates regardless of the size of the mutation effect or the strength of correlation between competing events when the data were generated under the CO or BS models, highlighting the flexibility of the BS model and its robustness to the misspecified TDE model.

We also extended Uno's C-index to account for both competing risks and TDC/TDE simultaneously. The time-dependent Uno's C-index was derived to evaluate the discriminative ability of models, which is applicable to TDC/TDE in the analysis of clustered competing risk data, and the variance of TDUC was derived to account for the clustering effect. The TDUC estimates the probability that the penetrance for randomly selected subject *i* is greater than the penetrance for randomly selected subject *j* if subject *i* experiences the event earlier than randomly selected subject *j* at the time for subject i experiences the event. The main difference of the proposed C-index to the conventional C-index is that the penetrance estimates of two subjects are compared at minimum observed times for two subjects. In contrast, the conventional C-index compares penetrance estimates obtained at each subject's observed time, while assuming the rank of two penetrance estimates to be constant. However, once TDC/TDE is incorporated, the rank of two penetrance estimates may change over time. Finally, we used the linear relationship between Kendall's tau and the C-index in combination with the Delta method to estimate the variance of our proposed C-index.

We analyzed HBOC family data recruited through BCFR to assess the time-dependent effect of risk-reducing salpingo-oophorectomy on the risk of developing breast cancer in the presence of ovarian cancer or death as the first event. Using a data subset of individuals who underwent RRSO, we compared the prediction ability of the correlated frailty competing risks model with different TDE models (PE, CO, BS) with respect to discrimination (TDUC) and calibration (Brier score). According to TDUC, the BS model obtained the highest discrimination, followed by the CO and PE models. Model performance with respect to calibration was assessed using the Brier score. The BS model obtained the smallest prediction errors with short time intervals, whereas the CO model obtained the smallest prediction errors with large time intervals. Since the measures of discrimination and calibration can quantify different prediction abilities, the choice of the model is subject to the purpose of the study.

7.2 Limitation and further work

This thesis has several possible limitations. First, we have considered MSs and RRSO as external binary TDCs. Kalbfleisch and Prentice (2002) classified TDCs into two different categories: external or internal covariates. An external covariate is external to the subject, meaning that it is not dependent on the survival of the subject, but it may influence the occurrence of the failure at time t. In other words, the occurrence of the external covariate is not affected by the subject's event status. The measure of air pollution on the frequency of asthma is the example of the external covariate, where such measure is not affected by the occurrence of asthma. In contrast, an internal covariate is dependent on the current event status of the individuals in the study, where the internal covariate requires the survival of the subject for its existence. For example, when a subject's blood pressure is measured over time, the measure of blood pressure is no longer available once the individual dies. Then, the measure of blood pressure ensures that the subject has not experienced the event, indicating the survival probability of death is 1. Thus, the effect of internal covariate may not be correctly estimated as its value varies based on the time of the failure. The hazard function and corresponding survival function can only be defined

up to the time of survival, but no further. We assume MSs and RRSO as the external covariates to address the problem of the interval covariate since the status of the screenings and RRSO are not directly related to breast cancer risks.

In this thesis, we have selected the location of the interior knots based on the quantiles of the difference between the subjects' last observed times and RRSO times to ensure an approximately equal number of events in each interval. Also, only a small number of degrees (2, 3) were considered to compare the efficiency of the model. However, the equidistance knot arrangement is not necessarily an optimal choice. Instead of using the quantile, the proper locations and number of knots can be selected by comparing the AIC for models with varying knot numbers or using generalized cross-validation (GCV) (Nan et al., 2005). The optimal interior knots can be selected by choosing a model that minimizes the AIC. Alternatively, the GCV can be used, where the placement of the knots can be chosen to minimize the GCV function. However, both AIC and GCV methods require intensive mathematical computations. Similarly, different degrees of the BS basis function can be used to provide a more flexible estimation of the effect of RRSO. However, there is a trade-off between roughness and smoothness in choosing the number of interior knots and degrees. The small number of knots and degrees leads to overly smooth, but it may be biased. In contrast, using a high number of knots and degrees conversely leads to unbiased estimates but increases the variability in the fit, resulting in overfitting.

Both simulation results and data application results demonstrated the flexibility of the BS model. The BS model obtained unbiased penetrance estimates in the simulation and obtained the smallest AIC and largest TDUC in the application, indicating that the BS model is the best-performing model. However, there are several limitations in the data. In contrast to the effect of RRSO, we only considered the CO model as TDEs of three different screenings because Choi et al. (2021) demonstrated that the effects of the three screenings under the CO model are significant. Under this model, the effect of screenings is exponentially decaying over time and eventually converges to a certain value. However, the effects of MSs could also be modelled considering the BS, which can flexibly estimate the effect of screenings. However, once the BS model is used, the

choice of the number of interior knots and degrees would be the problem. It may increase the variability of the coefficients related to the BS as more parameters are used for the screenings and RRSO.

Second, although the primary event of interest is the first occurrence of BC in our analysis, subjects may experience one of OC or death from other causes, where the occurrence of one event precludes the occurrence of other events. Hence, we proposed a model while considering those three events as competing risks. However, successive BC after the first BC can be the main interest in the competing risk analysis. Individuals in the study may experience several events, such as developing OC before experiencing BC, dying after the first BC, etc. However, our model does not allow the successive BCs after the first BC. Once we consider the successive events, the effects of RRSO or screenings might be different depending on the number of experienced BC. Also, such effects might differ between individuals who experienced other events first. Furthermore, we have assumed that the screenings and RRSO only affect the BC risks. However, those interventions might also alter the probability of experiencing other events. Then, a joint nested frailty model can be used for the recurrent events while considering the screenings and RRSO as TDC. The joint frailty model accounts for the dependence between successive within a subject. The nested frailties can be used to model the clustered data by including two nested random effects.

Moreover, although we have extended the standard C-index to account for time-dependent effects of time-dependent covariates within clustered competing risk model, the proposed measure has not been evaluated. The proposed C-index referred to as time-dependent Uno's C-index has potential limitations. First, the TDUC will tend to 0.5 when a small number of variables is used to model. By definition of the C-index, subject pairs with tied penetrance estimates are counted as 0.5, but they are not counted as comparable when both subjects experience the event. Since the proposed C-index uses the penetrance estimates at the minimum time between two subjects' observed times, using a small number of variables leads to many tied pairs. To further evaluate the proposed C-index, a simulation study could be conducted. The interest lies in how the number of variables and number/size of families, which may affect the frailty parameters, affect the C-index in the

analysis of clustered competing risk. Furthermore, another limitation is that the proposed C-index evaluates the prediction ability of a model with TDE/TDC but does not directly evaluate the time-dependent effect of a TDC. Since the difference between the penetrance estimates across different models might be caused by the other parameters involved in the models, other variables might affect the proposed C-index. Thus, to evaluate only the effect of TDC/TDE, a new measure would be needed. In addition, since only 166 (6%) individuals underwent RRSO among 2650 individuals, only those individuals are used to evaluate the prediction accuracy to discern the effect of RRSO. Also, among 166 individuals, only 28 subjects experienced breast cancer, which may cause all models to obtain similar values of the TDUC. By definition of the C-index, subjects with shorter observed time must experience the event to compare the pairs of two subjects. Then, there might be a small number of concordant and comparable pairs. Those pairs might have similar penetrance estimates and have similar TDUC across different models.

Appendix A: Additional plots and tables

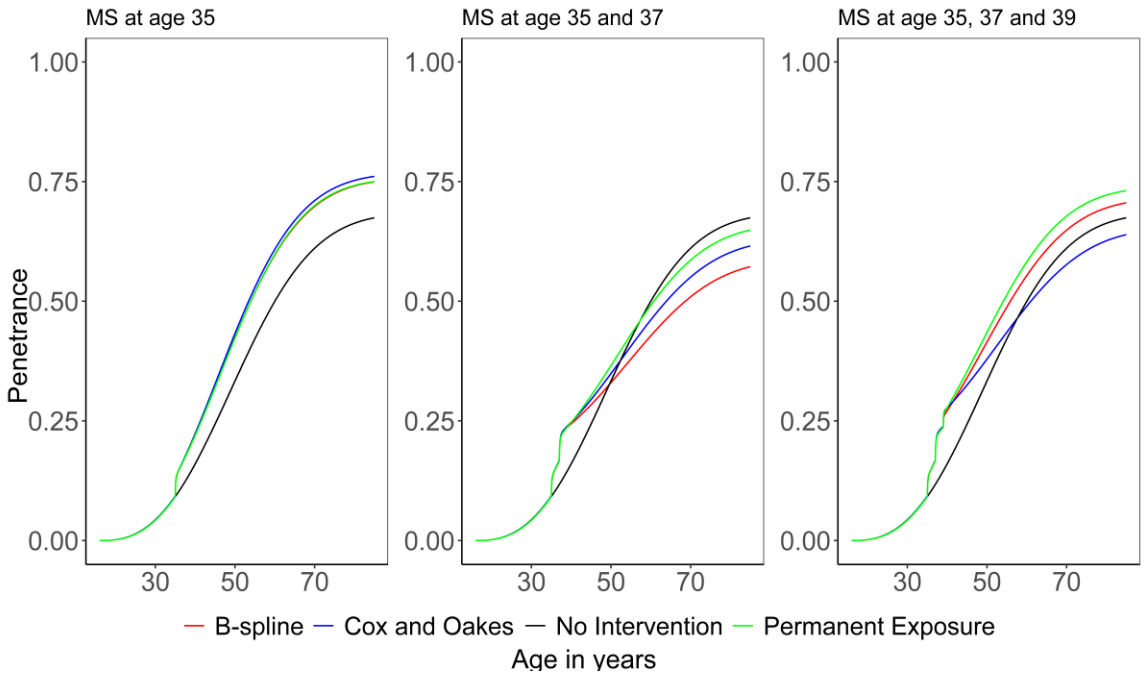

Figure A.1: Penetrance estimates for breast cancer with respect to one to three mammographic screenings (MS) at age 35 with the consecutive screening gap times of 2 years among those who had no risk-reducing salpingo-oophorectomy in the BRCA 1 families.

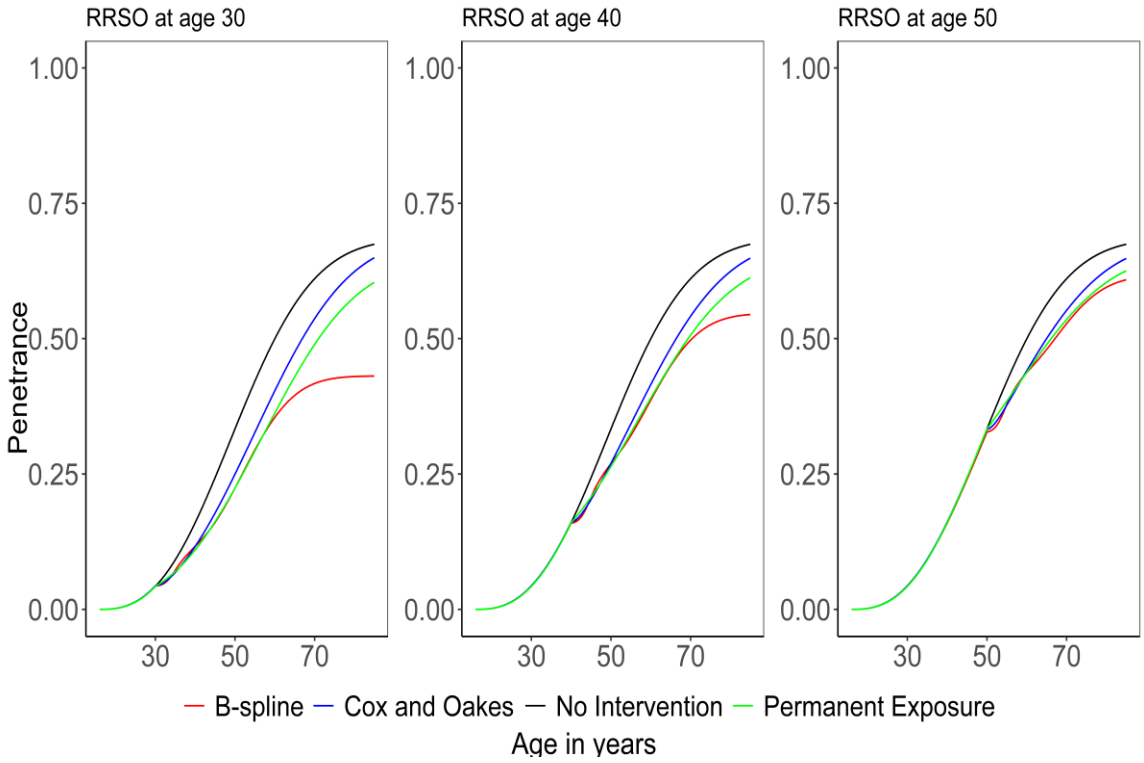

Figure A.2: Penetrance estimates for breast cancer with risk-reducing salpingo-oophorectomy (RRSO). The left most plot presents the penetrance with RRSO at age 30. To the right, they describe penetrance estimates with RRSO at age 40 and 50.

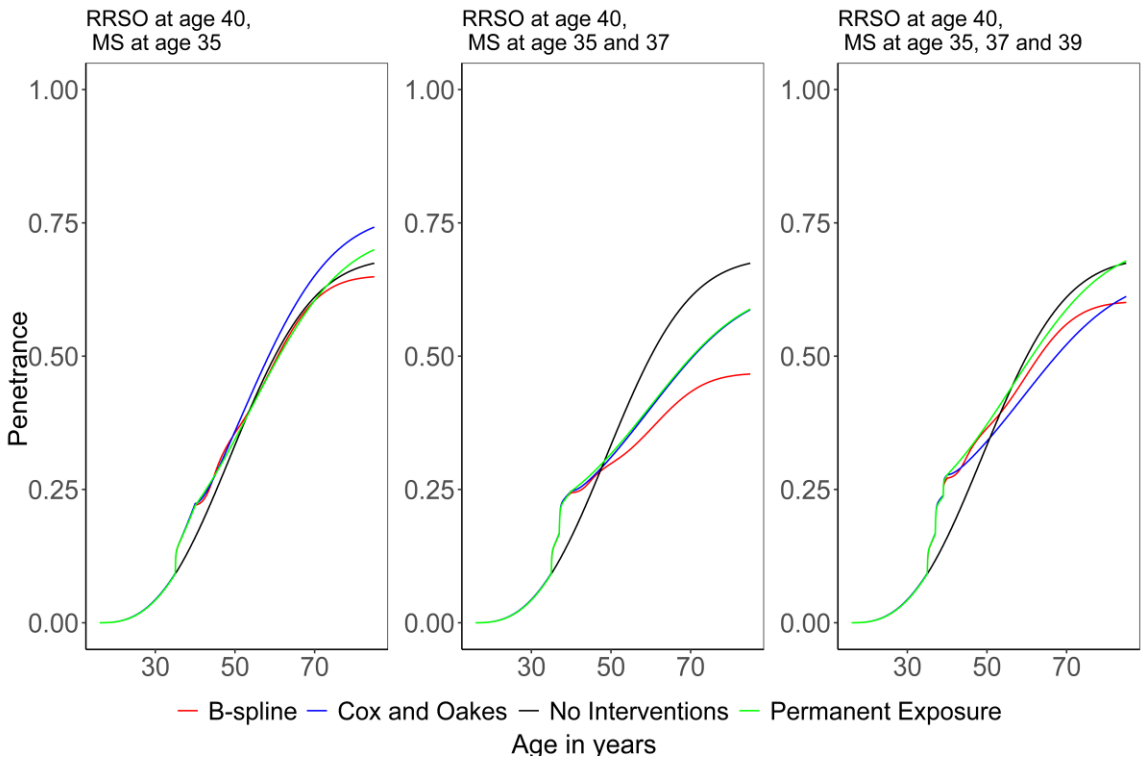

Figure A.3: Penetrance estimates for breast cancer with respect to one to three mammographic screenings (MS) at age 35 with the consecutive screening gap times of 2 years and risk-reducing salpingo-oophorectomy (RRSO) at age 40.

Table A.1: Hazard ratios and their 95% confidence intervals measuring the time-dependent effect of risk-reducing salpingo-oophorectomy (RRSO) on breast cancer under different time-dependent effect models (B-spline, Cox and Oakes, Permanent Exposure) for BRCA 1 mutation families.

Years after	Permanent Exposure		Cox and Oakes		B-spline	
RRSO	Estimate	95% CI	Estimate	95% CI	Estimate	95% CI
0.5	0.546	(0.127, 0.965)	0.204	(-0.060, 0.467)	0.133	(-0.194, 0.460)
1	0.546	(0.127, 0.965)	0.304	(0.041, 0.568)	0.206	(-0.122, 0.534)
2	0.546	(0.127, 0.965)	0.472	(0.186, 0.758)	0.419	(0.071, 0.767)
3	0.546	(0.127, 0.965)	0.572	(0.289, 0.854)	0.683	(0.195, 1.172)
4	0.546	(0.127, 0.965)	0.622	(0.341, 0.902)	0.892	(0.183, 1.601)
5	0.546	(0.127, 0.965)	0.645	(0.362, 0.927)	0.933	(0.194, 1.672)
6	0.546	(0.127, 0.965)	0.655	(0.368, 0.942)	0.789	(0.254, 1.323)
7	0.546	(0.127, 0.965)	0.660	(0.368, 0.951)	0.647	(0.240, 1.053)
8	0.546	(0.127, 0.965)	0.660	(0.366, 0.958)	0.553	(0.196, 0.911)
9	0.546	(0.127, 0.965)	0.662	(0.363, 0.962)	0.494	(0.159, 0.828)
10	0.546	(0.127, 0.965)	0.662	(0.361, 0.965)	0.460	(0.140, 0.779)
11	0.546	(0.127, 0.965)	0.663	(0.359, 0.967)	0.446	(0.139, 0.753)
12	0.546	(0.127, 0.965)	0.663	(0.357, 0.969)	0.451	(0.152, 0.751)
13	0.546	(0.127, 0.965)	0.663	(0.356, 0.970)	0.476	(0.170, 0.782)
14	0.546	(0.127, 0.965)	0.663	(0.355, 0.971)	0.505	(0.171, 0.839)
15	0.546	(0.127, 0.965)	0.663	(0.355, 0.971)	0.531	(0.154, 0.909)
16	0.546	(0.127, 0.965)	0.663	(0.354, 0.972)	0.554	(0.126, 0.983)
17	0.546	(0.127, 0.965)	0.663	(0.354, 0.972)	0.573	(0.093, 1.054)
18	0.546	(0.127, 0.965)	0.663	(0.354, 0.972)	0.588	(0.061, 1.115)
19	0.546	(0.127, 0.965)	0.663	(0.354, 0.973)	0.598	(0.035, 1.161)
20	0.546	(0.127, 0.965)	0.663	(0.354, 0.973)	0.603	(0.017, 1.189)

CI stands for confidence interval and RRSO stands for risk-reducing salpingo-oophorectomy

Appendix B: R codes for the illustration of the time-dependent C-index and its variance calculation

```
## The exemplified data used in Chapter 5
data <- data.frame(famID = c(1,1,1,2,2,2,2),
                   i = c(1,2,3,4,5,6,7),
                   time = c(23,37,63,41,49,60,69),
                   status = c(0,1,2,1,2,0,1),
                   x = c(1,0,1,0,0,1,1),
                   F_0 = c(0.59, 0.71, 0.46, 0.67, 0.51, 0.73, 0.55),
                   F_1 = c(0.55, 0.66, 0.39, 0.61, 0.45, 0.67, 0.52),
                   KM = c(1.00, 0.92, 0.42, 0.83, 0.71, 0.56, 0.14))
> data
  famID i time status x  F_0  F_1   KM
1     1 1   23      0 1 0.59 0.55 1.00
2     1 2   37      1 0 0.71 0.66 0.92
3     1 3   63      2 1 0.46 0.39 0.42
4     2 4   41      1 0 0.67 0.61 0.83
5     2 5   49      2 0 0.51 0.45 0.71
6     2 6   60      0 1 0.73 0.67 0.56
7     2 7   69      1 1 0.55 0.52 0.14

## ex_data function provides all combinations of the original data with
## penetrance estimates. pen_i and pen_j correspond to F̂1(t_fi|x_fi) and
## F̂1(t_gj|x_gj), respectively, and KM_i and KM_j are the Kaplan Meier
## estimates for censoring.

expand_data <- ex_data(data)

> expand_data
i j time famID_i t_i status_i pen_i KM_i famID_j t_j status_j pen_j KM_j
1 2   23       1  23        0  0.55 1.00       1  37        1  0.59 0.92
1 3   23       1  23        0  0.55 1.00       1  63        2  0.55 0.42
1 4   23       1  23        0  0.55 1.00       2  41        1  0.59 0.83
1 5   23       1  23        0  0.55 1.00       2  49        2  0.59 0.71
1 6   23       1  23        0  0.55 1.00       2  60        0  0.55 0.56
1 7   23       1  23        0  0.55 1.00       2  69        1  0.55 0.14
2 1   23       1  37        1  0.59 0.92       1  23        0  0.55 1.00
2 3   37       1  37        1  0.71 0.92       1  63        2  0.66 0.42
2 4   37       1  37        1  0.71 0.92       2  41        1  0.71 0.83
2 5   37       1  37        1  0.71 0.92       2  49        2  0.71 0.71
2 6   37       1  37        1  0.71 0.92       2  60        0  0.66 0.56
2 7   37       1  37        1  0.71 0.92       2  69        1  0.66 0.14
3 1   23       1  63        2  0.55 0.42       1  23        0  0.55 1.00
```

```
3 2   37       1  63        2  0.66 0.42       1  37        1  0.71 0.92
3 4   41       1  63        2  0.61 0.42       2  41        1  0.67 0.83
3 5   49       1  63        2  0.45 0.42       2  49        2  0.51 0.71
3 6   60       1  63        2  0.67 0.42       2  60        0  0.67 0.56
3 7   63       1  63        2  0.39 0.42       2  69        1  0.39 0.14
4 1   23       2  41        1  0.59 0.83       1  23        0  0.55 1.00
4 2   37       2  41        1  0.71 0.83       1  37        1  0.71 0.92
4 3   41       2  41        1  0.67 0.83       1  63        2  0.61 0.42
4 5   41       2  41        1  0.67 0.83       2  49        2  0.67 0.71
4 6   41       2  41        1  0.67 0.83       2  60        0  0.61 0.56
4 7   41       2  41        1  0.67 0.83       2  69        1  0.61 0.14
5 1   23       2  49        2  0.59 0.71       1  23        0  0.55 1.00
5 2   37       2  49        2  0.71 0.71       1  37        1  0.71 0.92
5 3   49       2  49        2  0.51 0.71       1  63        2  0.45 0.42
5 4   41       2  49        2  0.67 0.71       2  41        1  0.67 0.83
5 6   49       2  49        2  0.51 0.71       2  60        0  0.45 0.56
5 7   49       2  49        2  0.51 0.71       2  69        1  0.45 0.14
6 1   23       2  60        0  0.55 0.56       1  23        0  0.55 1.00
6 2   37       2  60        0  0.66 0.56       1  37        1  0.71 0.92
6 3   60       2  60        0  0.67 0.56       1  63        2  0.67 0.42
6 4   41       2  60        0  0.61 0.56       2  41        1  0.67 0.83
6 5   49       2  60        0  0.45 0.56       2  49        2  0.51 0.71
6 7   60       2  60        0  0.67 0.56       2  69        1  0.67 0.14
7 1   23       2  69        1  0.55 0.14       1  23        0  0.55 1.00
7 2   37       2  69        1  0.66 0.14       1  37        1  0.71 0.92
7 3   63       2  69        1  0.39 0.14       1  63        2  0.39 0.42
7 4   41       2  69        1  0.61 0.14       2  41        1  0.67 0.83
7 5   49       2  69        1  0.45 0.14       2  49        2  0.51 0.71
7 6   60       2  69        1  0.67 0.14       2  60        0  0.67 0.56

## Then, the time-dependent Uno's C-index is obtained as
td_C_50 <- comp_time_C_index_fun(expand_data, 16, 50)
> td_C_50
$U_C
[1] 0.8372327              ## TDUC with truncation time 50

$var_U_C
[1] 0.0001857506           ## Variance of the TDUC

$CI
[1] 0.8105198 0.8639456    ## 95% confidence interval for the TDUC

## TDUC = 0.8372327 with its variance of 0.0001857506 and 95%
## confidence interval (0.8105198, 0.8639456)
```

```
######  R codes for related functions
####  Expand dataset (generate all combinations of 2 subjects i and j)
ex_data <- function(data){
      n <- nrow(data)       ## total number of individuals
      i <- rep(1:n, each=n) ## all combinations for ith subject
      j <- rep(1:n, n)      ## all combinations for jth subject

      dat <- data[, c("famID", "time", "status", "x", "F_0", "F_1",
                  "KM")]
      ex_data <- cbind(i, j, dat[i, ], dat[j, ])
      names(ex_data) <- c("i", "j", paste0(c("famID", "t", "status",
                          "x", "F_0", "F_1", "KM"), "_i"),
                          paste0(c("famID", "t", "status", "x", "F_0",
                           "F_1", "KM"), "_j"))
      ex_data$time <- pmin(ex_data$t_i, ex_data$t_j)
      row.names(ex_data) <- 1:nrow(ex_data)

      pen_i <-  with(ex_data, ifelse(time == t_i & x_i == 0, F_0_i,
                                ifelse(time == t_i & x_i == 1, F_1_i,
                                       ifelse(time == t_j & x_i==0,
                                              F_0_j, F_1_j))))
      pen_j <-  with(ex_data, ifelse(time == t_i & x_j == 0, F_0_i,
                                ifelse(time == t_i & x_j == 1, F_1_i,
                                       ifelse(time == t_j & x_j==0,
                                              F_0_j, F_1_j))))

      ex_data$pen_i <- pen_i
      ex_data$pen_j <- pen_j

      raw_ex_data <- ex_data[, c("i", "j", "time", "famID_i", "t_i",
                              "status_i", "pen_i", "KM_i", famID_j",
                              "t_j", "status_j", "pen_j", "KM_j")]
      return(raw_ex_data)
}


####  Time-dependent Uno's C-index with truncation time
comp_time_C_index_fun <- function(data, trunc_time) {
      n <- length(unique(data$i))           ## number of individuals
      n_fam <- length(unique(data$famID_i)) ## number of families
      ## each family size
      n_f <- table(data[!duplicated(data$KM_i),]$famID_i)
      famID <- data[!duplicated(data$KM_i),]$famID_i

      # IPCW of the Kaplan Meier estimate of the censoring
      distribution
      km_t_i1 <- data$KM_i
      km_t_i2 <- data$KM_j
```

```
      # Penetrance
      pen_i <- data$pen_i   ## Penetrance estimates for subject i
      pen_j <- data$pen_j   ## Penetrance estimates for subject j

      # Subject indicator for all possible combination of pairs
      famID_i <- data$famID_i
      famID_j <- data$famID_j
      subject_i <- data$i

      # Denoting competing risk by 2
      status_i <- data$status_i
      status_j <- data$status_j
      t_i <- data$t_i            ## observed time for subject i
      t_j <- data$t_j            ## observed time for subject j

      # Weights
      km1_1 <- (km_t_i1)^(-2)
      km1_2 <- (km_t_i2)^(-2)
      km2 <- (km_t_i1 * km_t_i2)^(-1)

      ## sign and csign functions
      # sign functions
      sign <- (pen_i > pen_j) - (pen_i < pen_j)

      # csign function (with weights and truncation time)
       csign <- ((t_i <= t_j) * km1_1 + (t_i > t_j) * (status_j == 2) *
             km2) * (status_i == 1) * (t_i <     trunc_time) - ((t_i >=
             t_j) * km1_2 + (t_i < t_j) * (status_i == 2) * km2) *
             (status_j == 1) * (t_j < trunc_time)

      # Difference between the concordant and discordant pairs
      d_cs <- sign * csign
      # Comparable pairs
      d_c <- abs(csign)

      # Time-dependent Uno's C-index
      U_C <- 0.5*(sum(d_cs)/sum(d_c) + 1)

      ## Variance estimation
      var_U_C <- sample_var_C_index(d_c, d_cs, subject_i, famID, n_f,
                                    n_fam, n)
      ci <- U_C + c(-1, 1) * 1.96 * sqrt(var_U_C)
      return(list(U_C = U_C, var_U_C = var_U_C, CI = ci))
}


####  Variance estimation for C-index using sample variance
sample_var_C_index <- function(d_ijxx, d_ijxy, subject1, famID, n_f,
                               n_fam, n) {
```

```
        # n_f = each cluster size; n_fam = total number of families
        # n = total number of individuals across all families
        # Mean of individual i in family f
        ## weighted proportion of comparable pairs for each individual
        d_fixx <- aggregate(d_ijxx ~ subject1, FUN = mean)[,2]

        ## difference btw the weighted number of concordant and
        ## discordant pairs for each individual
        d_fixy <- aggregate(d_ijxy ~ subject1, FUN = mean)[,2]

        # Mean of each family
        ## weighted proportion of comparable pairs for each family
        d_fxx <- aggregate(d_fixx ~ famID, FUN = mean)[,2]

        ## difference btw the weighted number of concordant and
        ## discordant pairs for each family
        d_fxy <- aggregate(d_fixy ~ famID, FUN = mean)[,2]

        # Mean of all individuals
        ## average weighted proportion of comparable pairs
        d_xx <- sum(d_ijxx)/(n * (n-1))

        ## average difference btw the weighted number of concordant and
        ## discordant pairs
        d_xy <- sum(d_ijxy)/(n * (n-1))

        # Variance
        var_fixx <- sum(n_f * (d_fxx - d_xx)^2)/(n * (n_fam - 1))
        var_fixy <- sum(n_f * (d_fxy - d_xy)^2)/(n * (n_fam - 1))
        cov_fi <- sum(n_f * (d_fxx - d_xx) * (d_fxy - d_xy))/(n * (n_fam
                      - 1))

        var_d_xx <- 4/n * var_fixx
        var_d_xy <- 4/n * var_fixy
        cov_d_xx_d_xy <- 4/n * cov_fi

        output <- ifelse(d_xx == 0, 0, t(c(1/d_xx, -d_xy/d_xx^2)) %*%
                       matrix(c(var_d_xy, cov_d_xx_d_xy, cov_d_xx_d_xy,
                       var_d_xx), nrow = 2, ncol = 2) %*%
                        c(1/d_xx, -d_xy/d_xx^2)/4)
         return(output)
}
```

Bibliography

[1] Antolini, L., Boracchi, P., and Biganzoli, E. (2005). A time-dependent discrimination index for survival data. *Statistics in Medicine*, *24*(24), 3927–3944.

[2] Bamber, D. (1975). The area above the ordinal dominance graph and the area below the receiver operating characteristic graph. *Journal of Mathematical Psychology*, *12*(4), 387–415.

[3] Berry, S. D., Ngo, L., Samelson, E. J., and Kiel, D. P. (2010). Competing risk of death: An important consideration in studies of older adults. *Journal of the American Geriatrics Society*, *58*(4), 783–787.

[4] Beyersmann, J., Wolkewitz, M., and Schumacher, M. (2008). The impact of time-dependent bias in proportional hazards modelling. *Statistics in Medicine*, *27*(301), 6439–6454.

[5] Beyersmann, Jan, Latouche, A., Buchholz, A., & Schumacher, M. (2009). Simulating competing risks data in survival analysis. *Statistics in Medicine*, *28*(6), 956–971.

[6] Brier, G. W. (1950). Verification of forecasts expressed in terms of probability. *Monthly Weather Review*, *78*(1), 1–3.

[7] Burton, A., Altman, D. G., Royston, P., and Holder, R. L. (2006). The design of simulation studies in medical statistics. *Statistics in Medicine*, *25*(24), 2479–4292.

[8] Chen, S., Iversen, E. S., Friebel, T., Finkelstein, D., Weber, B. L., Eisen, A., Peterson, L. E., Schildkraut, J. M., Isaacs, C., Peshkin, B. N., Corio, C., Leondaridis, L., Tomlinson, G., Dutson, D., Kerber, R., Amos, C. I., Strong, L. C., Berry, D. A., Euhus, D. M., and Parmigiani, G. (2006). Characterization of BRCA1 and BRCA2 mutations in a large United States sample. *Journal of Clinical Oncology*, *24*(6), 863–871.

[9] Choi, Y. H., Jung, H., Buys, S., Daly, M., John, E. M., Hopper, J., Andrulis, I., Terry, M. B., and Briollais, L. (2021). A competing risks model with binary time varying covariates for estimation of breast cancer risks in BRCA1 families. *Statistical Methods in Medical Research*, *30*(9), 2165–2183.

[10] Clayton, D. G. (1978). A model for association in bivariate life tables and its application in epidemiological studies of familial tendency in chronic disease incidence. *Biometrika*, *65*(1), 141–151.

[11] Cliff, N., and Charlin, V. (1991). Variances and covariances of Kendall's tau and their estimation. *Multivariate Behavioral Research*, *26*(4), 693–707.

[12] Cox, D. R., and Oakes, D. (1984). *Analysis of survival data*. Chapman and Hall/CRC.

[13] Crowley, J., and Hu, M. (1977). Covariance analysis of heart transplant survival data. *Journal of the American Statistical Association, 72*(357), 27–36.

[14] De Boor, C. (1978). *A practical guide to splines*. New York: Springer-Verlag.

[15] Eilers, P. H., and Marx, B. D. (1996). Flexible smoothing with B-splines and penalties. *Statistical Science*, *11*(2), 89–102.

[16] Fine, J. P., and Gray, R. J. (1999). A proportional hazards model for the subdistribution of a competing risk. *Journal of the American Statistical Association*, *94*(446), 496–509.

[17] Gerds, T. A., and Schumacher, M. (2006). Consistent estimation of the expected brier score in general survival models with right-censored event times. *Biometrical Journal*, *48*(6), 1029–1040.

[18] Gorfine, M., and Hsu, L. (2011). Frailty-based competing risks model for multivariate survival data. *Biometrics*, *67*(2), 415–426.

[19] Graf, E., Schmoor, C., Sauerbrei, W., and Schumacher, M. (1999). Assessment and comparison of prognostic classification schemes for survival data. *Statistics in Medicine*, *18*(17–18), 2529–2545.

[20] Gray, R. J. (1988). A class of K-Sample tests for comparing the cumulative incidence of a competing risk. *The Annals of Statistics*, *16*(3), 1141–1154.

[21] Hanley, J. A., and McNeil, B. J. (1982). The meaning and use of the area under a receiver operating characteristic (ROC) curve. *Radiology*, *143*(1), 29–36.

[22] Harrell, F. E., Califf, R. M., Pryor, D. B., Lee, K. L., and Rosati, R. A. (1982). Evaluating the yield of medical tests. *JAMA*, *247*(18), 2543–2546.

[23] Harrell, F. E., Lee, K. L., and Mark, D. B. (1996). Multivariable prognostic models: issues in developing models, evaluating assumptions and adequacy, and measuring and reducing errors. *Statistics in Medicine*, *15*(4), 361–387.

[24] Hastie, T., and Tibshirani, R. (1993). Varying-Coefficient Models. *Journal of the Royal Statistical Society: Series B, Methodological*, *55*(4), 757–779.

[25] Henderson, R., Jones, M., and Stare, J. (2001). Accuracy of point predictions in survival analysis. *Statistics in Medicine*, *20*(20), 3083–3096.

[26] Hinchliffe, S. R., and Lambert, P. C. (2013). Flexible parametric modelling of cause-specific hazards to estimate cumulative incidence functions. *BMC Medical Research Methodology*, *13*(1), 13.

[27] Hosmer, D. W., Lemeshow, S., and Sturdivant, R. X. (2013). *Applied Logistic Regression*. John Wiley and Sons.

[28] Hougaard, P. (2000). *Analysis of Multivariate Survival Data*. New York: Springer.

[29] Hougaard, P. (1995). Frailty models for survival data. *Lifetime Data Analysis*, *1*(3), 255-273.

[30] John, E. M., Hopper, J. L., Beck, J. C., Knight, J. A., Neuhausen, S. L., Senie, R. T., Ziogas, A., Andrulis, I. L., Anton-Culver, H., Boyd, N., Buys, S. S., Daly, M. B., O'Malley, F. P., Santella, R. M., Southey, M. C., Venne, V. L., Venter, D. J., West, D. W., Whittemore, A. S., and Seminara, D. (2004). The breast cancer family registry: an infrastructure for cooperative multinational, interdisciplinary and translational studies of the genetic epidemiology of breast cancer. *Breast Cancer Research : BCR*, *6*(4), 375–389.

[31] Kalbfleisch, J. D., and Prentice, R. L. (2002). *The statistical analysis of failure time data*. John Wiley and Sons.

[32] Kang, L., Chen, W., Petrick, N. A., and Gallas, B. D. (2015). Comparing two correlated C indices with right-censored survival outcome: a one-shot nonparametric approach. *Statistics in Medicine*, *34*(4), 685–703.

[33] Kendall, M. G. (1938). A new measure of rank correlation. *Biometrika*, *30*(1/2), 81–93.

[34] Keown-Stoneman, C. D. G., Horrocks, J., and Darlington, G. (2018). Exponential decay for binary time-varying covariates in cox models. *Statistics in Medicine*, *37*(5), 776–788.

[35] Larsen, M. J., Thomassen, M., Gerdes, A. M., and Kruse, T. A. (2014). Hereditary breast cancer: clinical, pathological and molecular characteristics. *Breast Cancer: Basic and Clinical Research*, *2014*, 145–155.

[36] Munda, M., Rotolo, F., and Legrand, C. (2012). parfm: parametric frailty models in R. *Journal of Statistical Software*, *51*(11).

[37] Nan, B., Lin, X., Lisabeth, L. D., and Harlow, S. D. (2005). A varying-coefficient cox model for the effect of age at a marker event on age at menopause. *Biometrics*, *61*(2), 576–583.

[38] Nelder, J. A. and Mead, R. (1965). A simplex method for function minimization. *Computer Journal*, 7, 308-313.

[39] Pankratz, V. S., De Andrade, M., and Therneau, T. M. (2005). Random-effects cox proportional hazards model: general variance components methods for time-to-event data. *Genetic Epidemiology*, *28*(2), 97–109.

[40] Penciana, M. J., and D'Agostino, R. B. (2004). Overall C as a measure of discrimination in survival analysis: model specific population value and confidence interval estimation. *Statistics in Medicine*, *23*(13), 2109–2123.

[41] Petrucelli, N., Daly, M. B., and Pal, T. (2022). BRCA1- and BRCA2- associated hereditary breast and ovarian cancer. *GeneReviews*. https://www.ncbi.nlm.nih.gov/books/NBK1247/.

[42] Putter, H., Fiocco, M., and Geskus, R. B. (2007). Tutorial in biostatistics: competing risks and multi-state models. *Statistics in Medicine*, *26*(11), 2389–2430.

[43] R Core Team. (2018). R: A language and environment for statistical computing. R Foundation for Statistical Computing, Vienna, Austria. URL http"//www.Rproject.org/.

[44] Ring, K. L., and Modesitt, S. C. (2018). Hereditary cancers in gynecology: what physicians should know about genetic testing, screening, and risk reduction. *Obstetrics and Gynecology Clinics of North America*, *45*(1), 155–173.

[45] Ripatti, S., and Palmgren, J. (2000). Estimation of multivariate frailty models using penalized partial likelihood. *Biometrics*, *56*(4), 1016–1022.

[46] Rueten-Budde, A. J., Putter, H., and Fiocco, M. (2019). Investigating hospital heterogeneity with a competing risks frailty model. *Statistics in Medicine*, *38*(2), 269–288.

[47] Satagopan, J. M., Offit, K., Foulkes, W., Robson, M. E., Wacholder, S., Eng, C. M., Karp, S. E., and Begg, C. B. (2001). The lifetime risks of breast cancer in Ashkenazi Jewish carriers of BRCA1 and BRCA2 mutations. *Cancer Epidemiology Biomarkers and Prevention*, *10*(5), 467–473.

[48] Schmid, M., and Potapov, S. (2012). A comparison of estimators to evaluate the discriminatory power of time-to-event models. *Statistics in Medicine*, *31*(23), 2588–2609.

[49] Schoop, R., Beyersmann, J., Schumacher, M., and Binder, H. (2011). Quantifying the predictive accuracy of time-to-event models in the presence of competing risks. *Biometrical Journal*, *53*(1), 88–112.

[50] Sleeper, L. A., and Harrington, D. P. (1990). Regression splines in the Cox model with application to covariate effects in liver disease. *Journal of the American Statistical Association*, *85*(412), 941–949.

[51] Steyerberg, E. W., Vickers, A. J., Cook, N. R., Gerds, T., Gonen, M., Obuchowski, N., Pencina, M. J., and Kattan, M. W. (2010). Assessing the performance of prediction models: a framework for traditional and novel measures. *Epidemiology, 21*(1), 128–138.

[52] Suissa, S. (2008). Immortal time bias in pharmacoepidemiology. *American Journal of Epidemiology*, *167*(4), 492–499.

[53] Therneau, T. M., and Grambsch, P. M. (2000). *Modeling Survival Data: Extending the Cox Model*. Springer, New York, NY.

[54] Uno, H., Cai, T., Pencina, M. J., D'Agostino, R. B., and Wei, L. J. (2011). On the C-statistics for evaluating overall adequacy of risk prediction procedures with censored survival data. *Statistics in Medicine, 30*(10), 1105–1117.

[55] Vaupel, J. W., Manton, K. G., and Stallard, E. (1979). The impact of heterogeneity in individual frailty on the dynamics of mortality. *Demography*, *16*(3), 439–454.

[56] Warwick, J., Tabar, L., Vitak, B., and Duffy, S. W. (2004). Time-dependent effects on survival in breast carcinoma: results of 20 years of follow-up from the Swedish two-county study. *Cancer*, *100*(7), 1331–1336.

[57] Wolbers, M., Blanche, P., Koller, M. T., Witteman, J. C., and Gerds, T. A. (2014). Concordance for prognostic models with competing risks. *Biostatistics*, *15*(3), 526–539.

[58] Wolbers, M., Koller, M. T., Witteman, J. C., and Steyerberg, E. W. (2009). Prognostic models with competing risks methods and application to coronary risk prediction. *Epidemiology*, *20*(4), 555–561.

[59] Yashin, A. I., Vaupel, J. W., and Iachine, I. A. (1995). Correlated individual frailty: an advantageous approach to survival analysis of bivariate data. *Mathematical Population Studies*, *5*(2), 145–159.

[60] Zhou, B., Fine, J., Latouche, A., and Labopin, M. (2012). Competing risks regression for clustered data. *Biostatistics*, *13*(3), 371–383.

[61] Zou, G. (2021). Confidence interval estimation for treatment effects in cluster randomization trials based on ranks. *Statistics in Medicine*, *40*(14), 3227–3250.

[62] Zou, G., Smith, E., & Jairath, V. (2022). A nonparametric approach to confidence intervals for concordance index and difference between correlated indices. *Journal of Biopharmaceutical Statistics*, 1–28.

Curriculum Vitae

Name:	Seungwoo Lee
Post-secondary Education and Degrees:	University of Waterloo Waterloo, Ontario, Canada 2011-2016 B.Math. The University of Western Ontario London, Ontario, Canada 2019-2022 M.Sc.
Honours and Awards:	Schulich Graduate Scholarship 2019-2021
Related Work Experience	Research Assistant The University of Western Ontario 2019-2022